AD-A098 509 KUHN (RICHARD E) NEWPORT NEWS VA F/G 20/4
AN ENGINEERING METHOD FOR ESTIMATING THE INDUCED LIFT ON V/STOL--ETC(U)
JAN 81 R E KUHN N62269-80-C-0366
UNCLASSIFIED NADC-80246-60 NL

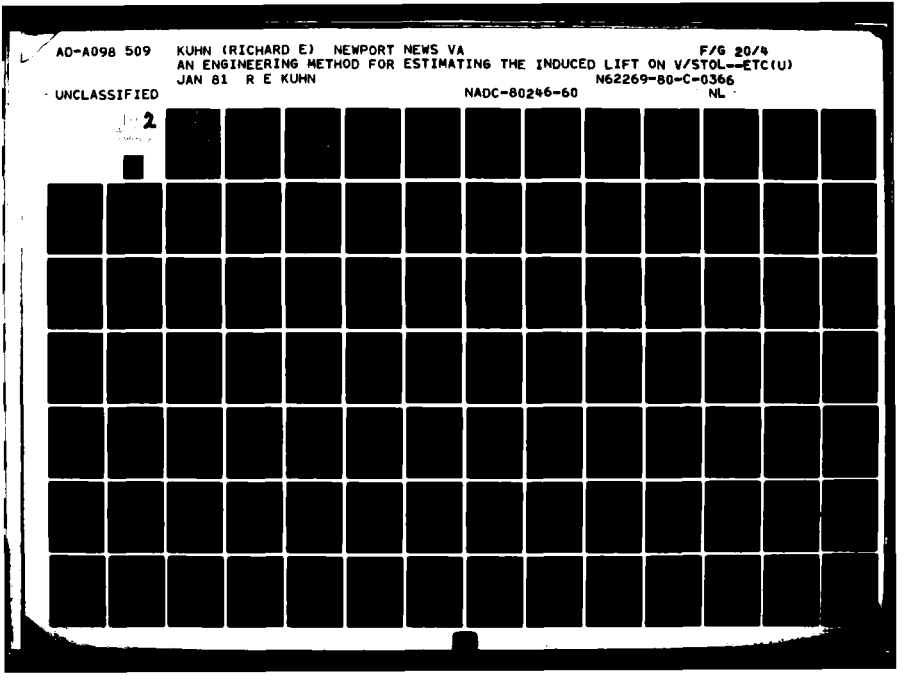

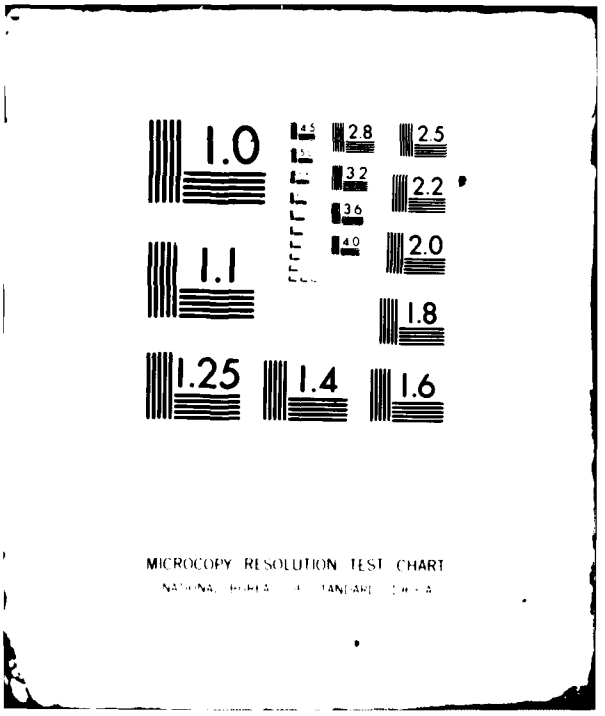
1.0
1.1
1.25
1.4
1.6
1.8
2.0
2.2
2.5
2.8
3.2
3.6
4.0
MICROCOPY RESOLUTION TEST CHART

REPORT NO. NADC-80246-60

LEVEL II

12

AN ENGINEERING METHOD FOR ESTIMATING THE INDUCED LIFT ON V/STOL AIRCRAFT HOVERING IN AND OUT OF GROUND EFFECT

JANUARY 1981

Richard E. Kuhn
V/STOL Consultant
111 Mistletoe Dr.
Newport News, Virginia 23606

AIRTASK NO. A03V-320D/01B/7F41-400-000

Prepared for
NAVAL AIR DEVELOPMENT CENTER
Department of the Navy
Warminster, Pennsylvania 18974

NOTICES

REPORT NUMBERING SYSTEM - The numbering of technical project reports issued by the Naval Air Development Center is arranged for specific identification purposes. Each number consists of the Center acronym, the calendar year in which the number was assigned, the sequence number of the report within the specific calendar year, and the official 2-digit correspondence code of the Command Office or the Functional Directorate responsible for the report. For example: Report No. NADC-78015-20 indicates the fifteenth Center report for the year 1978, and prepared by the Systems Directorate. The numerical codes are as follows:

CODE	OFFICE OR DIRECTORATE
00	Commander, Naval Air Development Center
01	Technical Director, Naval Air Development Center
02	Comptroller
10	Directorate Command Projects
20	Systems Directorate
30	Sensors & Avionics Technology Directorate
40	Communication & Navigation Technology Directorate
50	Software Computer Directorate
60 ✓	Aircraft & Crew Systems Technology Directorate
70	Planning Assessment Resources
80	Engineering Support Group

APPROVED BY: 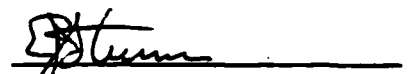 DATE: 3-11-81

E. J. STURM
CAPT USN

UNCLASSIFIED

SECURITY CLASSIFICATION OF THIS PAGE (When Data Entered)

REPORT DOCUMENTATION PAGE

READ INSTRUCTIONS BEFORE COMPLETING FORM

1. REPORT NUMBER: NADC-80246-60	2. GOVT ACCESSION NO.: AD-A098509
3. RECIPIENT'S CATALOG NUMBER:	
4. TITLE (and Subtitle): An Engineering Method For Estimating The Induced Lift On V/STOL Aircraft Hovering In And Out Of Ground Effect.	5. TYPE OF REPORT & PERIOD COVERED: Final Technical Report.
	6. PERFORMING ORG. REPORT NUMBER:
7. AUTHOR(s): Richard E. Kuhn	8. CONTRACT OR GRANT NUMBER(s): N62269-80-C-0366
9. PERFORMING ORGANIZATION NAME AND ADDRESS: Richard E. Kuhn, V/STOL Consultant, 111 Mistletoe Dr., Newport News, Va. 23606	10. PROGRAM ELEMENT, PROJECT, TASK AREA & WORK UNIT NUMBERS: AIRTASK No. A03V-320D/ 01B/7F41-400-000
11. CONTROLLING OFFICE NAME AND ADDRESS: Naval Air Development Center, Warminster, Pa. 18974	12. REPORT DATE: Jan[illegible]1981
	13. NUMBER OF PAGES: 93
14. MONITORING AGENCY NAME & ADDRESS(if different from Controlling Office)	15. SECURITY CLASS. (of this report): Unclassified
	15a. DECLASSIFICATION/DOWNGRADING SCHEDULE:

16. DISTRIBUTION STATEMENT (of this Report)

Unlimited

DTIC ELECTE MAY 5 1981 S

17. DISTRIBUTION STATEMENT (of the abstract entered in Block 20, if different from Report)

18. SUPPLEMENTARY NOTES

19. KEY WORDS (Continue on reverse side if necessary and identify by block number)

V/STOL
Ground Effects
Suckdown
Fountain Lift
Multiple Jets

20. ABSTRACT (Continue on reverse side if necessary and identify by block number)

An examination and correlation of available data has shown that two different methods must be used to estimate the jet induced lift on Fan and Jet V/STOL aircraft in hovering flight. The Basic Method developed in this study is used for configurations with widely spaced jets, and the h' Method is used for configurations with closely spaced jets. The methods account for the effects of jet arrangement, configuration planform, wing height, body contour and Lift Improvement Devices (LIDs) but are limited to configurations with essen-

DD FORM 1 JAN 73 1473 EDITION OF 1 NOV 65 IS OBSOLETE
S/N 0102-LF-014-6601

UNCLASSIFIED
SECURITY CLASSIFICATION OF THIS PAGE (When Data Entered)

tially vertical, circular jets of equal size and thrust. Suggestions for further work to evaluate and refine the methods are included.

TABLE OF CONTENTS

TABLE OF CONTENTS - Concluded

LIST OF FIGURES

LIST OF FIGURES - Continued

LIST OF FIGURES - Concluded

LIST OF TABLES

LIST OF SYMBOLS

A	Total jet area, m^2
d	Diameter of individual jet, m
d_e	Diameter of equivalent single jet having area A, m
D	Diameter of equivalent circular planform having area S, m
$\bar{D}$	Angular mean diameter of planform, see fig. 2, m
e	Half the distance between adjacent jets, see fig. 1, m
E	Length to width ratio of jet pattern
h	Height of lowest surface of configuration above ground, m
Δh	Height of wing above configuration's lowest surface, m
h'	Critical height in h' Method, m
K_A	Constant in expression for contribution of fountain arms
K_C	Constant in expression for contribution of fountain core, see eq. 13
λ_A	Exponent in expression for contribution of fountain arms
λ_C	Exponent in expression for contribution of fountain core, see eq. 12
K'	Constant in h' Method, see eq. 20 and 21
λ'	Exponent in h' Method, see eq. 18 and 19
K_r	Constant in expression for calculating fountain life of contoured bodies, see eq. 26
K_S	Constant in expression for multiple jet suckdown, see eq. 6
λ_S	Exponent in expression for multiple jet suckdown, see eq. 6
L	Length of configuration, m
ΔL	Net induced lift increment, N
ΔL_∞	Lift loss increment induced out of ground effect, N
ΔL_S	Suckdown induced by ground proximity, N
ΔL_F	Lift increment induced by fountain, N
ΔL_A	Lift increment induced by fountain arms, N
ΔL_C	Lift increment induced by fountain core, N
N	Number of jets
P'	Ratio of perimeter closed by LIDs to total perimeter of LID planform
$\frac{P_n}{p}$	Nozzle pressure ratio

LIST OF SYMBOLS - Concluded

r	Radius or effective radius of contoured body, m
S	Total planform area, m^2
S'	Actual surface area between jets, see fig. 1a and b, m^2
S''	Potential surface area between jets, see fig. 1a and b, m^2
S_C	Area enclosed by lines connecting jet centers, see fig. 1c, m^2
S'_C	Actual surface area inside S_C, see fig. 1c, m^2
S_L	Area enclosed by LIDs, see fig. 1c, m^2
T	Total jet thrust, N
W	Width of configuration, m
w	Half body width on line between jets when jets are external to planform, see fig. 1c, w = e when jets are contained within the planform of the configuration, m
y	Spanwise extent of planform on fountain arm centerline, see fig. 1a and b, m
Y	Maximum spanwise extent of planform between jets, see fig. 1a and b, m
θ	Half the included angle between adjacent jets, see fig. 1b, deg.
θ'	Ratio of jet pattern perimeter blocked by jets to total perimeter, see eq. 21

Subscripts

exp	indicates experimental data or increments derived from experimental data
hw	indicates high wing
b	indicates body alone
wb	indicates wing-body
m	indicates multijet
s	indicates single jet
h	indicates data calculated at height, h
h+Δh	indicates data calculated at height, h+Δh

SUMMARY

An examination and correlation of available data has shown that two different methods must be used to estimate the jet induced lift on Fan and Jet V/STOL aircraft in hovering flight. The Basic Method developed in this study is used for configurations with widely spaced jets, and the h' Method is used for configurations with closely spaced jets. The methods account for the effects of jet arrangement, configuration planform, wing height, body contour and Lift Improvement Devices (LIDs) but are limited to configurations with essentially vertical, circular jets of equal size and thrust. Suggestions for further work to evaluate and refine the methods are included.

INTRODUCTION

In hovering flight forces are induced on fan and jet powered V/STOL aircraft by the entrainment action of the exiting jets. Out of ground effect a small download is produced by the suction pressures induced on the lower surface of the aircraft by the downward directed jet streams. In ground effect the jets impinge on, and spread across the ground in a wall jet under the aircraft greatly increasing the entrainment surface area and the resulting suckdown. However, with two or more jets an upflow is created where the wall jets, flowing outward from their respective impingement points, meet. This upflow or "fountain" induces positive pressures on the underside of the aircraft which act to reduce the lift loss or in some cases produce a net positive lift.

The generally accepted method for estimating the ground induced suckdown of a single jet configuration was developed by Wyatt, Ref. 1. His method, with a small modification to account for nozzle pressure ratio effects, was used as the starting point in an attempt, reported in ref. 2, to develop an empirical method for predicting the ground effects of multiple jet configurations. An "air cushion" analogy used in that method to account for the fountain effects has been found to have limited applicability, particularly for configurations with widely spaced jets.

More recently Yen, ref. 3, developed relatively simple analytical expressions for the vertical momentum in the fountain. Yen's work has been used in the present study as the starting point for estimating the fountain forces. However, it was found that the method based on this approach was only applicable to widely spaced jets. A second method, similar to that of ref. 2, has been developed for closely spaced jet configurations.

The present methods are intended for use only in preliminary design work and to give a general indication of the effects of the primary configuration variables. The induced effects are a complex function of many configuration variables and the development of a V/STOL aircraft will require careful experimental investigations to accurately determine the induced forces.

DEVELOPMENT OF METHODS

The methods developed in this study assume that the total induced lift on a fan or jet V/STOL aircraft in hovering flight can be expressed as:

$$\frac{\Delta L}{T} = \frac{\Delta L_\infty}{T} + \frac{\Delta L_S}{T} + \frac{\Delta L_F}{T} + \frac{\Delta L_L}{T} \tag{1}$$

where:

$\frac{\Delta L_\infty}{T}$ is the lift loss induced out of ground effect. The methods for estimating this term were reviewed and presented in reference 2. For the present methods:

$$\frac{\Delta L_\infty}{T} = -.000253 \sqrt{\frac{S}{A}} \left[\left(\frac{P_n}{p} \right)^{-.64} \frac{\Sigma \pi d}{d_e} \right]^{1.58} \tag{2}$$

$\frac{\Delta L_S}{T}$ is the additional lift loss experienced in ground effect. The basic method for estimating this term for single jet configurations was developed by Wyatt (ref. 1) and modified slightly to account for the effects of pressure ratio in reference 2. For the present methods the ground induced suckdown for multiple jets is calculated by multiplying Wyatt's expression for single jet suckdown by the factor K_S:

$$\frac{\Delta L_S}{T} = K_S(-.15) \left[\frac{h/d_e}{\frac{\bar{D}}{d_e} - 1.0} \right]^{-\left[2.2 - .24 \left(\frac{P_n}{p} - 1 \right)\right]} \tag{3}$$

where $K_S = 1.0$ for a single jet configuration. A method for estimating K_S for multiple jet configurations has been developed in the present study and is presented in later sections.

$\frac{\Delta L_F}{T}$ and $\frac{\Delta L_L}{T}$ are terms for the positive lift due to fountain effects and Lift Improvement Devices (LIDs) respectively. Methods for estimating these effects have been developed in the present study and are presented in later sections.

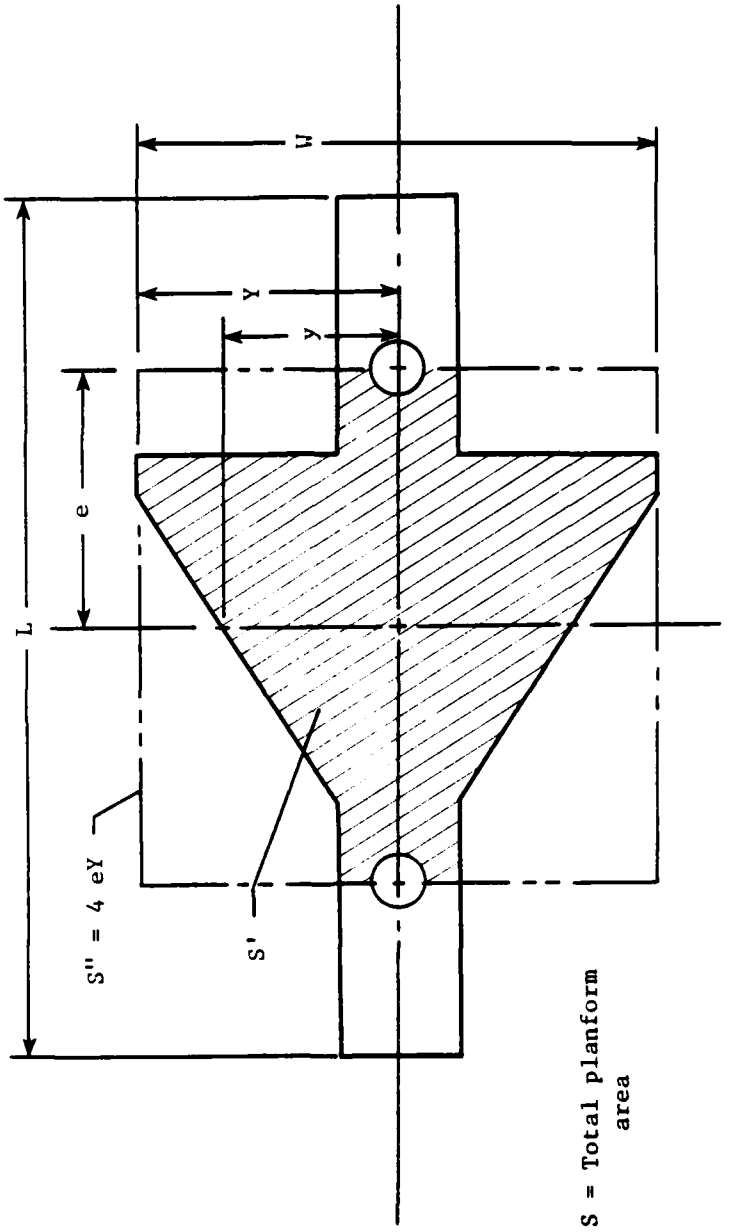

(a) Two jet configurations.

Figure 1.- Configuration geometry terms used in the analysis.

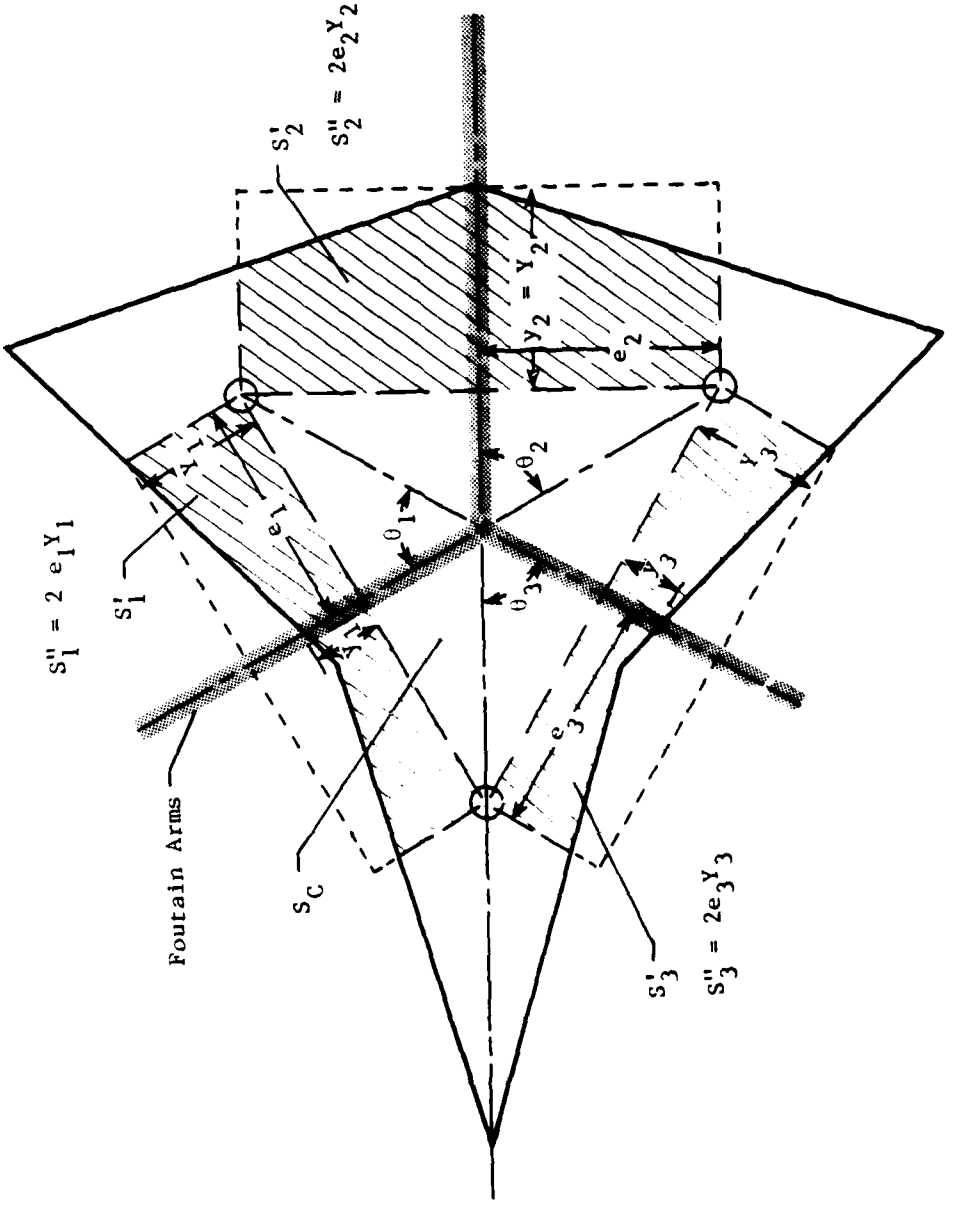

(b) Configurations with three or more jets.

Figure 1.- Continued.

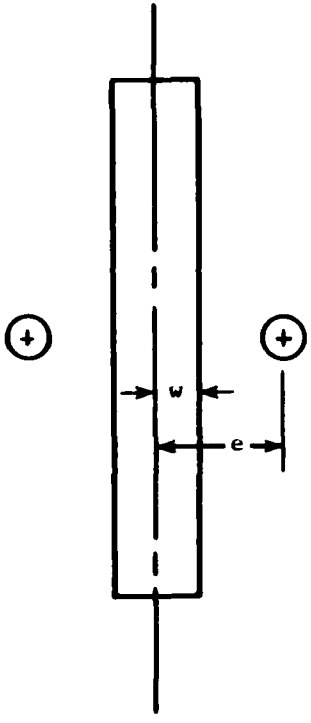

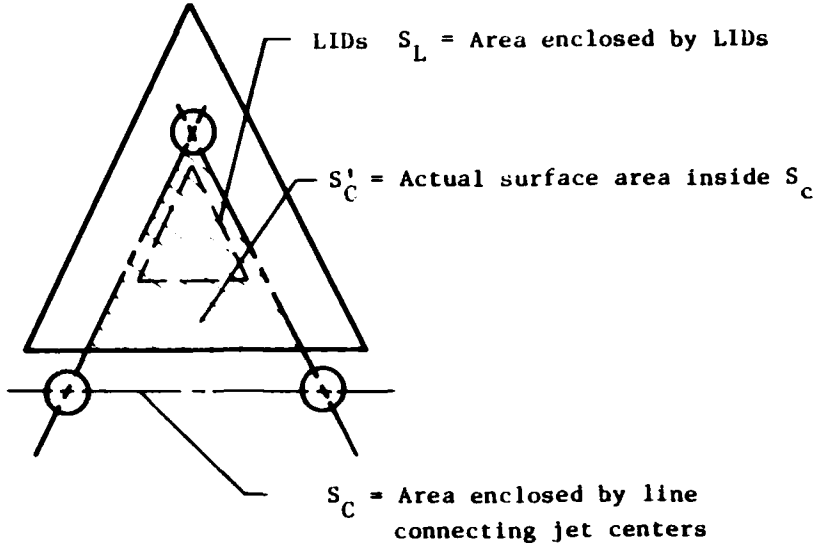

(c) Lift improvement devices and jets external to planform.

Figure 1.- Concluded.

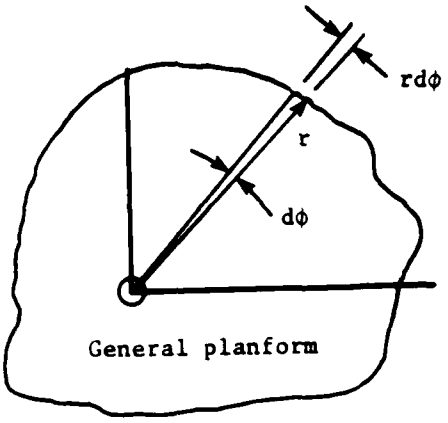

$$\bar{D} = \frac{1}{\pi} \int_0^{2\pi} r\,d\phi$$

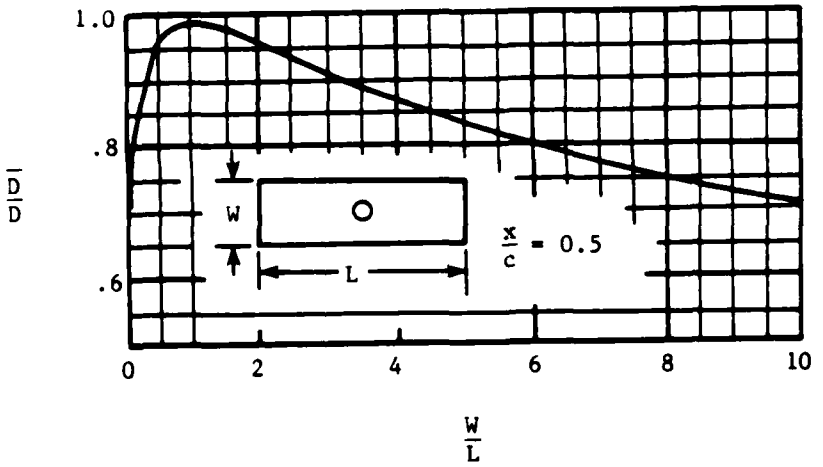

Figure 2.- Values of $\bar{D}$ for several regular planforms.

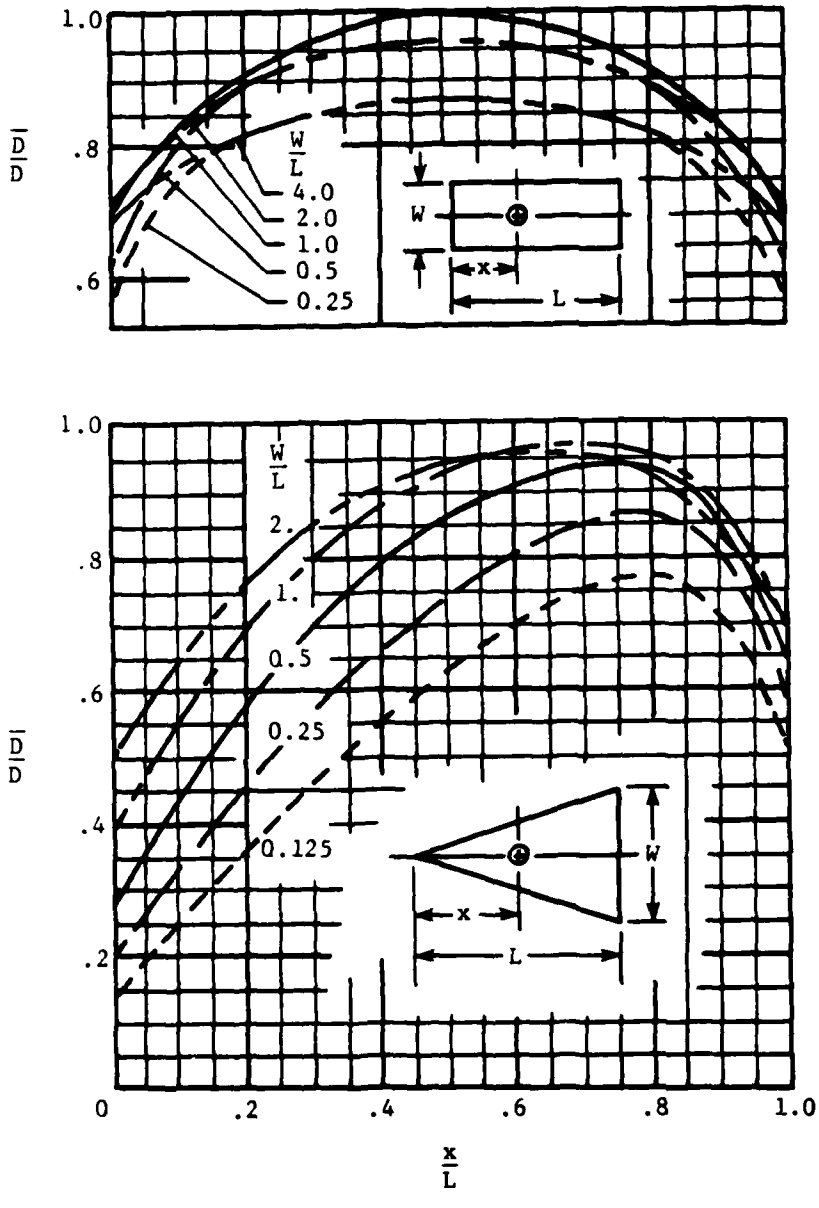

Figure 2.- Concluded.

The principle geometric parameters used in the methods developed here are defined in figure 1. The definition of $\bar{D}$ and its value for several regular planforms are presented in figure 2.

Basic Method

Basis of Method:

The flow from the jets of a V/STOL aircraft hovering in ground effect impinge on the ground and flow radially outward in a wall jet from the point of impingement. With multiple jets an upflow is created where these wall jets meet. With two jets of equal size and thrust this upflow rises vertically on the plane of symmetry between the jets and is a relatively thin fan-shaped sheet as depicted in figure 3. A plate or airplane configuration interrupting this upflow will experience a lift force. Yen, in reference 3, developed an expression for this force which can be written as:

$$\frac{\Delta L_A}{T} = K_A \left(\frac{e}{e + h}\right)^{\lambda_A} \frac{y}{\sqrt{(y^2 + (e + h)^2)}} \tag{4}$$

where the constant K_A and the exponent λ_A depend on the configuration geometry and the jet decay and entrainment rates. Methods for estimating both K_A and λ_A will be developed empirically in later sections.

With 3 or more vertical jets an essentially vertical "fountain core" is created at the centroid of the jet pattern where the inward flowing wall jets meet (fig. 4). Also between each pair of jets there is a vertical sheet or "fountain arm" similar to that created in the 2 jet case. Yen's expression for the lift force due to the fountain core can be written as:

$$\frac{\Delta L_C}{T} = K_C \left(\frac{e}{e + h}\right)^{\lambda_C} \cos \theta \tag{5}$$

where the constant K_C and the exponent λ_C depend on the configuration geometry and on the jet decay and entrainment rates and are determined empirically in later sections. The angle θ is defined as half the

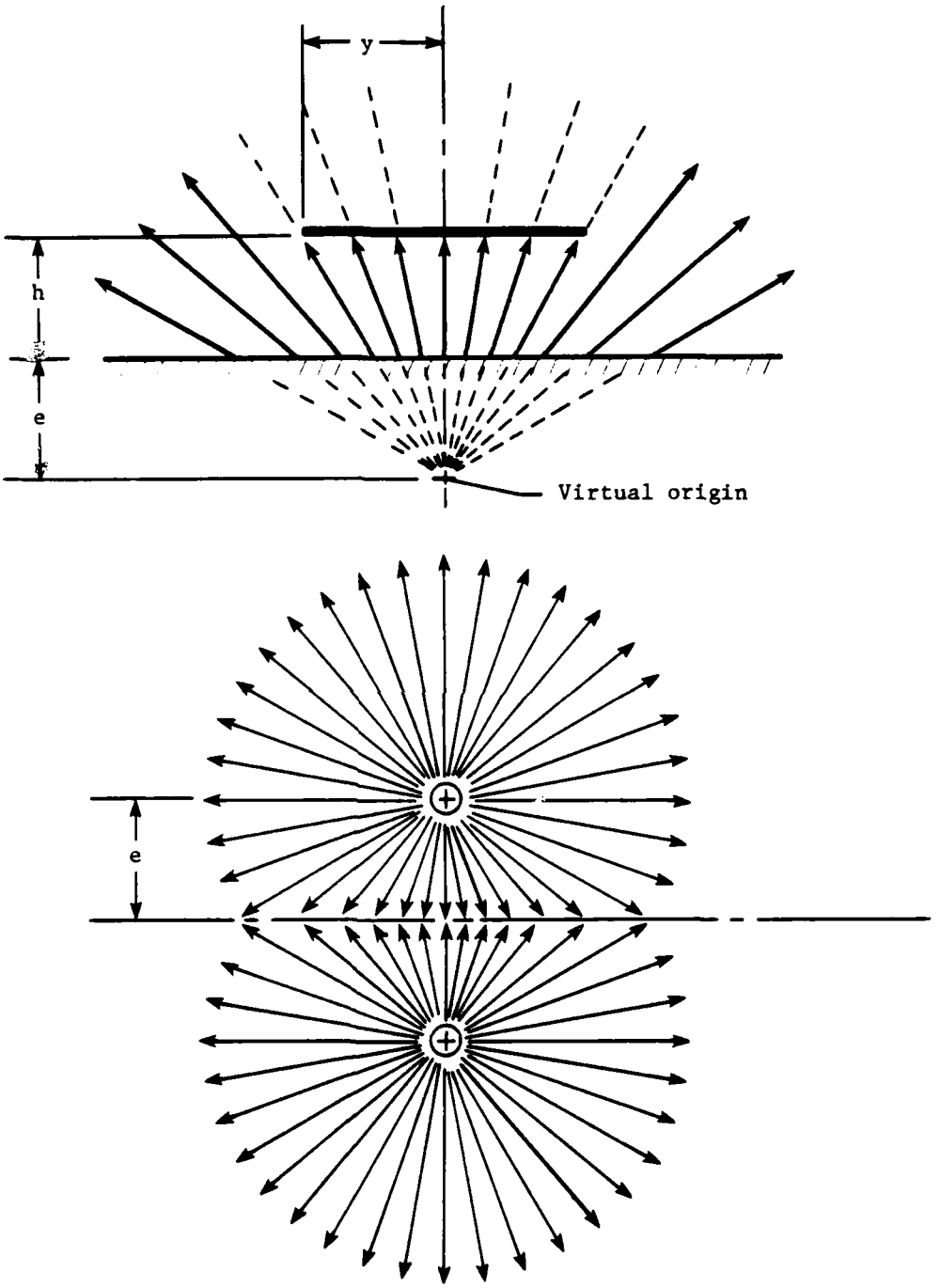

Figure 3.- "Fountain" flow generated by a two jet configuration.

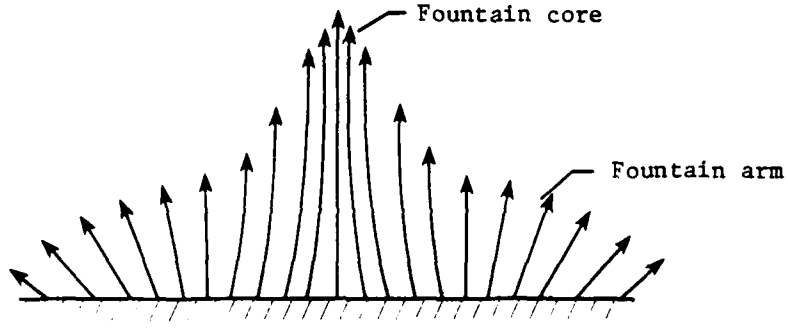

View A-A

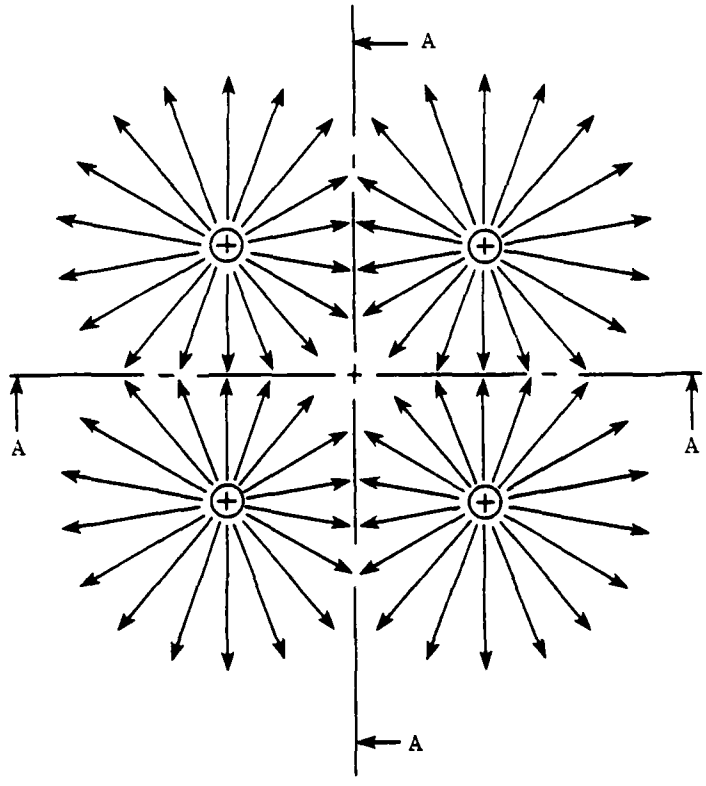

Figure 4.- "Fountain core and arms" generated by a configuration with 3 or more jets.

included angle between adjacent jets (see fig. 1b). Note that for the two jet cases θ equals 90° and the core lift $\frac{\Delta L_C}{T}$ is zero.

For a two jet configuration the fountain lift term, $\frac{\Delta L_F}{T}$, in equation (1) is given by equation (4) above $\left(\frac{\Delta L_F}{T} = \frac{\Delta L_A}{T}\right)$. For three or more jets the contributions of both the core and fountain arms must be included $\left(\frac{\Delta L_F}{T} = \frac{\Delta L_A}{T} + \frac{\Delta L_C}{T}\right)$. The contribution of the fountain arms, $\frac{\Delta L_A}{T}$, can be estimated by a modification of equation (4) which will be developed in later sections.

Unfortunately it is not possible to determine K_A, K_C, λ_A and λ_C directly from the experimental data because, as pointed out by Yen, the above expressions represent only the upward momentum and do not include the additional induced suckdown. As pointed out by Karemaa (ref. 4), the fountain flows that produce the upward momentum also act to increase the suckdown above that which would be expected from an equivalent single jet. The net lift gain or loss measured experimentally is the difference between the induced suckdown and the fountain lift experienced by the plate or airplane configuration. A method for estimating the suckdown must also be developed so that the difference between the estimated suckdown and fountain lift can be compared with the experimental data.

Multiple Jet Suckdown and Fountain Lift (2 Jet Case):

Estimating the multi-jet suckdown requires knowledge of the areas and strengths of the entrainment surfaces. For the single jet case the entrainment surface is the area projection of the plate or aircraft configuration planform on the ground surface and is defined by Wyatt's "mean angular diameter" $\bar{D}$ (fig. 2).

For the multiple jet case, Kotansky, et al. (ref. 5) have pointed out that additional entrainment surfaces exist as depicted in figure 5. For 2 jets the flow in the wall jets meet on a line between the jets and is projected upward in the fountain. Both sides of this upward flowing sheet of air can entrain air. Also that part of the flow that impinges on the plate of lower surface of the aircraft is again redirected and flows outward along the lower surface. This is also an entraining

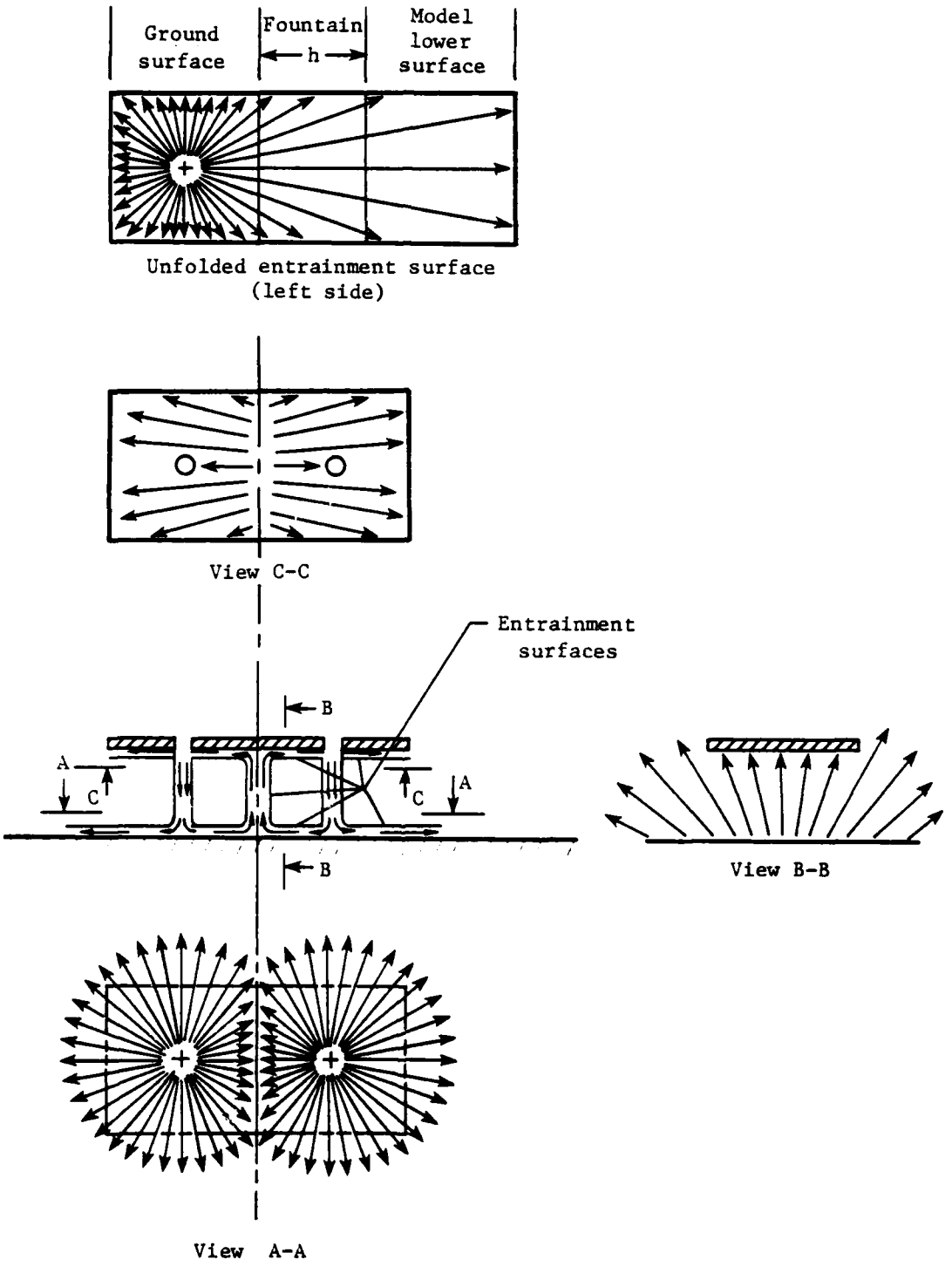

Figure 5.- Assumed fountain flow on model lower surface, arrows indicate flow direction, not vector magnitude.

surface and is equal in area to that on the ground. It is not as effective in entraining air and lowering the pressure between the plate and the ground as the flow on the ground surface, however, because of the energy loss that has occurred due to jet spreading and decay.

The blockage created by the fountain itself also tends to increase the suckdown. A single jet configuration entrains air from all sides. With two jets part of the path by which air flows in to satisfy the entrainment action of the wall jet on the ground is blocked by the fountain. This blockage of the inflow path acts to increase the suction pressures and the ground induced suckdown.

The first attempt to quantify the increased suckdown with two jet configurations was to unfold the entrainment surface as shown at the top of figure 5 and calculate a new $\bar{D}$ for each half of the configuration. The reduced entrainment effectiveness of the fountain and of the flow on the bottom of the plate was approximated by placing the origin for the calculation of $\bar{D}$ at the impingement point on the ground part of the unfolded surface. These values of $\bar{D}$ (which increase with height), were used in Wyatt's expression to calculate the multijet suckdown, $\left(\frac{\Delta L_S}{T}\right)_m$. The resulting values of multijet suckdown were used in extracting the fountain lift from the experimental data using equation (1):

$$\left(\frac{\Delta L_A}{T}\right)_{exp} = \left(\frac{\Delta L}{T}\right)_{exp} - \frac{\Delta L_\infty}{T} - \left(\frac{\Delta L_S}{T}\right)_m$$

When the data thus obtained are plotted, as shown by the 3 examples presented in figure 6, a value for the exponent λ_A of about 2, which is reasonable, but a little higher than Yen (ref. 3) expected, is obtained for the middle range of heights. At very low heights (high values of $\left(\frac{e}{e+h}\right)$), however, the data indicate a very rapid increase in $\frac{\Delta L_A}{T}$. Either there is another mechanism producing a rapid increase in the fountain force or the download is being over-estimated at these heights.

The most likely explanation is that the download is over-estimated at the lower heights by the above approach. Karemaa, et. al. in ref. 4

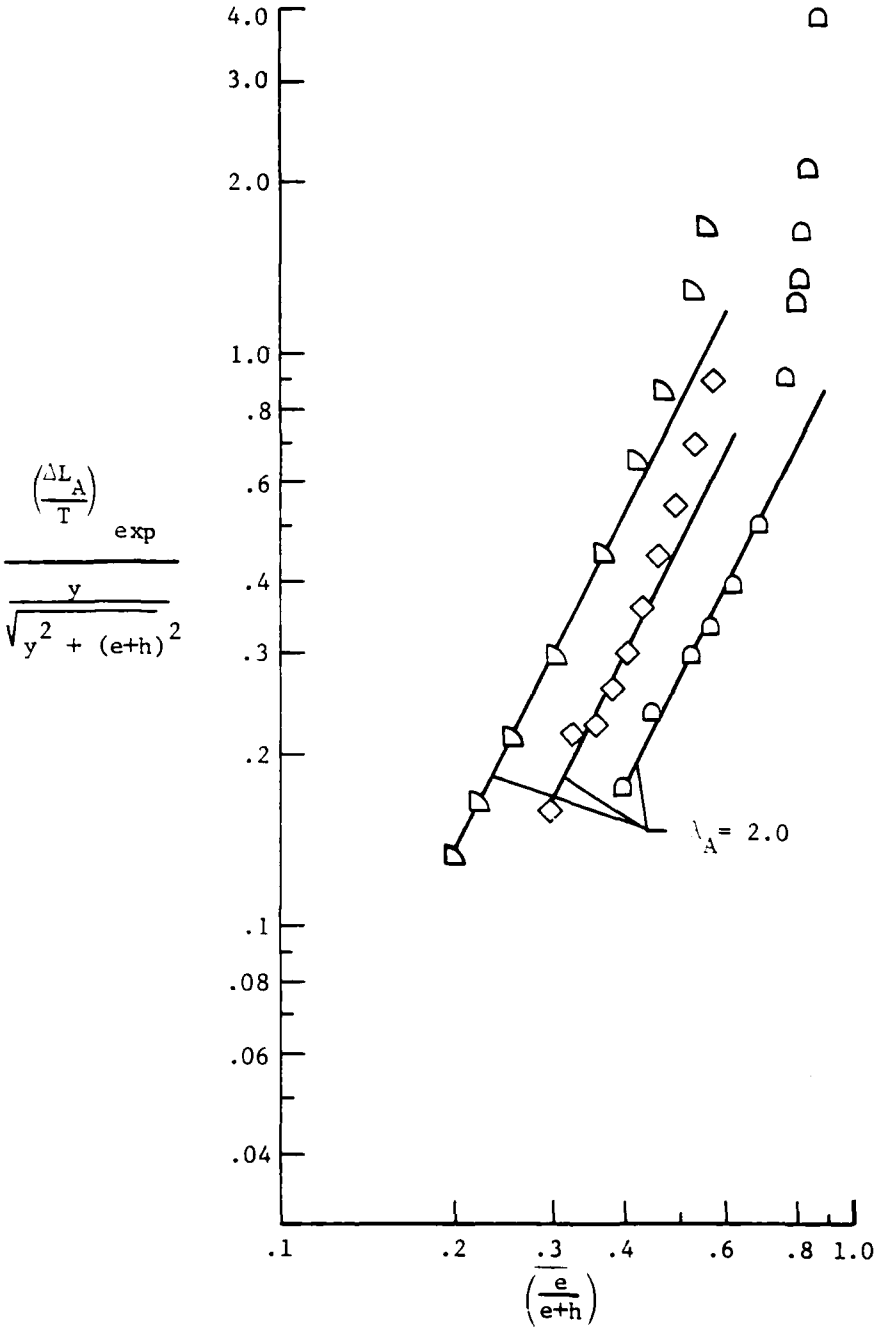

Figure 6.- Preliminary evaluation of λ_A for three sample sets of data.

have shown that the fountain loses strength as the ground is approached because it is being entrained by the wall jet on the ground surface thus partially satisfying the wall jets entrainment appetite and reducing the suction pressures being created.

An iterative approach was used in arriving at the expressions for the Basic Method as derived in this study. First the values of λ_A and K_A for the middle range of heights (as in examples shown in figure 6) were derived from the data to calculate interim values of $\frac{\Delta L_A}{T}$. These values of fountain lift were used to extract the "experimental" multijet download from the data: $\left(\frac{\Delta L_S}{T}\right)_m = \left(\frac{\Delta L}{T}\right)_{exp} - \frac{\Delta L_\infty}{T} - \frac{\Delta L_A}{T}$ and to calculate the ratio of the multijet download to that for an equivalent single jet, $K_S = \frac{\left(\frac{\Delta L_S}{T}\right)_m}{\left(\frac{\Delta L_S}{T}\right)_S}$ from the data. The resulting values of K_S are presented in figure 7. Although there is considerable scatter, the data for most configurations, approach a variation given by: $K_S = 4.5 \left[\frac{h/d_e}{\frac{\bar{D}}{d_e} - 1.0}\right]^{1/4}$ at the higher heights. The reduction in K_S at the lower heights was found to be a function of the configuration geometry ($\frac{\bar{D}}{d_e}$, width/length ratio W/L, and the ratio of actual to circumscribing rectangle area, S/WL).

$$K_S = 4.5 \left[\frac{h/d_e}{\frac{\bar{D}}{d_e} - 1.0}\right]^{1/4} \left[1 - \left(\frac{h/d_e}{.08 \frac{\bar{D}}{d_e} \frac{W}{L}}\right)^{\lambda_S}\right] \quad (6)$$

where

$$\lambda_S = -1.7 \left[\frac{W}{L}\left(\frac{S}{WL}\right)^{.36}\right]^{1.38}$$

The fountain lift was finally derived from the data using the expression for multijet download derived above. The resulting data, presented in figure 8, indicates that a value of the exponent of $\lambda_A = 2.0$ provides a reasonable fit with most of the data. The constant K_A was found to be a function of the ratio of configuration width to the jet spacing $\frac{Y}{e}$, and

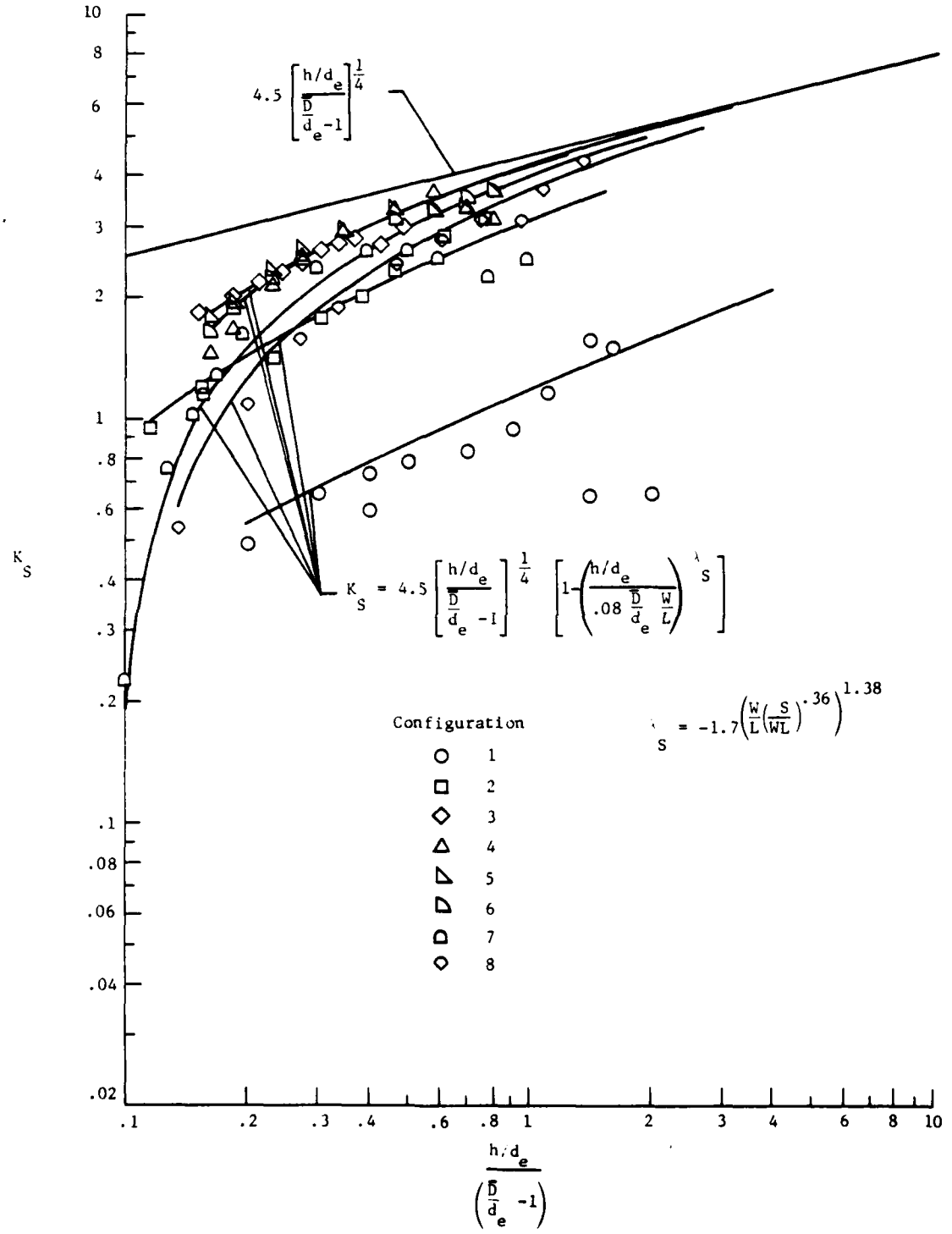

Figure 7.- Variation of multiple jet suckdown fact or K_S with height and configuration.

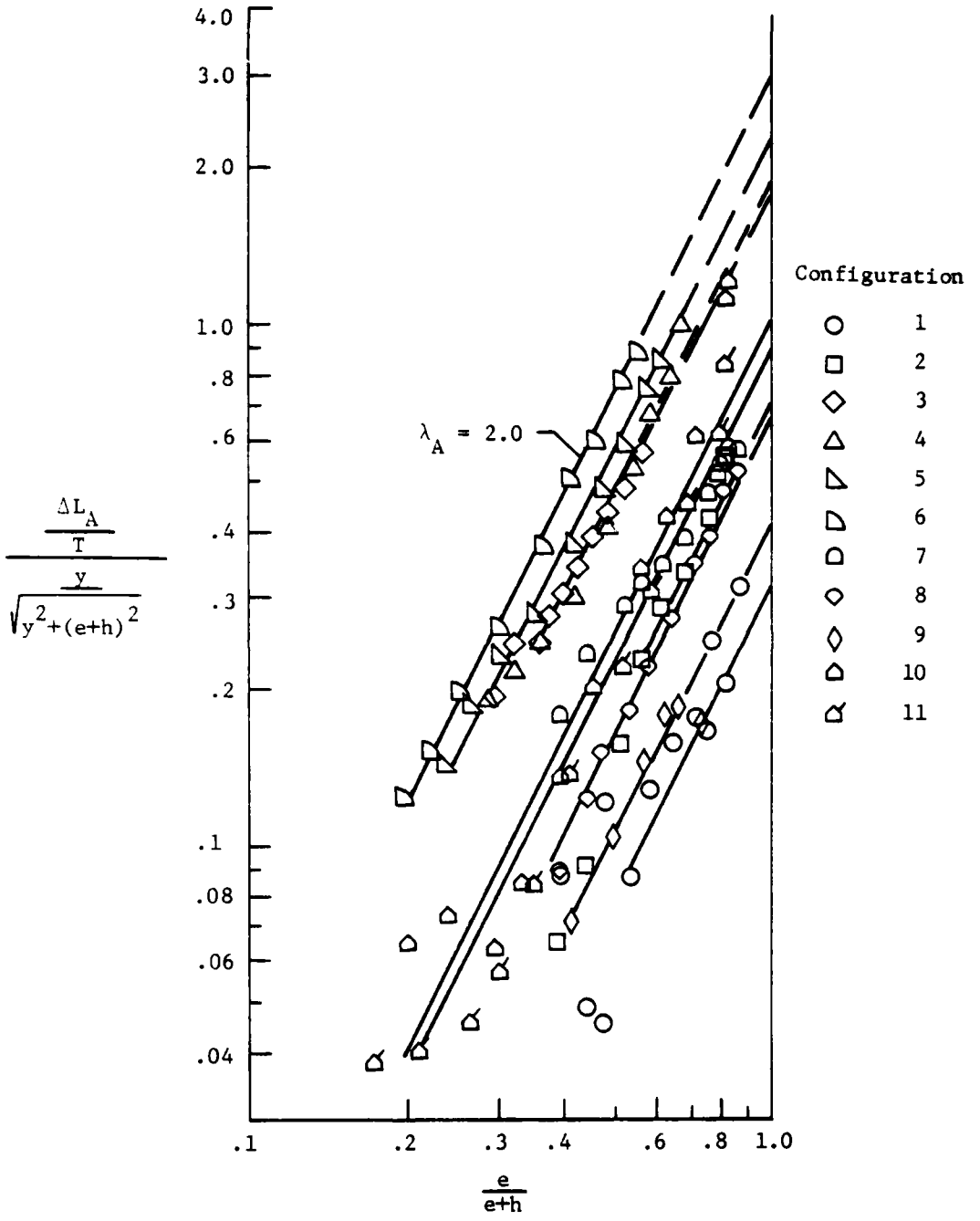

Figure 8.- Fountain lift derived from Experimental data, 2 jet configurations.

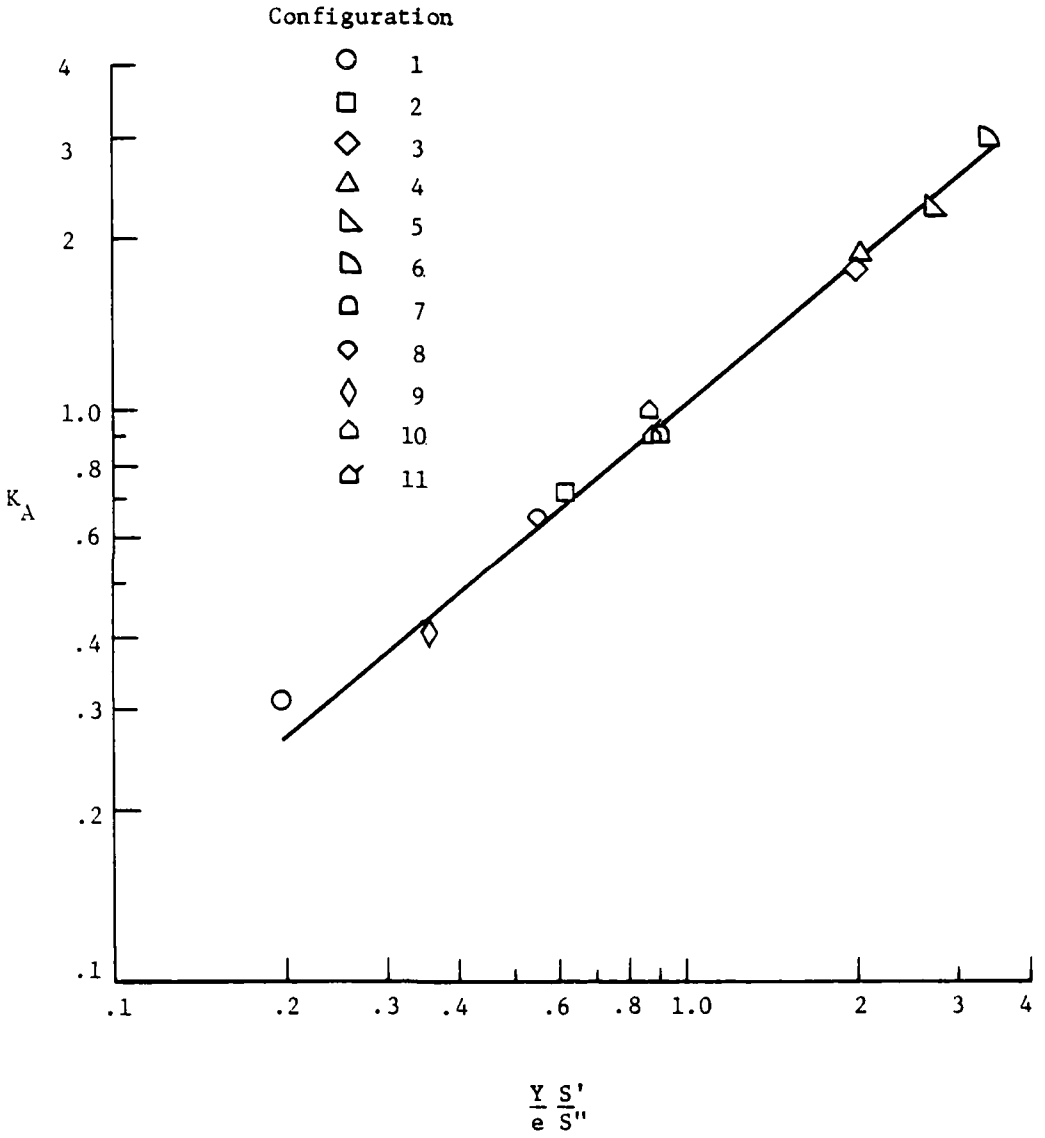

Figure 9.- Correlation of K_A with configuration geometry.

of the ratio of actual to potential area between the jets $\frac{S'}{S''}$ (see fig. 1a) as shown in figure 9 and is given by:

$$K_A = \left(\frac{Y}{e}\frac{S'}{S''}\right)^{.835}$$

The expression for the fountain lift contribution for 2 jet configurations in the Basic Method can then be written as:

$$\frac{\Delta L_A}{T} = \left(\frac{Y}{e}\frac{S'}{S''}\right)^{.835}\left(\frac{e}{e+h}\right)^{2.0}\frac{y}{\sqrt{y^2+(e+h)^2}} \qquad (7)$$

The net induced lift calculated by the Basic Method for 2 jet configurations (equations 1, 2, 3, 6 and 7) is compared with experimental data for 12 configurations in figure 19. (Configuration 12 is the only configuration not used in the development of the method.) In general the agreement is good. However the h' method, to be presented later, shows better agreement for the configurations with the smaller jet spacings, for which it was developed.

Fountain Lift (3 or More Jets):

With 3 or more jets a "fountain core" is generated at the centroid of the jet pattern and "fountain arms" radiate from the core between each pair of jets (fig. 4). The fountain lift $\frac{\Delta L_F}{T}$ for these configurations must account for the contributions of both the core and the arms and can be expressed as:

$$\frac{\Delta L_F}{T} = \frac{\Delta L_A}{T} + \frac{\Delta L_C}{T}$$

Before developing expressions for the core and arm contributions to the fountain lift it is necessary to determine the suckdown $\left(\frac{\Delta L_S}{T}\right)_m$ increment with 3 or more jets. There are compensating factors at work. For a vanishingly small core the induced suckdown term would be expected to be increased, relative to that for the 2 jet case, because of the increased entrainment area provided by the multiple fountain arms. (The 2 jet case can be thought of as having 2 equal and opposite arms.)

However, the core has been found (ref. 4) to take up a significant amount of space within the jet pattern and therefore reduces the entrainment area. No significant difference between the suckdown increment for configurations with 3 or more jets and that for 2 jet configurations could be discerned from the data. Therefore the expression developed for estimating the suckdown increment for 2 jet configurations has been applied to all multi-jet configurations.

In the initial approach to developing the Basic Method for 3 or more jets it was assumed that all the jet flow inboard of the line connecting two adjacent jets (figure 1b) goes into making up the fountain core and all the air outboard goes into the arms. It was also assumed that the arms between each adjacent pair of jets had the characteristics of the fountain that would be developed between these two jets as a simple 2 jet configuration, and that the lift force would be half of that calculated for this 2 jet pair. The total contribution of the several arms would be given by summing the lift increment from the individual pairs and would therefore be given by:

$$\frac{\Delta L_A}{T} = \frac{\frac{\Delta L_{A,1}}{2} + \frac{\Delta L_{A,2}}{2} + \ldots + \frac{\Delta L_{A,N}}{2}}{T}$$

where $\Delta L_{A,x}$ for each jet pair is defined in equation 9 below.

When these expressions for the arm contribution were used in studying the core contribution (presented below) it appeared that the arm contribution was over predicted. In effect the core effects are felt outside the line joining the jet centers (fig. 1b) and the fountain arms are not as strong as the initial assumptions would predict. In the final development the expression for the contribution of the fountain arms is given by:

$$\frac{\Delta L_A}{T} = \frac{\frac{1}{2}\left(\Delta L_{A,1} + \Delta L_{A,2} \ldots \Delta L_{A,N}\right)}{T} \left(0.7 \sqrt{\frac{h/d_e}{\frac{\bar{D}}{d_e} - 1.0}}\right) \qquad (8)$$

where

$$L_{A,x} = 2\,\frac{T}{N}\left(\frac{Y_x}{e_x}\,\frac{S'_x}{S''_x}\right)^{.835}\left(\frac{e_x}{e_x + h}\right)^2 \frac{y_x}{\sqrt{y_x^2 + (e_x + h)^2}} \tag{9}$$

The core contribution to the net induced force was extracted from the data by using equations 8 and 9 to calculate the fountain arm contribution and subtracting it and the out-of-ground-effect and multi-jet lift losses from the experimental data;

$$\left(\frac{\Delta L_C}{T}\right)_{exp} = \left(\frac{\Delta L}{T}\right)_{exp} - \frac{\Delta L_\infty}{T} - \left(\frac{\Delta L_S}{T}\right)_m - \frac{\Delta L_A}{T}$$

Samples of the data thus obtained are shown in figure 10. Because, for most configurations, the distance between jets in the pairs making up a multijet arrangement are not equal the data are presented as a function of the average spacing to height parameter, $\left(\frac{e}{e + h}\right)_{ave}$.

In order to accommodate configurations with non-uniform jet spacing it was assumed that the core contribution could be expressed as:

$$\frac{\Delta L_C}{T} = \frac{\Delta L_{C,1} + \Delta L_{C,2} + \ldots + \Delta L_{C,N}}{T} \tag{10}$$

where

$$\Delta L_{C,x} = TK_c \left(\frac{e_x}{e_x + h}\right)^{\lambda_c} \cos\theta_x \tag{11}$$

and the constant K_C and the exponent λ_C are to be determined from the data such as shown in figure 10. Single values for K_C and for λ_C for each configuration could not be determined from the data because of the nonlinearities seen in figure 10. However, the data can be represented by two slopes and two constants. It was determined that a value of $\lambda_C = 2.5$ fit most of the configurations at low heights (higher values of $\left(\frac{e}{e + h}\right)_{ave}$). Above a transition height, h_C, some configurations showed an increase in slope and others a decrease. Unfortunately it was difficult to determine accurate values of the slope (exponent λ_C) because most of the configurations were not carried to high enough heights. The exponent λ_C appears to be proportional to the number of jets, N,

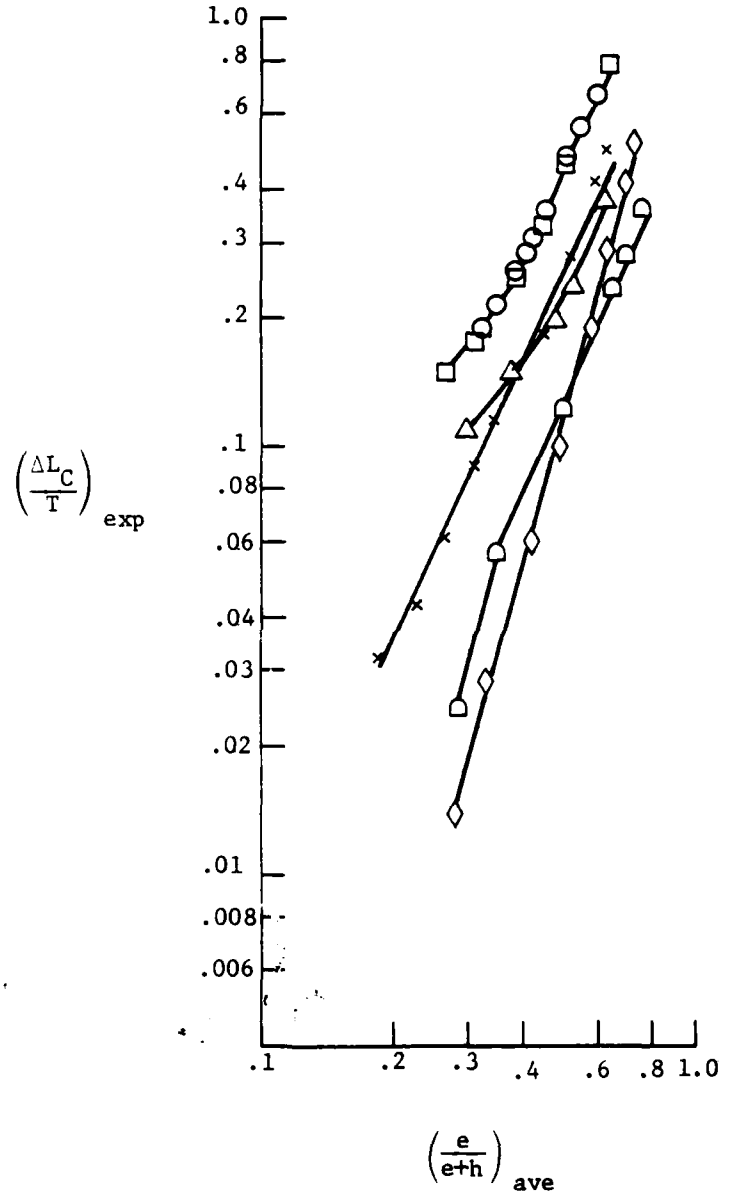

Figure 10.- Fountain core contribution for several sample sets of data.

the length/width ratio of the jet pattern, E, and to be inversely proportional to the relative size of the jet pattern $\frac{\sqrt{S_C}}{d_e}$, (fig. 11). For the Basic Method the exponent λ_C is defined as:

$$\left.\begin{array}{ll} @\ h < h_C & \lambda_C = 2.5 \\ @\ h > h_C & \lambda_C = \dfrac{N\ E}{\dfrac{\sqrt{S_C}}{d_e}} \end{array}\right\} \qquad (12)$$

The corresponding values for the constants were found to be a function of the size and shape of the planform as well as of the jet pattern parameters (fig. 11):

$$\left.\begin{array}{ll} @\ h < h_C & K_C = .12N \dfrac{\left(\dfrac{\bar{J}}{d_e}\right)\left(\dfrac{W}{L}\right)(E)^{.25}}{\dfrac{\sqrt{S_C}}{d_e}} \\ @\ h > h_C & K_C = .31N\left(\dfrac{\bar{D}}{d_e}\right)^{.35}\left(\dfrac{W}{L}\right)^{.65}\left(\dfrac{S'_C}{S_C}\right)^{.5}\left(\dfrac{E}{\dfrac{\sqrt{S_C}}{d_e}}\right)^{1.8} \end{array}\right\} \qquad (13)$$

Note that it is not necessary to calculate the value of h_C directly. The height, h_C, is the point at which the curves intersect:

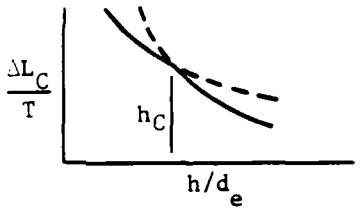

The net induced lift for configurations with 3 or more jets as calculated by the Basic Method (equations 1 to 3, 6, and 8 to 13) are compared with experimental data for the 11 configurations on which the method is based in figure 20.

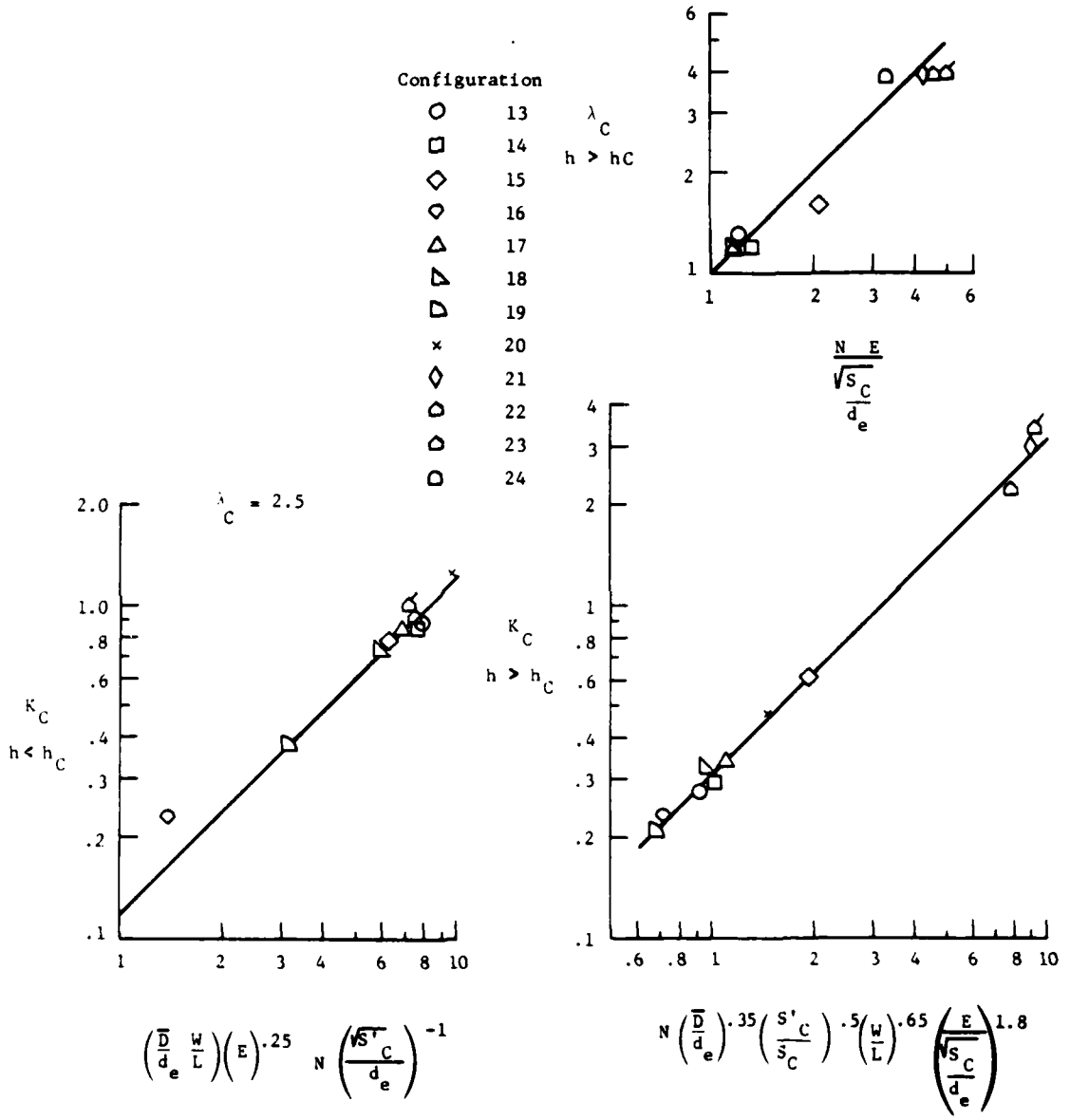

Figure 11.- Correlation of K_C and λ_C with configuration geometry.

h' Method

The Basic Method appears to work well for the configurations with widely spaced jets for which it was developed. However, configurations with closely spaced jets exhibit an abrupt increase in fountain lift at low heights that is not predicted by the Basic Method (fig. 12). Apparently at low heights the pressure between the jets is greater than that predicted by the Basic Method and increases rapidly as the jet spacing is reduced. However the ability to retain this pressure breakdown as the height increases, probably as a result of the jets beginning to merge before reaching the ground. Under these conditions the assumptions implicit in the Basic Method no longer apply and another approach must be taken for closely spaced jets.

The fountain lift increment extracted from the data for configurations with closely spaced jets was found to exhibit characteristics that can be illustrated by the two examples configurations presented in figure 12. The data for configuration 26 (fig. 12) is representative of most of the data. The data at both low and high heights can be represented by an equation of the form:

$$\frac{\Delta L_F}{T} = K' \left(\frac{h}{d_e}\right)^{\lambda'} \tag{14}$$

However, the two curves did not intersect but were joined by a straight line transition that was tangent to the curve for the data at low heights and projected to $\frac{\Delta L}{T} = 0$ at a height defined as h'. The data for configuration 25 (fig. 12) does not extend to low enough heights to show the lower curve; only the transition tangent is present in the available data.

The critical height, h', was found to depend on the jet spacing and nozzle pressure ratio. For configurations with 3 or more jets, (fig. 13);

$$\frac{h'}{d_e} = 2 \left(\frac{e}{d}\right)^{.5}_{ave} \left(\frac{P_n}{p}\right)^{.5} \tag{16}$$

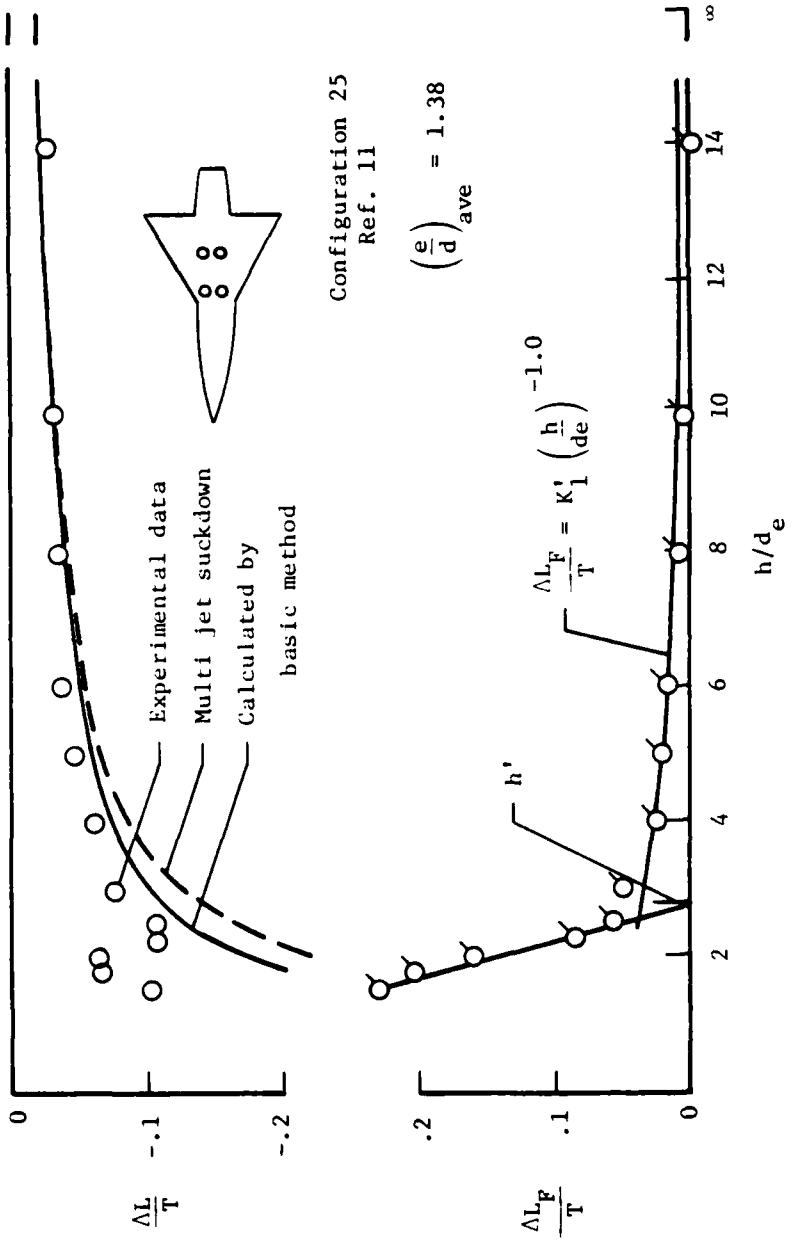

Figure 12.- Typical characteristics of configurations with close jet spacing illustration of basis of h' method.

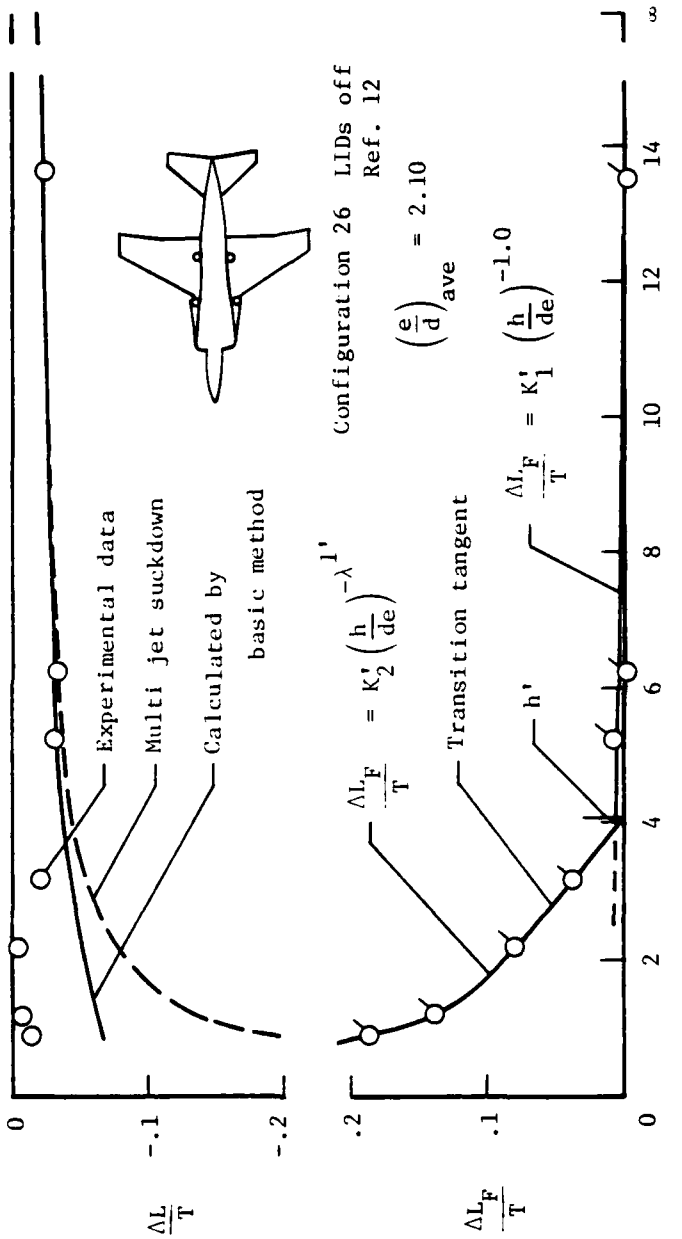

Figure 12.- Concluded.

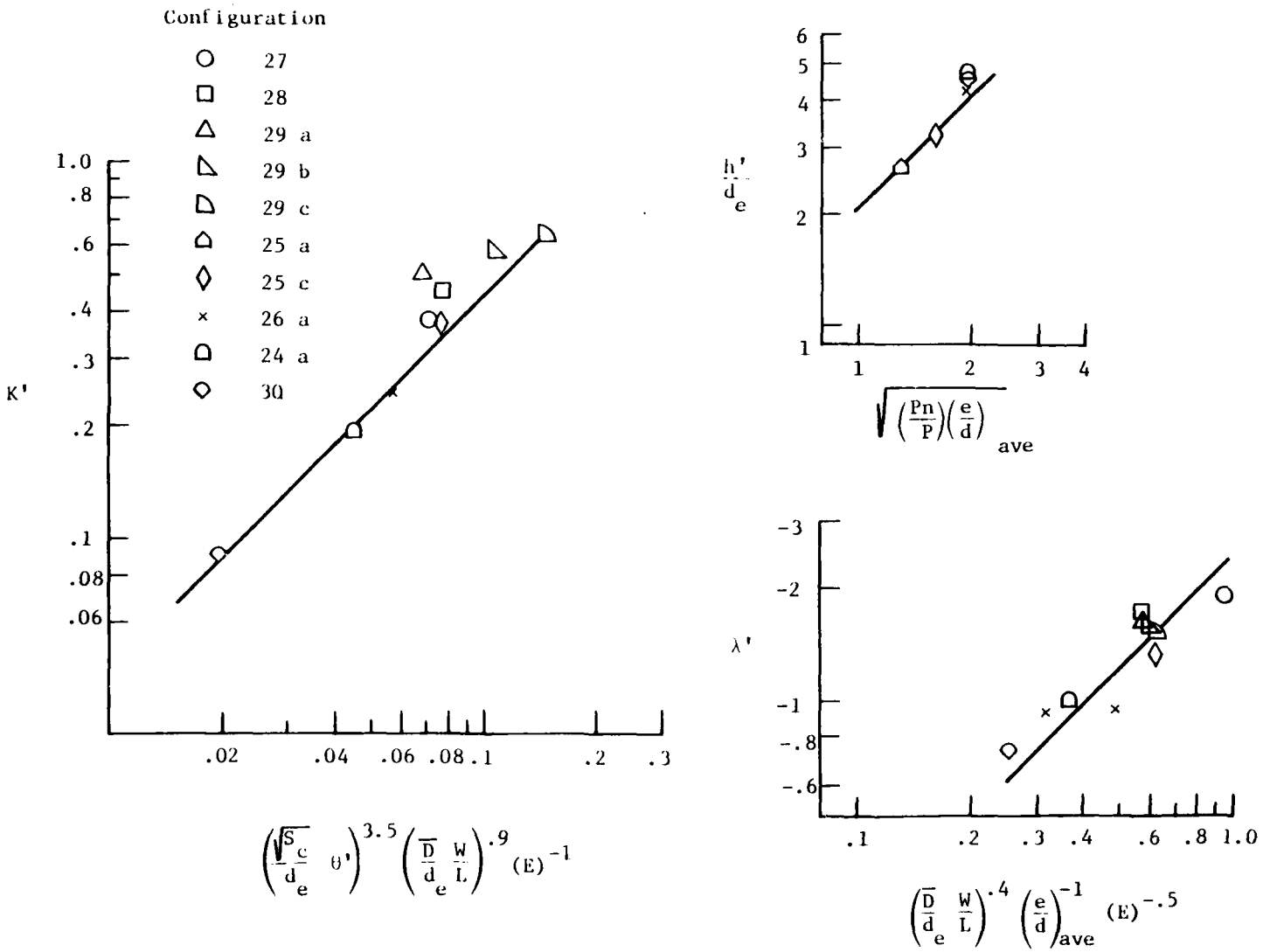

Figure 13.- Correlation of h', K' and λ' with configuration geometry for configurations with 3 or more jets. h<h'

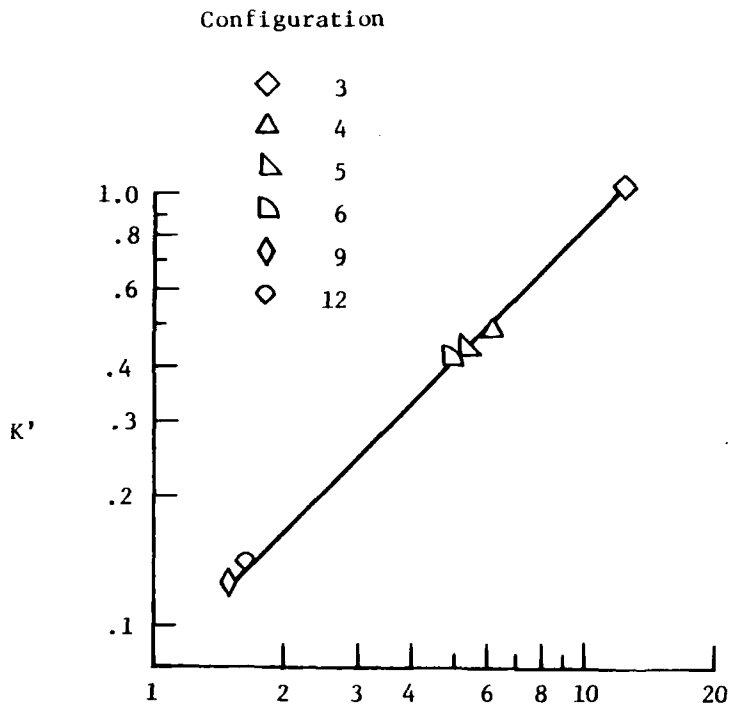

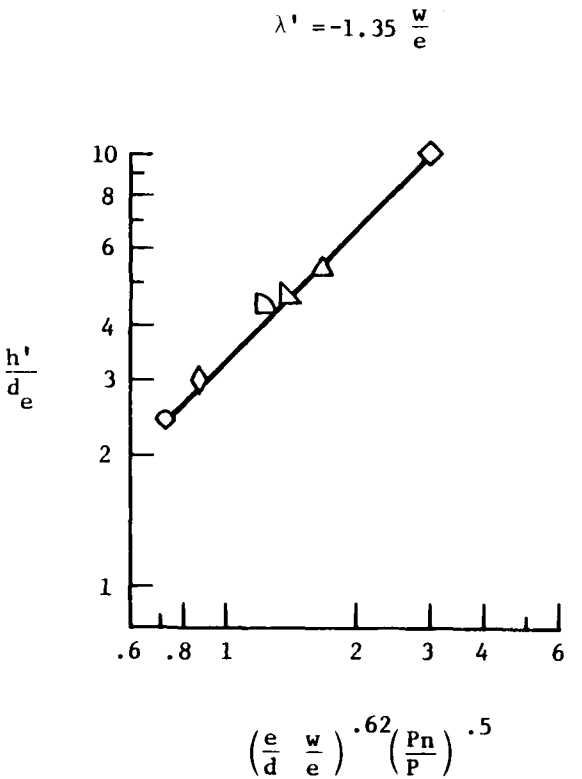

Figure 14.- Correlation of h' and K' with configuration geometry for 2 jet configurations. h<h'

and for 2 jet configurations, (fig. 14)

$$\frac{h'}{d_e} = 3.6 \left(\frac{e}{d}\frac{w}{e}\right)^{.62} \left(\frac{P_n}{p}\right)^{.5} \tag{17}$$

Note that the factor $\frac{w}{e}$ is inserted to accommodate cases (such as conf. 10 and 12) where the jets are external to the planform. (w is equal to half the width of the planform). For configurations in which the jets are contained within the planform, w is taken as equal to e; $\frac{w}{e} = 1.0$.

The fountain lift at intermediate heights (above h') was found to be a function of only the planform size and shape (fuselage size and shape in the case of high wing configurations (such as conf. 26) as will be discussed later) and to be inversely proportional to the height:

$$@\ h > h' \qquad \frac{\Delta L_F}{T} = \frac{.033 \ \frac{\bar{D}}{d_e}\frac{W}{L}}{(h/d_e)} \tag{15}$$

This expression was found to hold for 2 jet configurations as well as for configurations with 3 or more jets.

For heights less than h' it was found that all 2 jet configurations except those in which the jets were external to the planform (conf. 10 and 12) had the same rate of change with height; $\lambda' = -1.35$. To include those configurations with the jets external to the planform this was modified to:

$$@\ h < h' \qquad \lambda' = -1.35 \frac{w}{e} \text{ for 2 jet configurations} \tag{18}$$

For configurations with 3 or more jets the exponent was found to be inversely proportional to the size of the jet pattern as shown in figure 13:

$$@\ h < h' \qquad \lambda' = -2.4 \frac{\left(\frac{\bar{D}}{d_e}\frac{W}{L}\right)^{.4}}{E^{.5}\left(\frac{e}{d}\right)_{ave}} \tag{19}$$

for configurations with 3 or more jets.

The level of the fountain lift at heights below the critical height is determined by the constant K' which was derived as shown in figures 13 and 14:

$$@\ h < h' \qquad K' = .084 \left(\frac{e}{d}\right)^{.39} \left(\frac{y}{d}\frac{S'}{S''}\right)^{1.1} \quad \text{for 2 jet configurations} \qquad (20)$$

and

$$K' = 4.4 \left(\frac{\sqrt{S_C}}{d_e}\theta'\right)^{3.0} \left(\frac{\bar{D}}{d_e}\ \frac{W}{L}\right)^{.9} (E)^{-1.0} \quad \text{for conf. with 3 or more jets} \qquad (21)$$

and

$$\theta' = \frac{Nd}{2(e_1 + e_2 + \ldots e_N)}$$

Estimates using the h' Method (equations 14 to 21) are compared with experiment for 2 jet configurations in figure 19. Agreement is good for those configurations with closely spaced jets, $\frac{e}{d} < 3.0$ (conf. 3 to 6, 9 and 12), for which it was developed. It is unfortunate that the data for most of these configurations does not extend to high enough heights to determine if the predicted break in the variation of induced lift with height is really there. The method over predicts the induced lift for configurations with wider jet spacing (conf. 10, $\frac{e}{d} = 3.7$, conf. 11, $\frac{e}{d} = 4.4$ and conf. 1 and 2, $\frac{e}{d} = 6.4$).

Comparisons of estimates using the h' Method with experimental data for configurations with 3 or more jets are presented in figure 21 and in figures 20a and b. Agreement is good for configurations with average spacing to diameter ratios of 3.0 or less.

Other Configuration Variables

Wing Height:

The data of reference 11 show that the out-of-ground-effect lift loss is reduced if the nozzle is extended below the surface. The out-of-ground-effect lift loss for a high wing configuration would therefore be lower than that for a similar low wing configuration. The data of reference 11 indicate that the reduction is proportional to the square root of the ratio of distance the nozzle projects (or wing height) to the nozzle diameter (Fig. 15a) and the wing contribution would be expected to decrease similarly as the wing height is increased. In the present methods the effects of wing height on the out-of-ground-effect lift loss is calculated by:

$$\left(\frac{\Delta L_\infty}{T}\right)_{hw} = \left(\frac{\Delta L_\infty}{T}\right)_b + \left[\left(\frac{\Delta L_\infty}{T}\right)_{wb} - \left(\frac{\Delta L_\infty}{T}\right)_b\right]\left[1 - .4\sqrt{\frac{\Delta h}{d_e}}\right] \tag{22}$$

where the lift loss for the body $\left(\frac{\Delta L_\infty}{T}\right)_b$ and for the wing-body $\left(\frac{\Delta L_\infty}{T}\right)_{wb}$ are calculated by equation (2).

Reference 2 showed that the effect of wing height on the in-ground-effect induced suckdown for single jet configurations could be calculated by:

$$\left(\frac{\Delta L_S}{T}\right)_{s,hw} = \left(\frac{\Delta L_S}{T}\right)_{s,b,h} + \left[\left(\frac{\Delta L_S}{T}\right)_{s,wb,h+\Delta h} - \left(\frac{\Delta L_S}{T}\right)_{s,b,h+\Delta h}\right]$$

where the subscript, s indicates single jet, hw indicates high wing, b indicates body, wb indicates wing-body (calculated as a low wing configuration at height $(h + \Delta h)$), h indicates height above the ground and Δh indicates wing height. The induced suckdown is calculated for each element by equation (3) using $K_S = 1.0$ for single jet.

Simply inserting the calculated induced suckdown increments for multijet configurations in the above expression and in the corresponding expression for fountain lift did not prove satisfactory for high wing multijet configurations. Apparently when the wing is not co-planer with the bottom of the body it does not "see" the same fountain flow as a low wing configuration and both the induced suckdown and the fountain lift contributions are changed. As indicated by the schematic in Figure 15b the fountain flow that impinges on the lower surface of the body is turned outward and does not reach the wing. Under these conditions only the body term at height, h, needs to be treated as a multijet configuration and the induced suckdown for high wing multijet configurations can be expressed as:

$$\left(\frac{\Delta L_S}{T}\right)_{m,hw} = \left(\frac{\Delta L_S}{T}\right)_{m,b,h} + \left[\left(\frac{\Delta L_S}{T}\right)_{s,wb,h+\Delta h} - \left(\frac{\Delta L_S}{T}\right)_{s,b,h+\Delta h}\right] \tag{23}$$

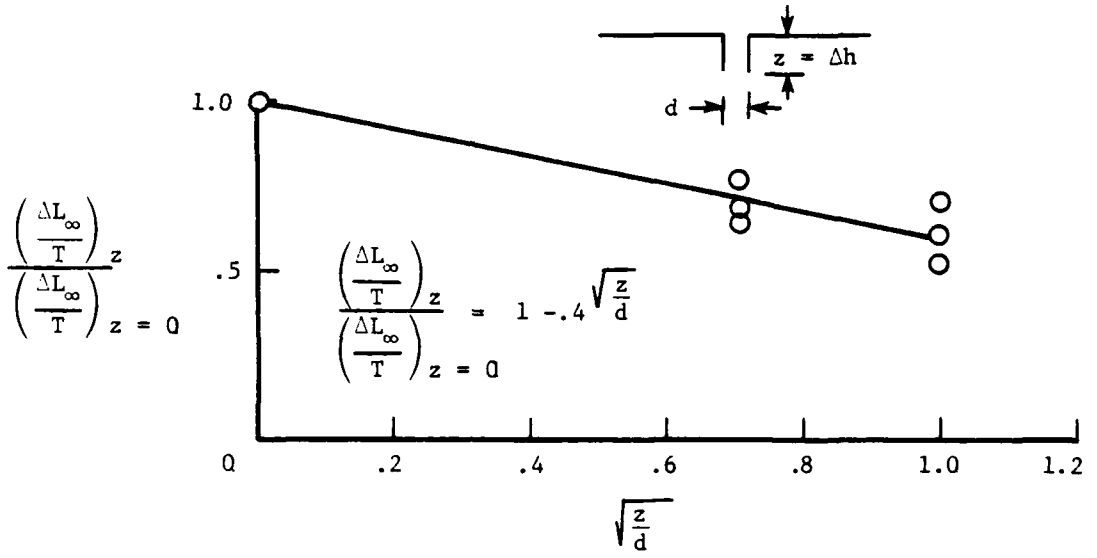

(a) Out of ground effect.

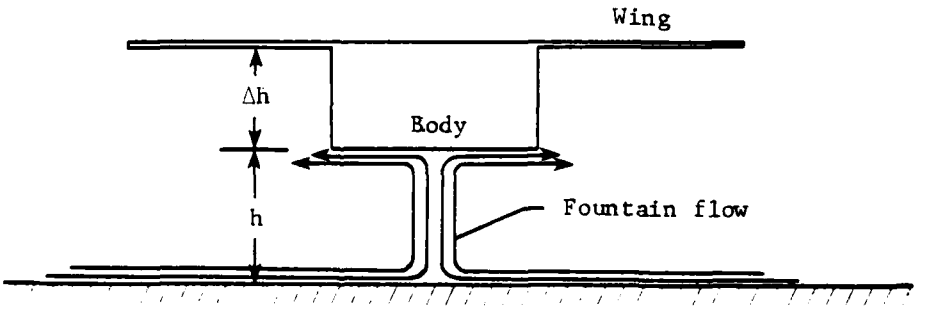

(b) Schematic of fountain flow with high wing configurations.

Figure 15.- Effects of wing height.

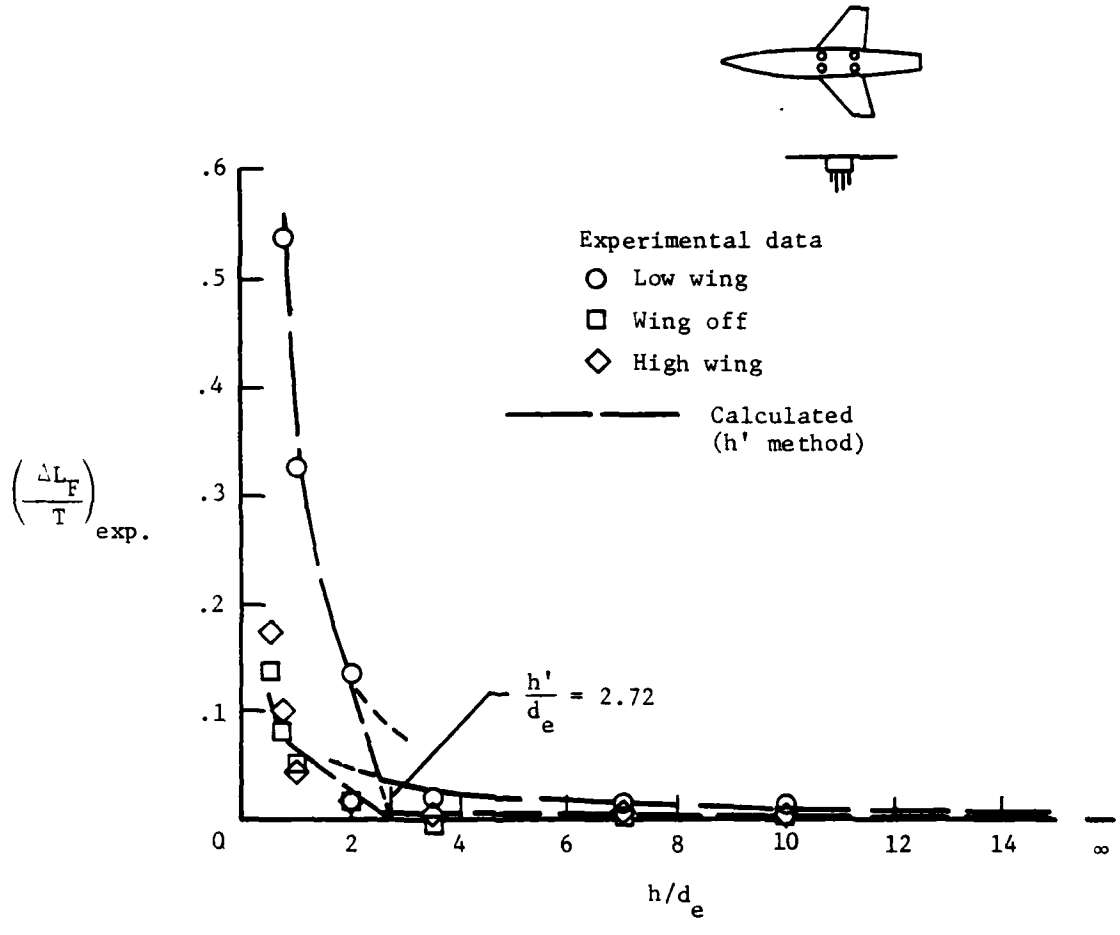

Figure 16.- Effect of wing height on fountain lift; configuration 31, ref 14.

When the above expression is used in extracting the fountain lift increment from the data for configuration 31 (fig. 16) it is seen that the fountain lift increment for the high wing configuration is essentially the same as that for the fuselage alone and very much smaller than that for the low wing configuration. The fountain lift term for the high wing configuration is therefore simply that calculated for the body alone:

$$\left(\frac{\Delta L_F}{T}\right)_{hw} = \left(\frac{\Delta L_F}{T}\right)_b \tag{24}$$

The above expression appears satisfactory for the configurations used in the present study when there is a clean break between the body lower surface and the wing; conf. 26 (fig. 21 f & g), conf. 27 (fig. 21 h, i & j) and conf. 31 (fig. 22). The above approach would not be expected to work for configurations with a rounded body lower surface coupled with a small wing height or for some of the blended wing-body configurations being developed. For these configurations it is suggested that the "equivalent height" approach suggested by Albang, Ref. 10, might be considered. However, this concept has not been evaluated in the present study.

Body Contour:

Most of the configurations used in developing both the Basic Method and the h' Method have been flat plate models. If the lower surface of the configuration is contoured the fountain lift will be reduced because all the fountain flow will not have been stopped and turned to the horizontal. Some of the flow will still have an upward component of momentum as indicated in the sketch at the top of figure 17. It is well known from Coanda turning studies that a thin sheet of air will turn through a greater angle than a thick sheet for the same radius. Therefore it would be expected that the relatively thin fan shaped fountain flow from a 2 jet configuration which is aligned with the body axis would follow the contour of the body more readily and the fountain lift will be reduced more than the relatively thicker core-and-arm fountain or a 2 jet fountain crosswise to the configuration.

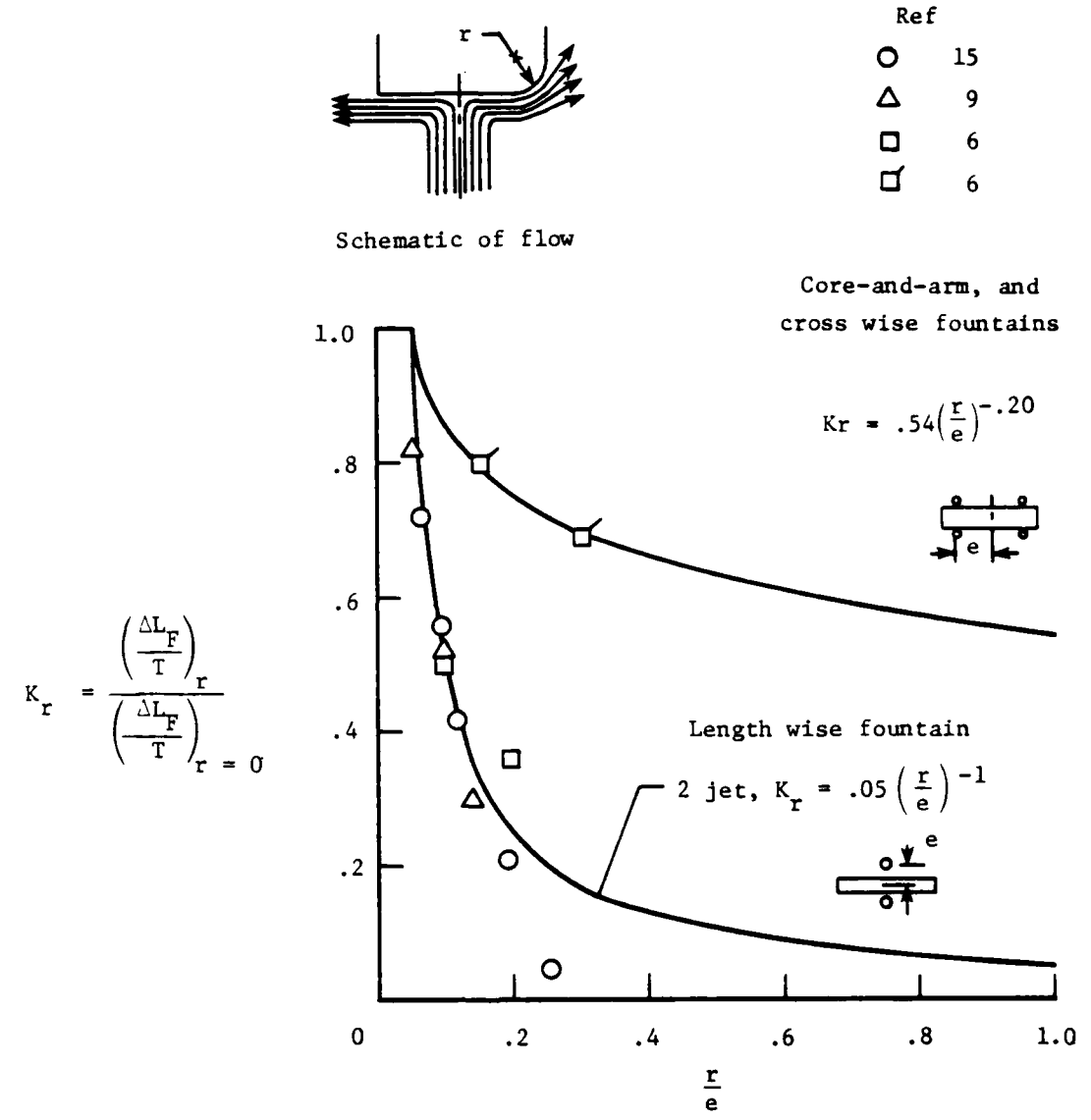

$$K_r = \frac{\left(\frac{\Delta L_F}{T}\right)_r}{\left(\frac{\Delta L_F}{T}\right)_{r=0}}$$

Figure 17.- Effect of lower surface contour.

Three sets of data for 2 jet configurations with a fountain aligned with the body axis show a reduction in fountain strength that is inversely proportional to the ratio of the corner radius, r, to the jet spacing parameter, e (fig. 17).

Only one set of data is available for a core-and-arm fountain and there is no data available for a crosswise fountain. Until better data is available it is recommended that the relationship shown in figure 17 be used for these types of configurations.

The fountain lift contribution produced by configurations with contoured bodies is therefore given by:

$$\left(\frac{\Delta L_F}{T}\right)_r = K_r \left(\frac{\Delta L_F}{T}\right)_{r=o} \tag{25}$$

where $K_r = .05 \left(\frac{r}{e}\right)^{-1.0}$ for lengthwise fountains

and $K_r = .54 \left(\frac{r}{e}\right)^{-.20}$ for core-and-arm, or crosswise fountains (see fig. 17) (26)

and $\left(\frac{\Delta L_F}{T}\right)_{r=o}$ is given by equations 15 - 21 for the h' method, and for the Basic Method $\left(\frac{\Delta L_F}{T}\right)_{r=o} = \frac{\Delta L_A}{T} + \frac{\Delta L_C}{T}$ which are given by equations 8 - 13.

Configuration 24 (fig. 21, a & b) is the only configuration providing a direct comparison of flat plate and contoured models. Configurations 26 (fig. 21, f) and 27, 28, and 29 (fig. 21, h-i) also involved estimating the effects of fuselage contour. For configuration 26 the effective radius of the gun pods was used in determining K_r.

Lift Improvement Devices

Frequently strakes, or "Lift Improvement Devices" (LIDs), are installed on the lower surface of the body in an attempt to increase the fountain lift. In theory if all the fountain flow could be contained and turned vertically downward the fountain lift could be doubled. However, practical configurations fall short of this. Usually there is insufficient space available for the LIDs to enclose sufficient area, and it may be impractical to enclose the complete perimeter (or the

rear portion may be lift open to direct the hot gasses aft in order to minimize ingestion of hot gasses into the inlet). Also if the LIDs are made shallow their effectiveness will suffer. Reference 7 indicated that the fountain lift increased with strake depth up to a depth of about 0.25d but there was little gain above that. Also reference 6 has shown that the LIDs must be contained within the jet pattern. LIDs external to the jet pattern can cause large lift losses rather than lift gains at low heights. Only LID configurations internal to the jet pattern and with depths greater than 0.25d were used in developing the present method.

In the present method the increment in fountain lift due to the installation of LIDs is defined as:

$$\frac{\Delta L_L}{T} = K_L \left(\frac{\Delta L_F}{T}\right) \tag{28}$$

The augmentation factor for LIDs, K_L, was found by subtracting the LID off experimental data from the data with LIDs on and dividing by the calculated fountain lift for the flat plate configuration. There is considerable scatter in the resulting data but there is a clear indication that K_L falls off rapidly at the lower heights. At the higher heights where the increments were very small there was even more scatter but K_L appeared to level off and an average value was used. The value of K_L was found to be related to the configuration geometry as shown in figure 18 and can be expressed as:

$$\begin{aligned} @\ h < h_L \qquad & K_L = .22\ \frac{h}{\sqrt{S_L}}\ (E^2)\left(\frac{S'_C}{S_C}\right)^{-1} \\ @\ h > h_L \qquad & K_L = 1.25\left(\frac{S_L}{S'_C}\right)(p')\left(\frac{\bar{D}}{d_e}\right)^{-.44} E^{-.5} \end{aligned} \tag{29}$$

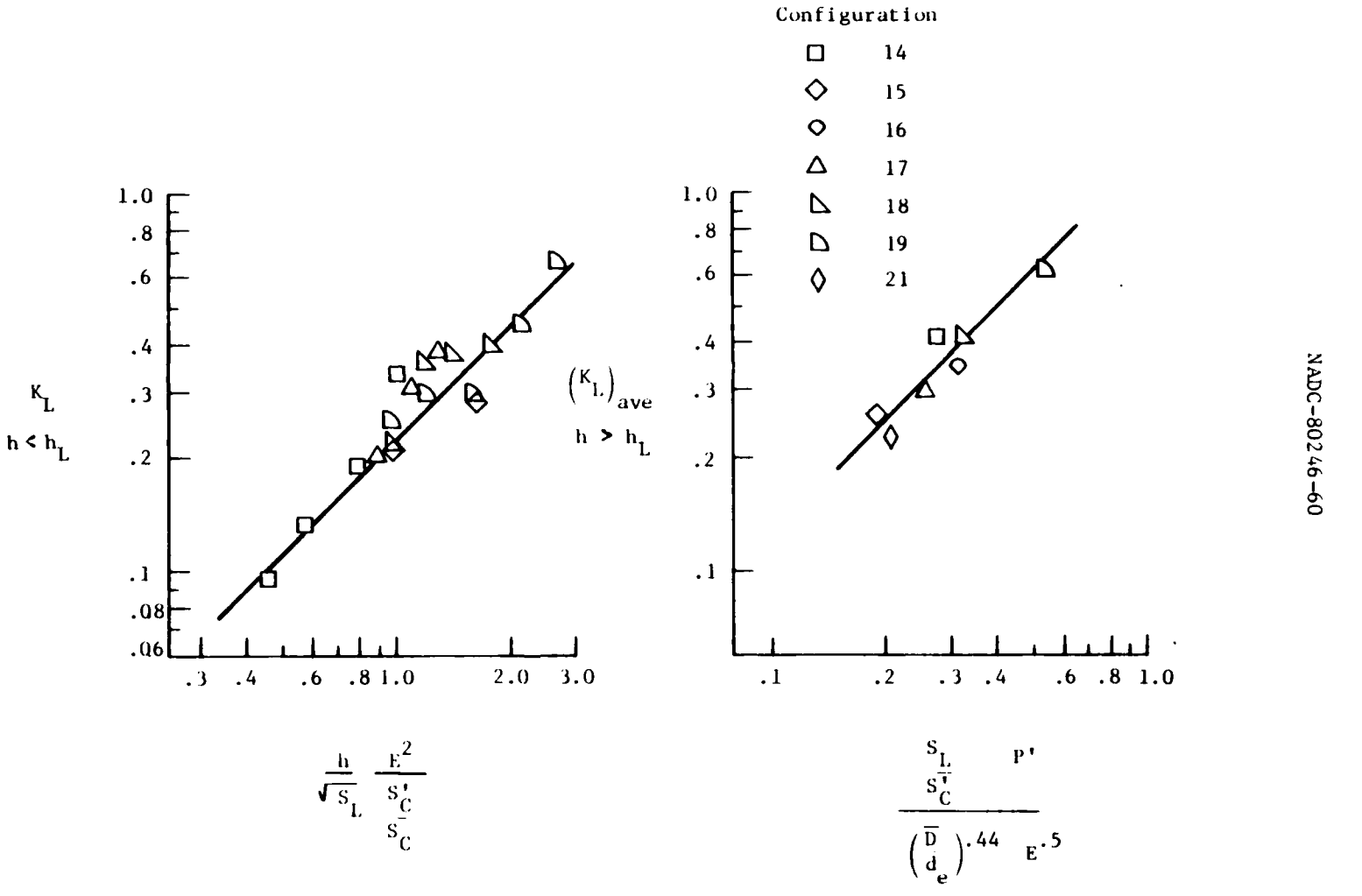

Figure 18.- Correlation of the LID factor K_L with configuration geometry.

PRESENTATION OF METHODS

The methods for estimating the induced lift for fan and jet V/STOL aircraft in hovering flight are recapped in this section for the convenience of the user. The net induced lift can be expressed as:

$$\frac{\Delta L}{T} = \frac{\Delta L_\infty}{T} + \frac{\Delta L_S}{T} + \frac{\Delta L_F}{T} + \frac{\Delta L_L}{T} \tag{1}$$

where;

ΔL_∞ is the lift loss out of ground effect;

$$\frac{\Delta L_\infty}{T} = -.000253 \sqrt{\frac{S}{A}} \left[\left(\frac{P_n}{P} \right)^{-.64} \frac{\Sigma \pi d}{d_e} \right]^{1.58} \tag{2}$$

ΔL_S is the additional suckdown induced by ground proximity;

$$\frac{\Delta L_S}{T} = K_S(-.015) \left[\frac{h/d_e}{\frac{\bar{D}}{d_e} - 1.0} \right] - \left[2.2 - .24 \left(\frac{P_n}{P} - 1.0 \right) \right] \tag{3}$$

where $K_S = 1.0$ for single jet configurations; and for multijet configurations,

$$K_S = 4.5 \left[\frac{h/d_e}{\frac{\bar{D}}{d_e} - 1.0} \right]^{1/4} \left[1.0 - \left(\frac{h/d_e}{.08 \frac{\bar{D}}{d_e} \frac{W}{L}} \right)^{\lambda_S} \right] \tag{6}$$

and

$$\lambda_S = -1.7 \left[\frac{W}{L} \left(\frac{S}{WL} \right)^{.36} \right]^{1.38}$$

ΔL_F is the fountain lift which is given by the Basic Method for widely spaced jets, and by the h' Method for closely spaced jets $\left(\frac{e}{d} < 3.0 \right)$.

Basic Method

The fountain lift is made up of 2 parts; the contribution of the core (ΔL_C) and the contribution of the arms (ΔL_A) which radiate from the core between each pair of adjacent jets.

$$\frac{\Delta L_F}{T} = \frac{\Delta L_C}{T} + \frac{\Delta L_A}{T}$$

For the two jet case, there is no core and;

$$\frac{\Delta L_F}{T} = \frac{\Delta L_A}{T} = \left(\frac{Y}{e}\frac{S'}{S''}\right)^{.835}\left(\frac{e}{e+h}\right)^{2.0}\frac{y}{\sqrt{y^2 + (e+h)^2}} \tag{7}$$

For 3 or more jets the arm contribution is given by;

$$\frac{\Delta L_A}{T} = \frac{\frac{1}{2}\left(\Delta L_{A,1} + \Delta L_{A,2} + \ldots + \Delta L_{A,N}\right)}{T}\left(.7\sqrt{\frac{h/d_e}{\frac{\bar{D}}{d_e} - 1.0}}\right) \tag{8}$$

where

$$\frac{\Delta L_{Ax}}{T} = 2\,\frac{T}{N}\left(\frac{y_x}{e_x}\frac{S'_x}{S''_x}\right)^{.835}\left(\frac{e_x}{e_x+h}\right)^{2.0}\frac{y_x}{\sqrt{y_x^2 + (e_x+h)^2}} \tag{9}$$

The core contribution is given by:

$$\frac{\Delta L_C}{T} = \frac{\Delta L_{C,1} + \Delta L_{C,2} + \ldots + \Delta L_{C,N}}{T} \tag{10}$$

where

$$\Delta L_{C,x} = TK_C\left(\frac{e_x}{e_x+h}\right)^{\lambda_C}\cos\theta_{,x} \tag{11}$$

and K_C and λ_C depend on the height:

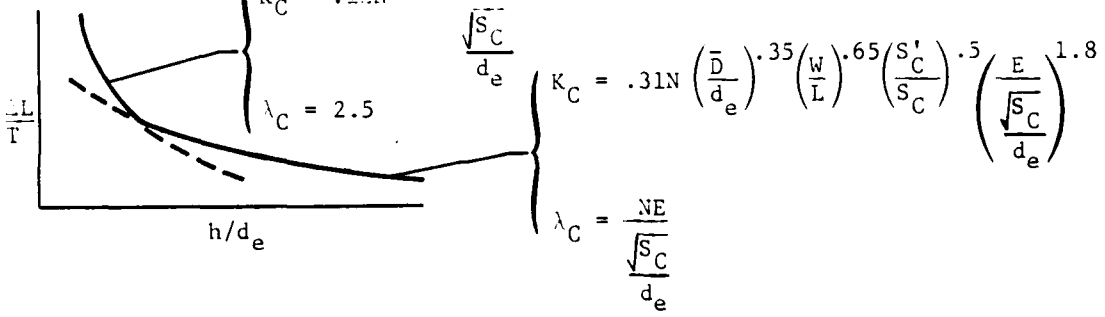

h' Method

The h' Method is used for configurations with closely spaced jets ($\left(\frac{e}{d}\right)_{ave} < 3.0$). These configurations show a sharp break in the induced lift curve which results from a discontinuity in the variation of fountain lift with height. The fountain lift is given by:

$$\frac{\Delta L_F}{T} = K' \left(\frac{h}{d_e}\right)^{\lambda'} \tag{14}$$

where;

$$\left.\begin{aligned} K' &= .084\left(\frac{e}{d}\right)^{.39}\left(\frac{y}{d}\,\frac{S'}{S''}\right)^{1.1} \\ \lambda' &= -1.35\left(\frac{w}{e}\right) \end{aligned}\right\} \text{for 2 jet conf.}$$

where;

$$\left.\begin{aligned} K' &= 4.4\left(\frac{\sqrt{S_C}}{d_e}\,\vartheta'\right)^3\left(\frac{\bar{D}}{d_e}\,\frac{W}{L}\right)^{.9} E^{-1.0} \\ \lambda' &= -2.4\left(\frac{\bar{D}}{d_e}\,\frac{W}{L}\right)^{.4} E^{-.5}\left(\frac{e}{d}\right)_{ave}^{-1.0} \end{aligned}\right\} \text{for 3 or more jets}$$

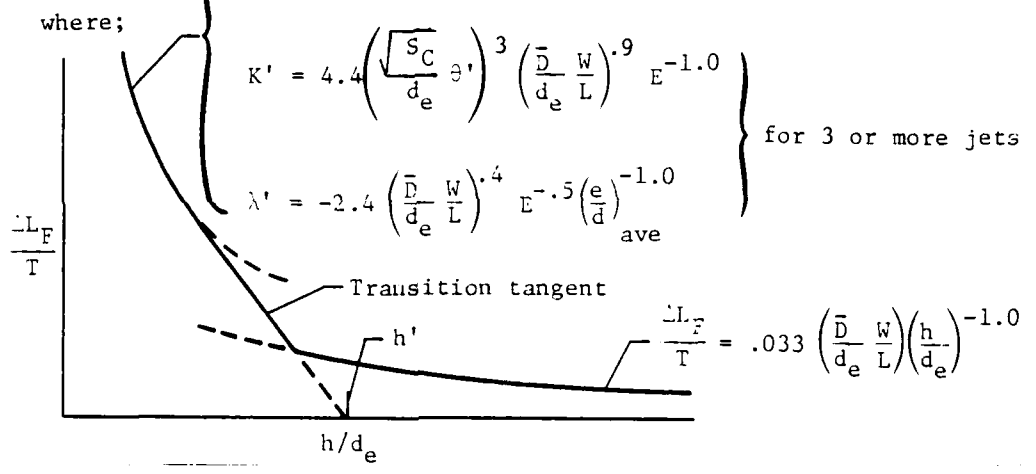

where $\vartheta' = \dfrac{Nd}{2(e_1 + e_2 + \ldots + e_N)}$

and,

$$h' = 3.6\left(\frac{e}{d}\,\frac{w}{e}\right)^{.62}\left(\frac{P_n}{p}\right)^{.5} \qquad \text{for 2 jet configurations}$$

$$h' = 2.0\left(\frac{e}{d}\right)_{ave}^{.5}\left(\frac{P_n}{p}\right)^{.5} \qquad \text{for 3 or more jets.}$$

Body Contour

The above expressions apply to flat plate configurations. A corner radius on the body reduces the fountain lift contribution:

$$\left(\frac{\Delta L_F}{T}\right)_{\text{contoured}} = K_r \left(\frac{\Delta L_F}{T}\right)_{\text{flat plate}}$$

where; $K_r = .05 \left(\frac{r}{e}\right)^{-1.0}$ for lengthwise fountains

and $K_r = .54 \left(\frac{r}{e}\right)^{-.20}$ for core-and-arm or crosswise fountains (see fig. 17)

Lift Improvement Devices

Lift Improvement Devices (LIDs) increase the fountain lift:

$$\frac{\Delta L_L}{T} = K_L \left(\frac{\Delta L_F}{T}\right)_{\text{flat plate}} \tag{28}$$

where

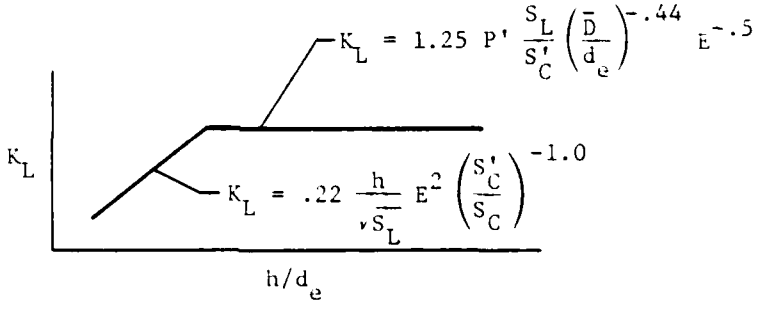

Wing Height

Raising the wing above the plane of the bottom of the body reduces most of the contributions to the induced lift:

Out of ground effect:

$$\left(\frac{\Delta L_\infty}{T}\right)_{nw} = \left(\frac{\Delta L_\infty}{T}\right)_b + \left[\left(\frac{\Delta L_\infty}{T}\right)_{wb} - \left(\frac{\Delta L_\infty}{T}\right)_b\right]\left[1 - .4\sqrt{\frac{\Delta h}{d_e}}\right] \tag{22}$$

The additional suckdown due to the proximity to the ground is felt only on the body for the high wing case:

$$\left(\frac{\Delta L_S}{T}\right)_{m,hw} = \left(\frac{\Delta L_S}{T}\right)_{m,b,h} + \left[\left(\frac{\Delta L_S}{T}\right)_{s,wb,h+\Delta h} - \left(\frac{\Delta L_S}{T}\right)_{s,b,h+\Delta h}\right] \tag{23}$$

The fountain lift is felt only on the body and therefore the contribution calculated for the body alone is used:

$$\left(\frac{\Delta L_F}{T}\right)_{hw} = \left(\frac{\Delta L_F}{T}\right)_b$$

NEED FOR ADDITIONAL RESEARCH

The methods developed in this study are based on data from a wide range of configurations but in most cases there was little systematic data available. The few cases in which only one configuration parameter was varied (such as the variation of $\frac{e}{d}$ in configurations 4 to 6 from reference 7) while the rest of the configuration was fixed were invaluable in determining the manner in which the various ground effect contributions varied with the key geometric parameters. In most cases an understanding of the flow involved, intuition and trial-and-error had to be relied on in arriving at the expressions developed. If the methods presented here are deemed worthy of further development some carefully structured experimental investigations would be of great help in evaluating and refining the present methods.

Multiple Jet Suckdown:

The additional ground induced suckdown associated with multiple jet configurations is the most important and most difficult element of the method to determine. The fact that in the h' Method, equation (15) for the fountain lift at the higher heights depends only on the configuration size and shape $\left(\frac{\bar{D}}{d_e}\frac{W}{L}\right)$ suggests that the multiple jet suckdown may be overestimated by the present formulation and also that a simpler formulation of the fountain lift may be possible. A systematic investigation of the effects of varying jet spacing over a wider range of values for several planform sizes and shapes would be of great help in reevaluating both the multiple jet suckdown and the fountain lift. Tests should start with simple rectangular planforms, first with 2 jet, then with equally spaced 4 jet arrangements before proceeding to more complex configurations.

Wing Height:

The method of handling wing height is based on very limited data. Data for a systematic variation of wing height for a wider range of configuration planforms would be desirable.

Body Contour:

There is no data available for the effects of body contour with crosswise fountains and only one set for core-and-arm fountains. In addition the effects of body contour other than simple radii need to be investigated and the combined effects of body contour and wing height should be studied.

Lift Improvement Devices:

There was a large amount of scatter in the limited amount of data available to use in developing the method to predict the effects of LIDs. And there were only 3 configurations that had gaps in the LIDs ($p' < 1.0$). Also the present method indicates that at low heights the LID effect is inversely proportional to the squareroot of the area enclosed by the LIDs, which is surprising. Some careful experiments to investigate these items would be helpful.

Non Vertical Jets:

The methods assume vertical jets of equal size and thrust. The data of reference 13 (conf. 27 to 29) indicated relatively little effect of small inclination and the jet inclination of these configurations was therefore ignored in developing the present methods. However, there is one isolated set of data in reference 16 which shows a significant increase in fountain lift with outward cant of the jets. Unfortunately the geometric characteristics of the configuration have been lost and the data of ref. 16 could not be used in the present study. The effects of jet inclination should be investigated systematically.

Thrust Differential:

The aft jets on configuration 22 to 24 were smaller, operated to higher pressure ratios, and produced less thrust than the front jets. The fountain lift contribution of these configurations were calculated using the appropriate thrust of each jet pair and by positioning the fountains in inverse ratio to the thrusts. Unfortunately when the thrusts are unequal the fountains will not be vertical, as is assumed in the Basic Method. The agreement shown for these configurations may therefore be

fortuitous or the method may have been biased by the inclusion of these data in the derivation. Specific experiments to investigate the effects of dissimilar jets size and thrust in a systematic manner are needed.

Non Circular Jets:

Kotansky and Glaze in reference 17 have shown that, with rectangular jets the wall jets on the ground are very nonradial. The wall jets from the sides tend to be two-dimensional and contain much more of the mass flow than the more nearly radial flow from the ends. Under these conditions both the suckdown and the fountain strengths would be altered. Vogler's data in reference 14 shows that the ground induced suckdown reduces as the length width ratio of the rectangular jet increases. Also the fountain strength would be expected to be reduced if rectangular jets are placed end to end, and increased if placed side by side. Two or more closely spaced circular jets would produce flow fields similar to rectangular jets and therefore similar induced lift effects. The data from configurations 24 and 31 may contain these effects and the h' Method developed here may have been biased by including them in its development. A systematic investigation of rectangular jets is currently underway and should help to quantify these effects.

Height Range:

Some of the data did not go to high enough heights (configurations 3 to 9 and 14 to 19 for example) and some did not go low enough (conf. 26) and some did not take enough points (conf. 31) to adequately define critical breaks in the variation of induced lift with height. The present method should be used to estimate the various lift loss and lift gain increments for each configuration to be investigated before testing to ensure that data is taken in all the critical height ranges.

Nozzle Pressure Ratio:

The critical height h' was found to be dependent on pressure ratio and previous work (ref. 2) has shown a small effect of pressure ratio on the suckdown for the single jet case. No other effects of pressure ratio were apparent in the data used in developing the present methods.

However, except for ref. 11 which showed the dependence of h' on pressure ratio, there have been no systematic investigations of pressure ratio on fountain lift and multiple jet suckdown. The pressure ratios used in the investigations which form the basis of the present methods ranged from 1.15 to over 2.0 and it is possible that the effects of pressure ratio are obscured by other effects. An investigation of the effects of pressure ratio on fountain lift and multiple jet suckdown is needed.

CONCLUDING REMARKS

The present study has shown that, with the empirical approach used here, two different methods are needed to predict the induced lift of Fan and Jet V/STOL aircraft in hovering flight. The Basic Method as developed here applies to configurations with widely spaced jets ($\frac{e}{d} > 3.0$), and the h' Method is applicable to closely spaced jets. The methods account for the effects of jet arrangement, configuration planform, wing height, body contour and Lift Improvement Devices (LIDs) but are limited to essentially vertical, circular jets of equal size and thrust.

The methods are based on correlation of data from a wide variety of configurations, however, there was little systematic variation in any of the data sets available. Suggestions for further work to evaluate and refine the methods are included.

REFERENCES

1. Wyatt, L. A. "Static Test of Ground Effect on Planforms Fitted With a Centrally-Located Round Lifting Jet." Ministry of Aviation, CP 749, June, 1962.
2. Kuhn, R. E. "An Empirical Method for Estimating Jet Induced Lift Losses of V/STOL Aircraft Hovering In and Out-Of-Ground Effect." Proceeding of the Workshop on V/STOL Aerodynamics, Naval Postgraduate School, Monterey, Calif. May 1979.
3. Yen, K. T. "On the Vertical Momentum of the Fountain Produced by Multi-Jet Vertical Impingement on a Flat Ground Plane." Naval Air Development Center, NADC-79273-60, Nov., 1979.
4. Karemaa, A., et al. "The Aerodynamic and Thermodynamic Characteristics of Fountains and Some Far-Field Temperature Distributions." ONR Report, ONR-CR212-237-1F, July, 1978.
5. Kotansky, D. R., et al. "Jet Induced Forces and Moments In and Out-of-Ground Effect." McDonnell Aircraft Company, NADC-77-229-30, June, 1977.
6. Foley, W. H. and Sansone, J. A. "V/STOL Propulsion-Induced Aerodynamics Hover Calculation Method." General Dynamics, NADC-78242-60, Feb. 1980.
7. Hill, W. G. and Jenkins, R. C. "Effect of Nozzle Spacing on Ground Interference Forces for a Two Jet V/STOL Aircraft." AIAA Paper No. 79-1856, Aug. 1979.
8. Kamman, J. H. and Hall, C. L. "Lift System Induced Aerodynamics of V/STOL Aircraft in a Moving Deck Environment." McDonnell Aircraft Company, NADC-77-107-30, Sept. 1978.
9. Wohllebe, F. A. and Migdal, D. "Some Basic Test Results of V/STOL Jet-Induced Lift Effects in Hover." AIAA Report No. 79-0339, Jan. 1979.
10. Albang, L. F. "Analysis of Spread Multi-Jet VTOL Aircraft in Hover." Old Dominion University, Report No. 74-T8, Dec. 1974.
11. Gentry, G. L. and Margason, R. J. "Jet-Induced Lift Losses on VTOL Configurations Hovering In and Out of Ground Effect." NASA TN D-3166, Feb. 1966.
12. Johnson, D. B., et al. "Powered Wind Tunnel Testing of the AV-8B; A Straightforward Approach Pays Off." AIAA Report No. 79-0333, Jan. 1979.
13. Shumpert, P. K. and Tibbetts, J. G. "Model Tests of Jet-Induced Lift Effects on a VTOL Aircraft in Hover." NASA CR-1297, March, 1969.
14. Vogler, R. D. "Interference Effects of Single and Multiple Round or Slotted Jets on a VTOL Model in Transition." NASA TN D-2380, Aug. 1964.

REFERENCES - Concluded

15. Spong, E. D., et al. "V/STOL Jet-Induced Interactions." McDonnell Aircraft Company, Proceedings of Workshop on V/STOL Aerodynamics, Naval Postgraduate School, Monterey, Calif. May, 1979.

16. Margason, R. J. "Review of Propulsion-Induced Effects on Aerodynamics of Jet V/STOL Aircraft." NASA TN D-5617, Feb. 1970.

17. Kotansky, D. R. and Glaze, L. W. "Investigation of Impingement Region and Wall Jet Formed by the Interaction of High Aspect Ratio Lift Jets and a Ground Plant." NASA CR152174, Sept. 1978.

TABLE I
GEOMETRY OF TWO JET CONFIGURATIONS

Conf.	$\frac{d}{cm}$	$\frac{d_e}{cm}$	$\frac{P_n}{p}$	$\frac{S}{A}$	$\frac{\bar{D}}{d_e}$	$\frac{W}{L}$	$\frac{S}{WL}$	$\frac{e}{d_e}$	$\frac{y}{d_e}$	$\frac{Y}{y}$	$\frac{S'}{S''}$	$\frac{w}{e}$
1	3.59	5.08	2.0	40.7	4.53	.096	1.0	4.5	.853	1.0	1.0	1.0
2	↓	↓	↓	127	10.18	.301	↓	4.5	2.75	↓	↓	↓
3	↓	↓	↓	165	12.55	.622	↓	2.34	4.63	↓	↓	↓
4	2.54	3.63	1.15	29.3	5.34	.719	↓	1.414	2.83	↓	↓	↓
5	↓	↓	↓	↓	↓	↓	↓	1.061	↓	↓	↓	↓
6	↓	↓	↓	↓	↓	↓	↓	.850	↓	↓	↓	↓
7	3.59	5.08	2.0	115	8.25	1.0	.27	4.5	9.13	↓	.447	↓
8	↓	↓	↓	77.5	6.25	1.0	.182	4.5	9.13	↓	.27	↓
9	2.54	3.63	1.15	5.09	1.704	.125	1.0	2.0	2.83	↓	.25	.25
10	5.9	8.34	1.5	37.9	5.33	.64	.396	2.63	2.92	1.19	.662	1.0
11	↓	↓	↓	↓	↓	↓	↓	3.09	2.37	1.46	.765	↓
(12) Body	4.83	6.82	1.15	6.66	2.011	.447	.376	1.05	—	1.0	.546	.355

TABLE II
GEOMETRY OF CONFIGURATIONS WITH THREE OR MORE JETS

Conf.	N	$\frac{d}{cm}$	$\frac{d_e}{cm}$	$\frac{P_n}{p}$	$\frac{S}{A}$	$\frac{\bar{D}}{d_e}$	$\frac{W}{L}$	$\frac{S}{WL}$	$\frac{\sqrt{S_c}}{d_e}$	$\frac{S'_c}{S_c}$	$\frac{r}{e}$	$\frac{S_L}{S_c}$	p'
13	4	3.35	6.70	2.0	63.0	7.89	.915	1.0	3.85	1.0	—	—	—
14		3.61	7.21		54.8	7.32	.915		3.58		—	.707	1.0
15		4.09	8.18		80.2	8.79	.64		4.36		—	.737	
16					29.5	4.67	.234			.798	—		
17	3	3.35	6.70		70	8.03	.85	.50	3.15	1.0	—	.728	
18					46.7	6.32				.884	—		
19					10.4	3.10				.728	—		
20		5.08	8.88	1.4	119	9.14	1.0	.48	3.19	1.0	—	—	—
21		$\frac{5.9}{1.46}$	6.25	$\frac{1.5}{4.4}$	67.4	7.11	.64	.396	2.56	1.0	—	1.16	.9
22		$\frac{4.17}{1.46}$							3.48	1.0	—	—	—
23									3.77	1.0	—	—	—
24	3	5.9	10.22	1.5	12.6	2.91	.85	.259	1.83	1.0	.101	.54	.9
25_a	4	2.87	5.73	2.08	39	5.9	.525	.31	1.23	1.0	—	—	—
25_b					39	5.9					—	—	—
25_c					34.5	5.41	.463				—	—	—
26 Body		$\frac{6.15}{7.33}$	13.5	$\frac{2.07}{1.80}$	23.5	2.075	.175	.502	2.08	.95	.16	.80	.71
27		4.64	9.28	2.0	31.6	4.59	.138	.784	.923	1.0	1.3	—	—
28	6	3.79							1.07		1.6	—	—
29_a	8	3.28							1.13		1.8	—	—
29_b									1.313			—	—
29_c									1.473			—	—
30	3	5.9	10.22	1.5	4.25	1.93	.51	.50	1.83	.9	—	—	—
$31_{(wb)}$	4	4.45	8.89	1.3	41.5	5.74	.52	.30	1.286	1.0	—	—	—
31 Body	4				24.95	3.58	.11	.79			—	—	—

TABLE II- Concluded
GEOMETRY OF CONFIGURATIONS WITH THREE OR MORE JETS

Conf.	$\frac{e_1}{d_e}$	$\frac{e_2}{d_e}$	$\left(\frac{y}{d_e}\right)_1$	$\left(\frac{y}{d_e}\right)_2$	$\left(\frac{Y}{d_e}\right)_1$	$\left(\frac{Y}{d_e}\right)_2$	θ_1 deg	θ_2 deg	$\left(\frac{S'}{S''}\right)_1$	$\left(\frac{S'}{S''}\right)_2$	E
13	2.08	1.77	1.60	1.60	1.60	1.60	49.5	40.5	1.0	1.0	1.18
14	1.94	1.66	1.48	1.48	1.48	1.48	↓	↓	↓	↓	1.17
15	3.26	1.46	1.72	1.71	1.72	1.72	65.9	24.1	↓	↓	2.23
16	↓	↓	0	1.71	0	1.71	↓	↓	—	↓	2.23
17	2.63	2.06	1.84	1.84	1.84	1.84	67	46	1.0	↓	1.28
18	↓	↓	↓	0	↓	—	↓	↓	1.0	—	↓
19	↓	↓	0	0	—	—	↓	↓	—	—	↓
20	2.96	1.80	2.02	5.1	3.66	5.66	72.5	35	.71	.79	1.64
21	3.54	.936	4.03	.898	4.03	.898	80.8	18.5	.518	1.0	3.78
22	← See Table III →										4.06
23	← See Table III →										4.77
24	1.86	.939	0	.813	1.01	.813	75.5	29	—	.64	1.98
25_a	1.0	.377	1.43	4.76	2.0	4.76	69.4	20.6	.71	1.0	2.65
25_b	↓	↓	↓	↓	↓	↓	↓	↓	↓	↓	↓
25_c	↓	↓	1.21	4.76	1.79	4.76	↓	↓	.68	1.0	↓
26 Body	← See Table III →										2.27
27	.425	.50	.543	4.7	5.43	4.7	40.4	49.6	1.0	1.0	.85
28	.347	.409	.634	↓	.634	↓	↓	↓	↓	↓	1.77
29_a	.301	.354	.689	↓	.689	↓	↓	↓	↓	↓	2.55
29_b	↓	.477	.566	↓	.566	↓	32.3	57.7	↓	↓	1.89
29_c	↓	.601	.442	↓	.442	↓	26.6	63.4	↓	↓	1.5
30	1.86	.939	0	0	0	0	75.5	29	—	—	1.98
$31_{(wb)}$	1.071	.386	2.05	3.73	3.32	3.73	70.2	19.8	.62	1.0	2.78
31 Body	↓	↓	.4	↓	.4	↓	↓	↓	1.0	↓	2.78

TABLE III
JET PATTERN GEOMETRY FOR CONFIGURATIONS WITH
UNEQUAL FRONT AND REAR JET SPACING

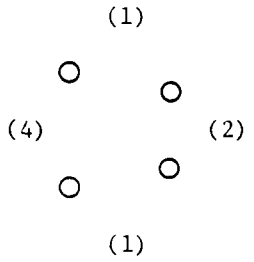

		$\frac{e}{d_e}$	$\frac{y}{d_e}$	$\frac{Y}{y}$	$\frac{\div}{\text{deg}}$	$\frac{S'}{S''}$
	Side (1)	3.507	4.62	1.0	75.4	.408
Conf. 22	Rear (2)	.936	.898		18.5	1.0
	Front (4)	.792	6.09		10.7	.752
	Side (1)	4.117	4.62		77.5	.424
Conf. 23	Rear (2)	.936	.898		15.9	1.0
	Front (4)	.792	5.32		9.1	.695
	Side (1)	2.13	0		46.5	—
Conf. 26	Rear (2)	.82	~2.		39	1.0
	Front (4)	1.06	~2.		48	1.0

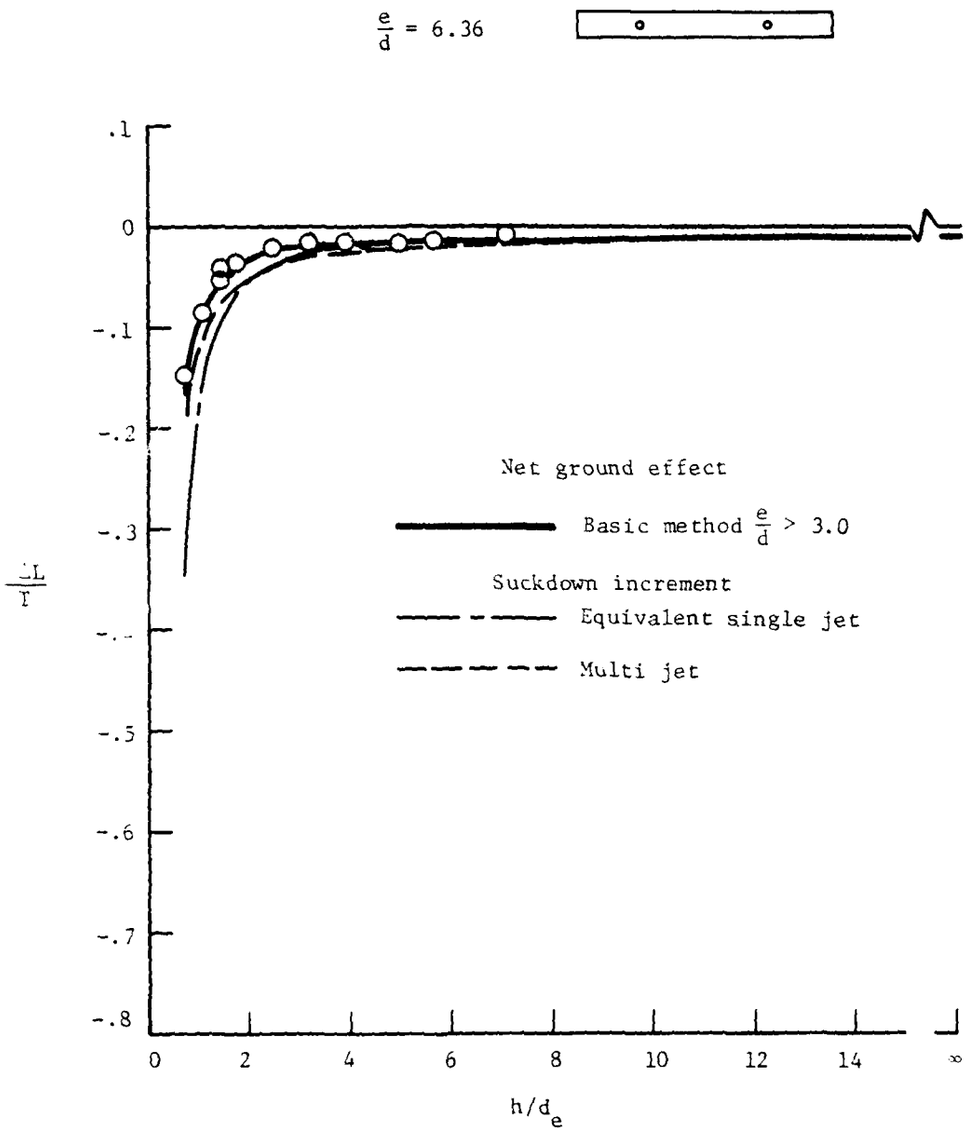

(a) Configuration 1 (ref 6)

Figure 19.- Comparison of calculated and measured ground effects for 2 jet configurations.

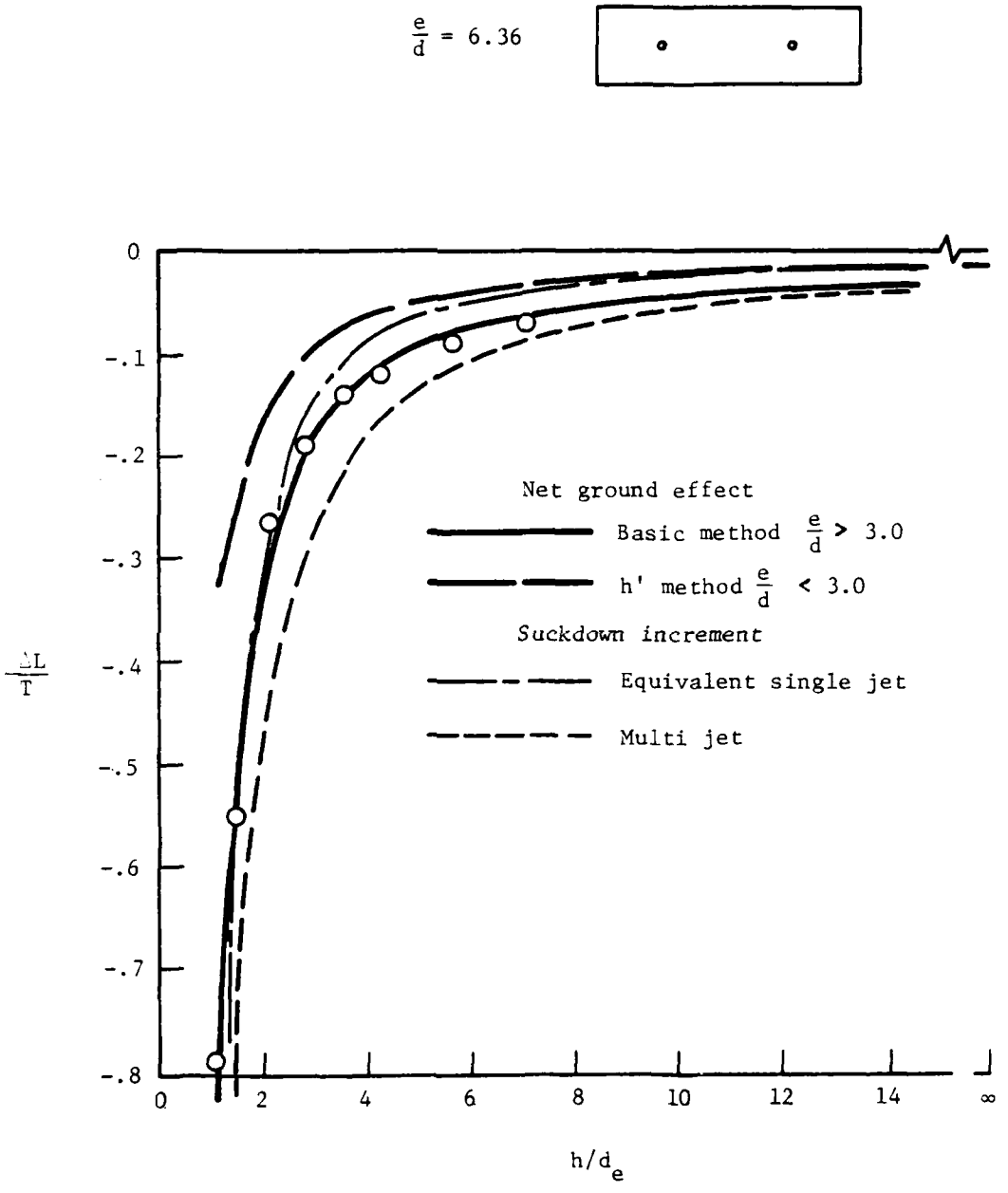

(b) Configuration 2 (ref 6)

Figure 19 .- Continued

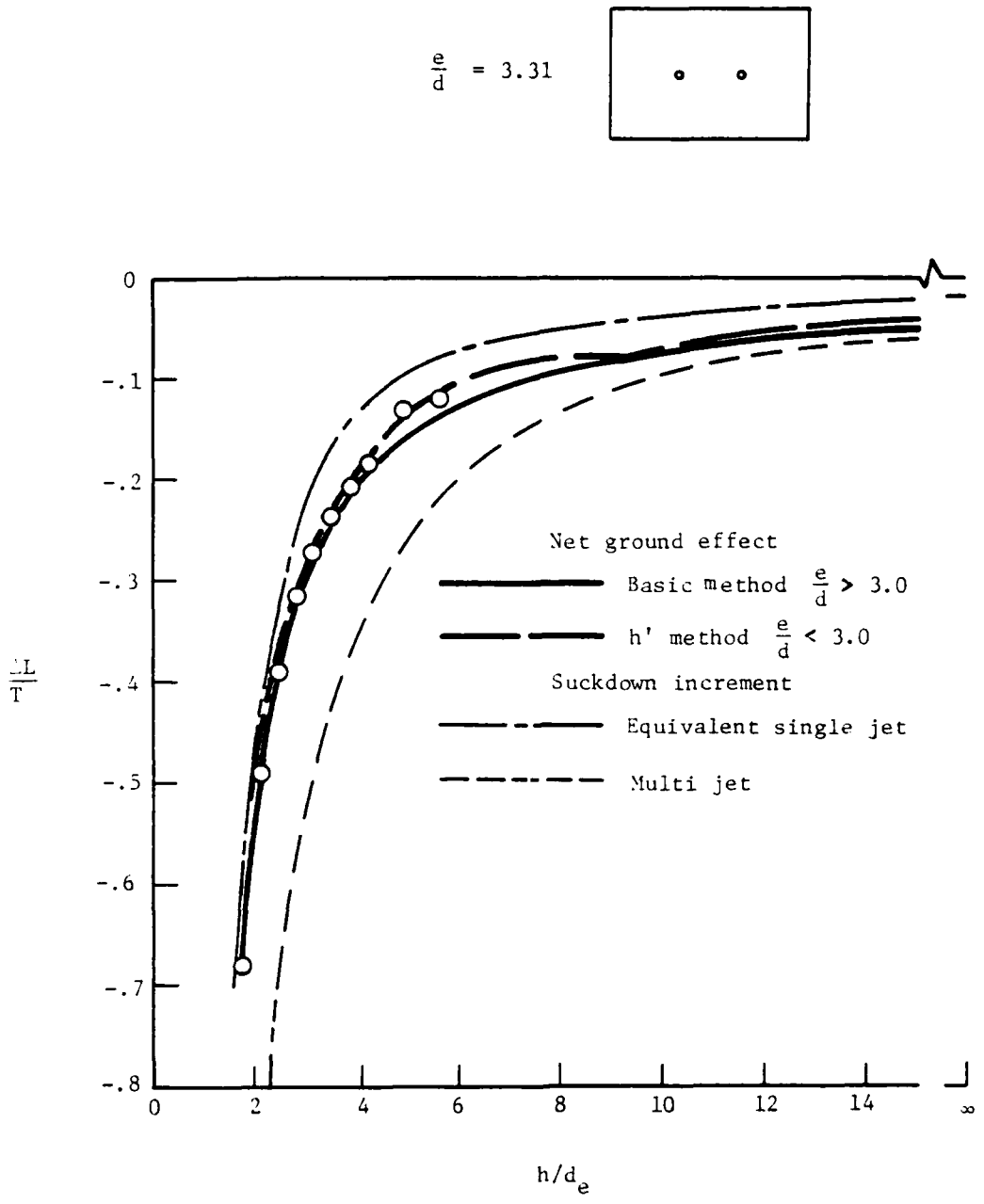

(c) Configuration 3 (ref 4)

Figure 19.- Continued.

$\frac{e}{d} = 2.0$

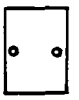

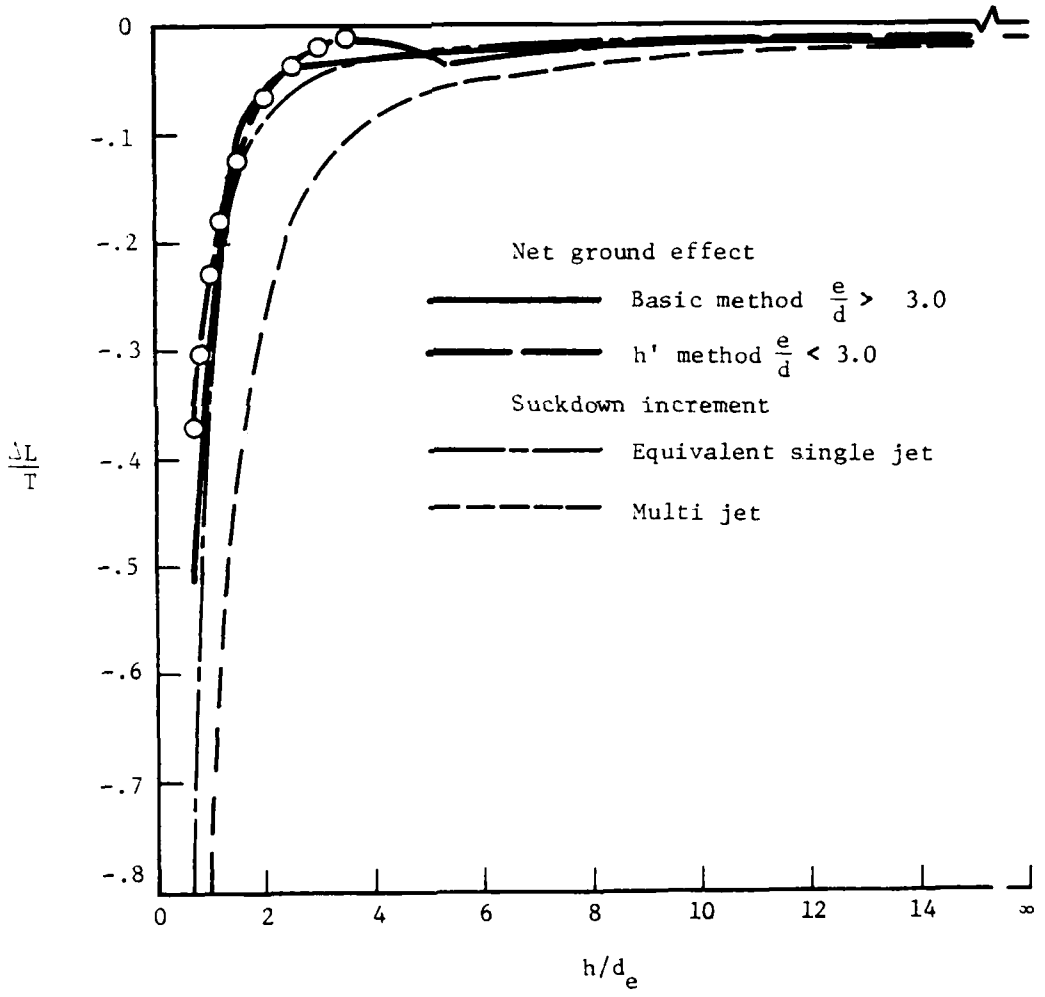

(d) Configuration 4 (ref 7)

Figure 19.- Continued

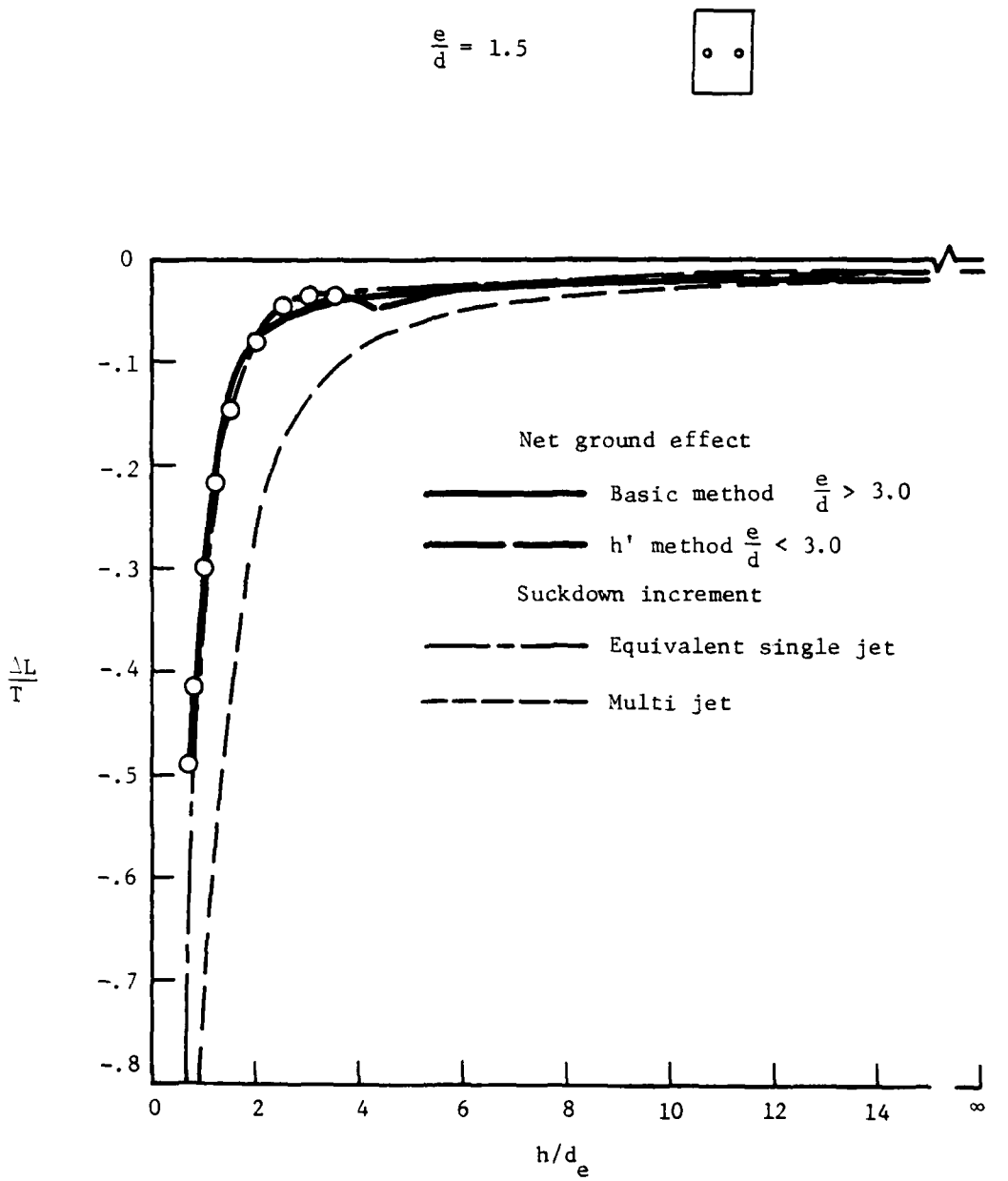

(e) Configuration 5 (ref 7)

Figure 19.- Continued.

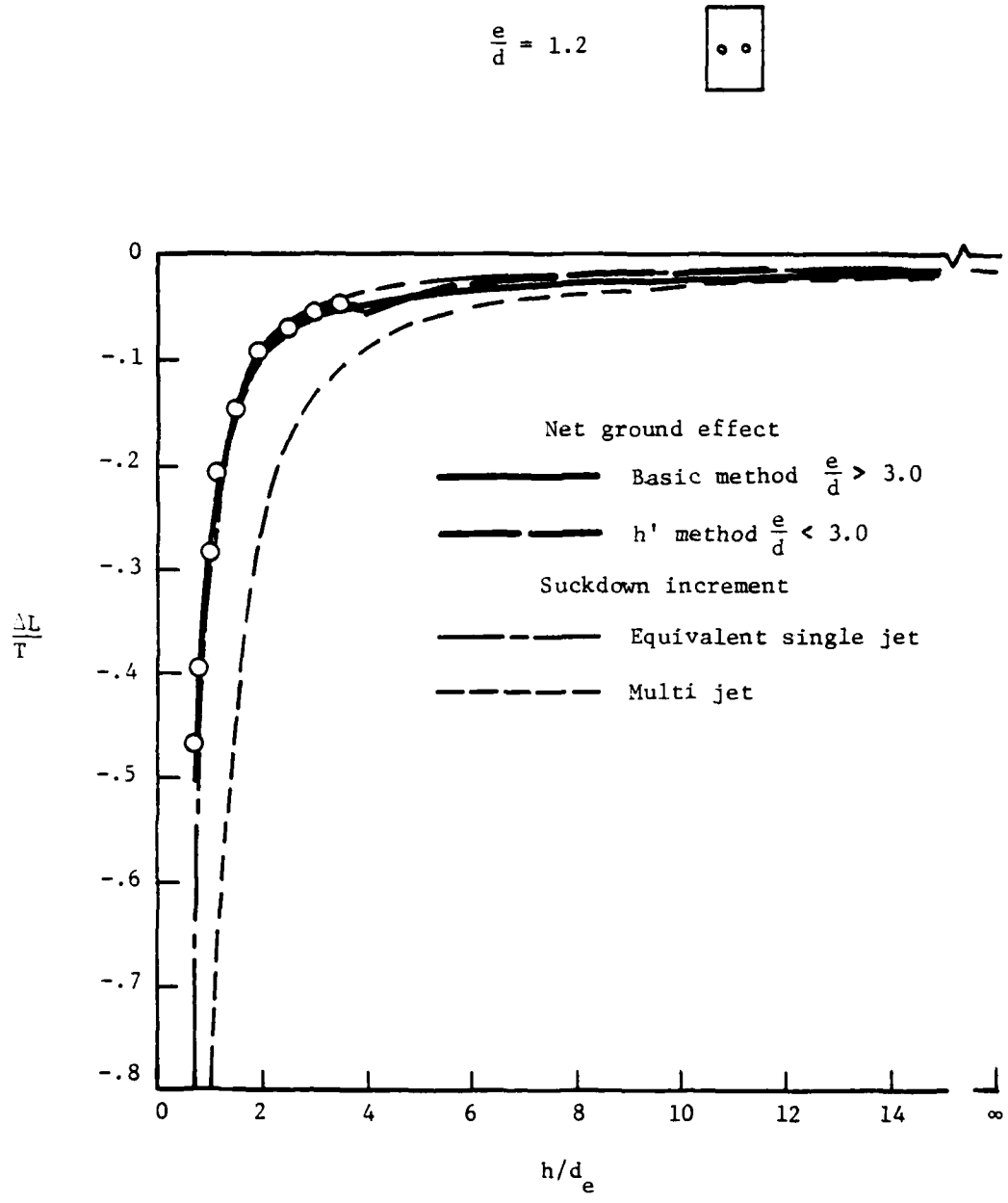

(f) Configuration 6 (ref 7)

Figure 19.- Continued

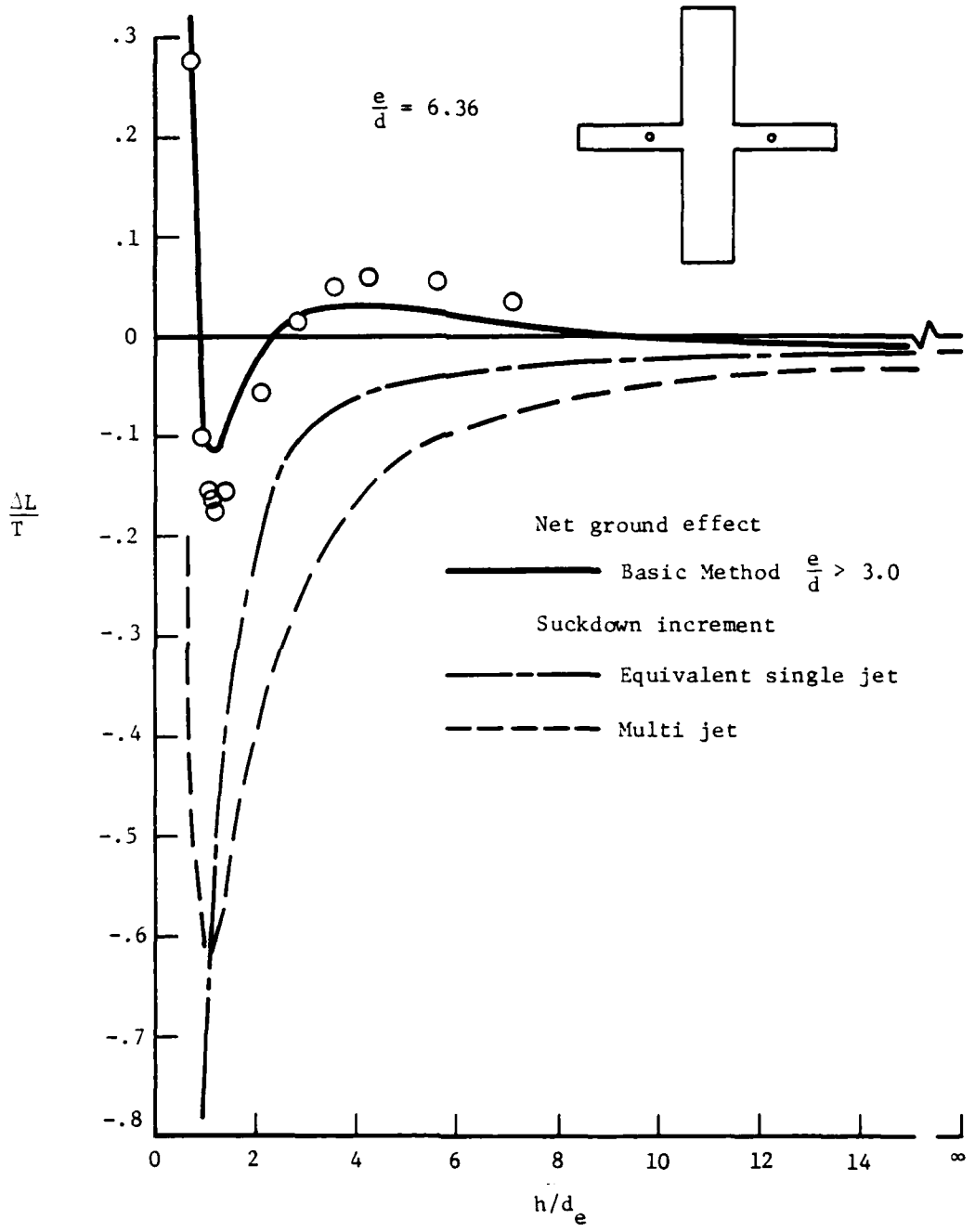

(g) Configuration 7 (ref 6)

Figure 19.- Continued

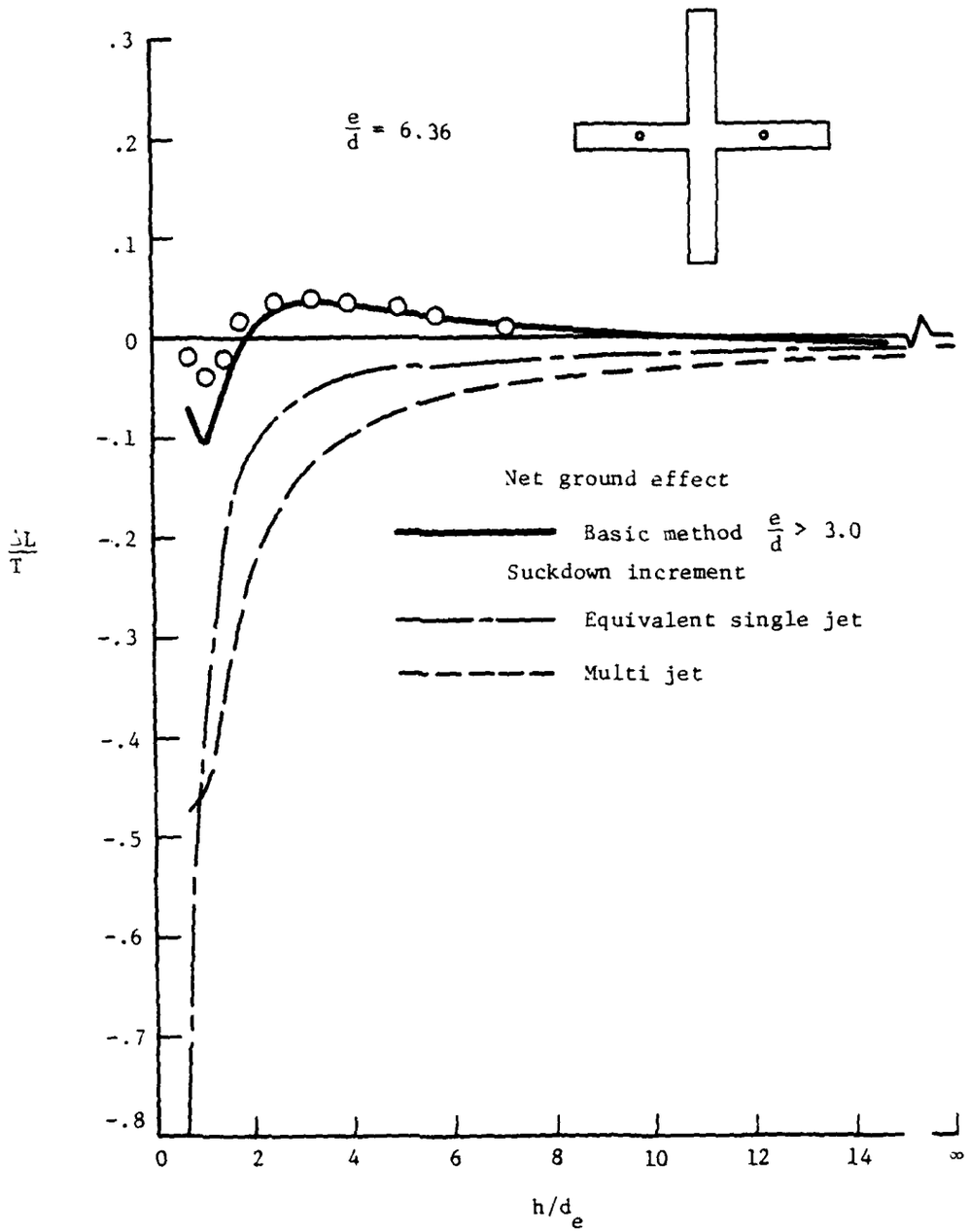

(h) Configuration 8 (ref 6)

Figure 19.- Continued.

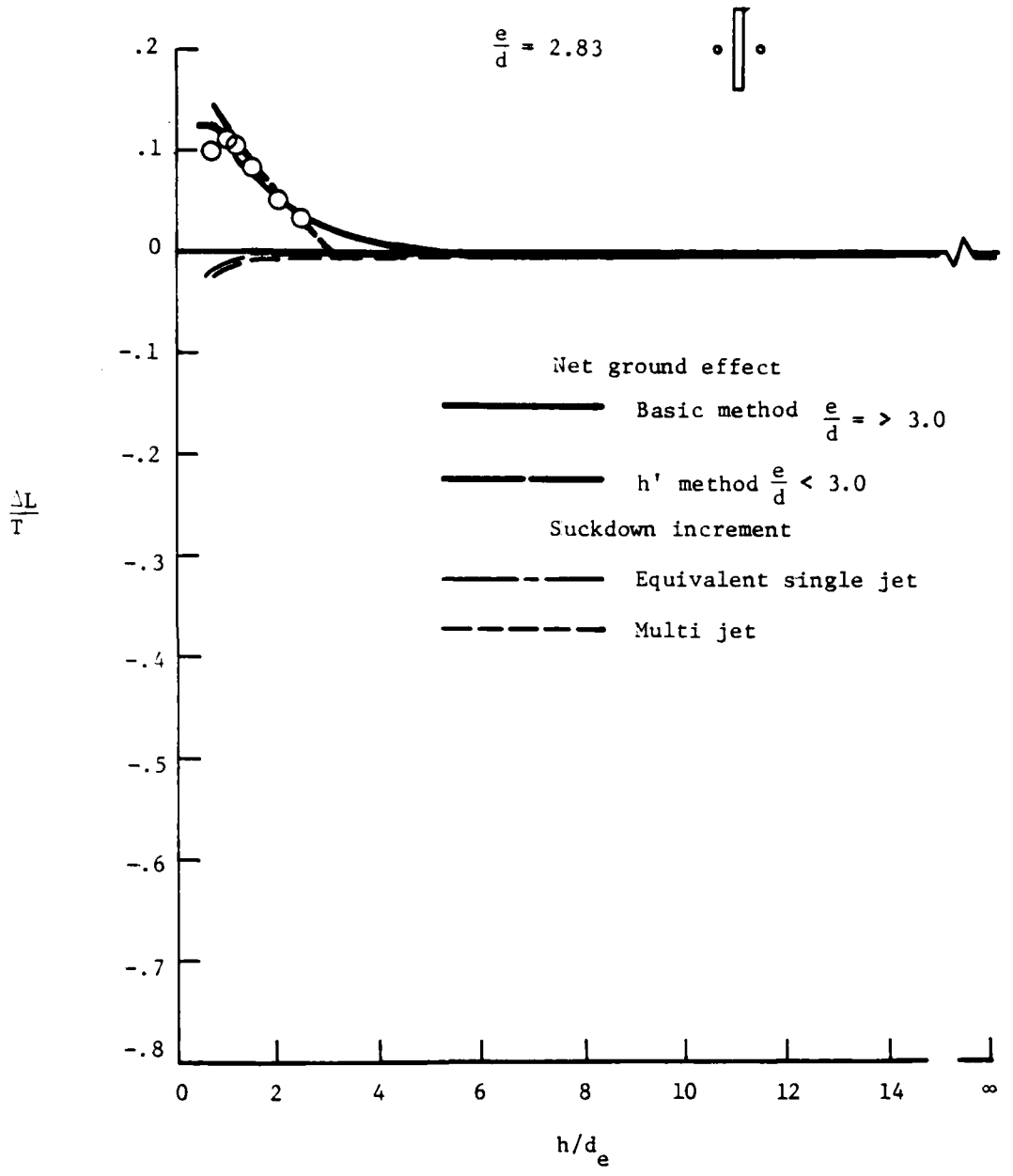

(i) Configuration 9 (ref 7)

Figure 19.- Continued.

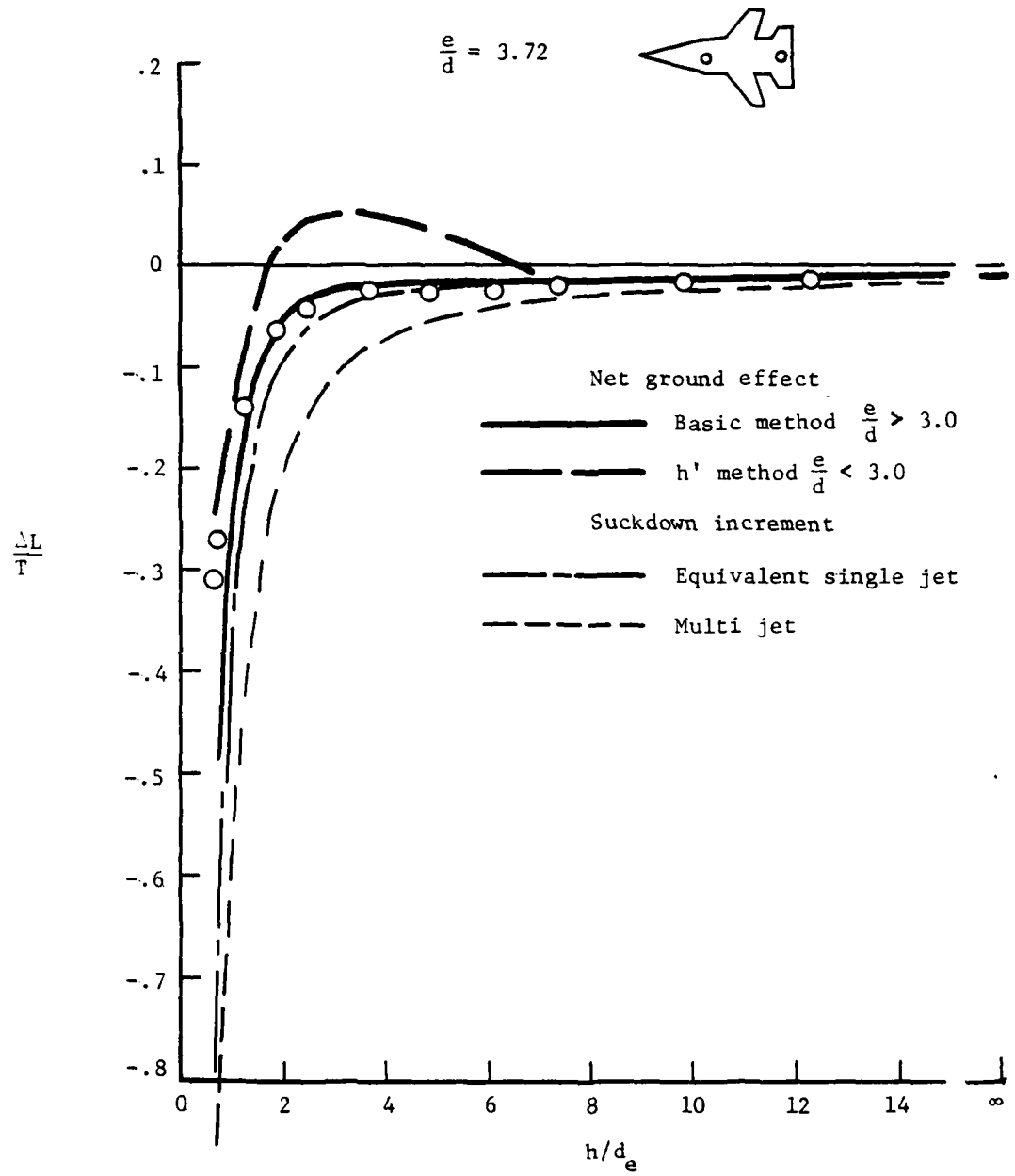

(j) Configuration 10 (ref 8)

Figure 19.- Continued

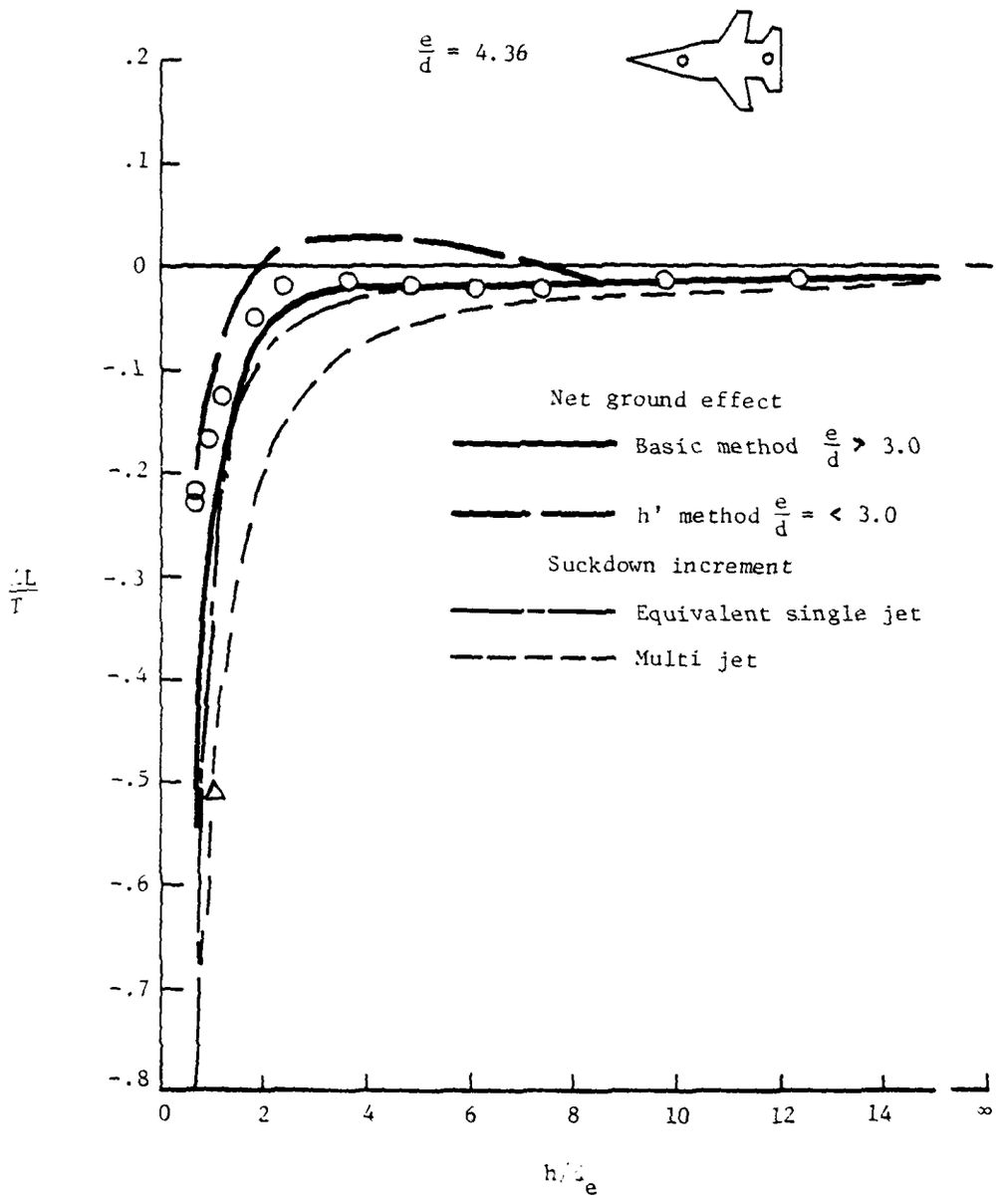

(k) Configuration 11 (ref 8)

Figure 19.- Continued.

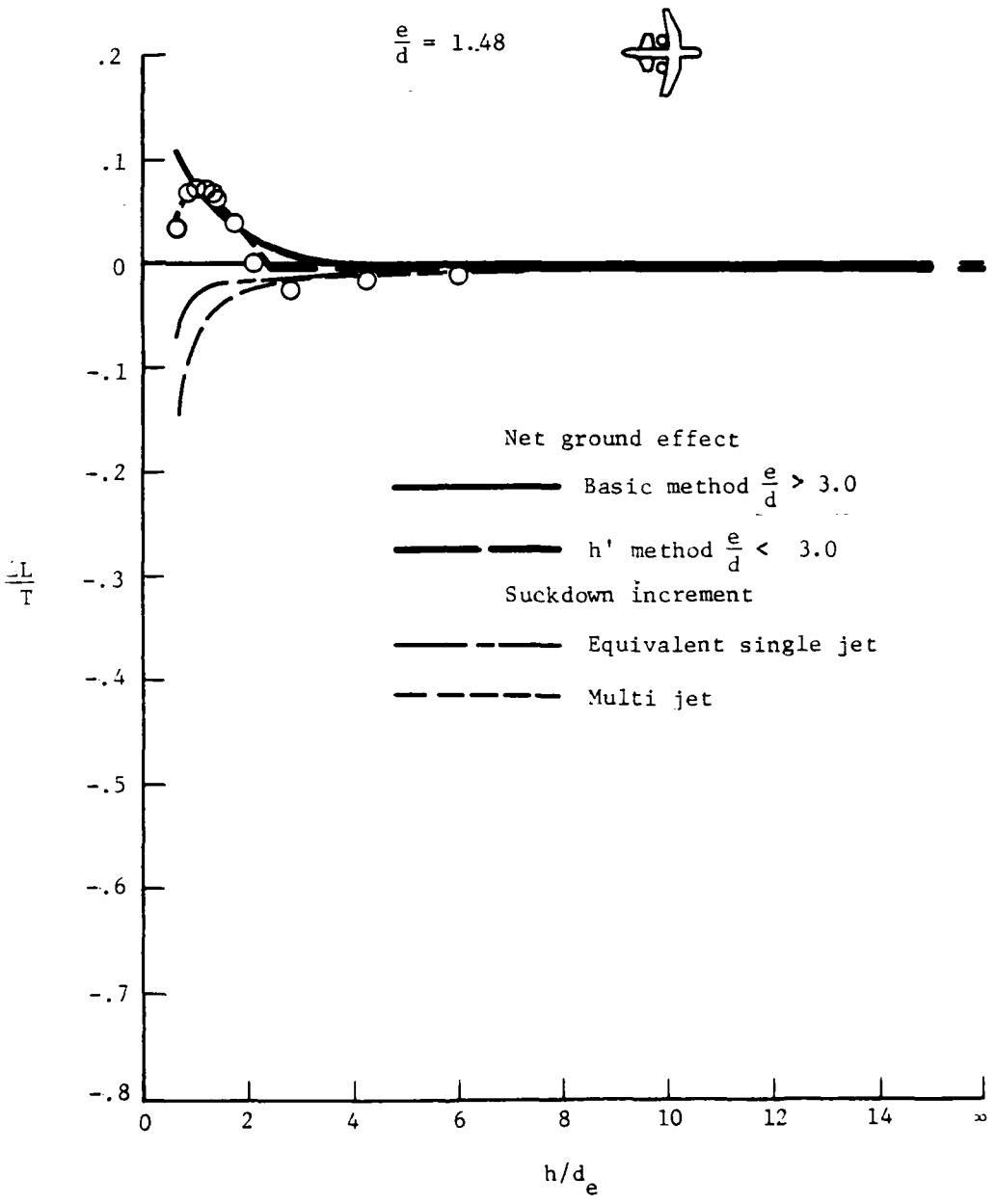

(l) Configuration 12 (ref 7)

Figure 19.- Concluded.

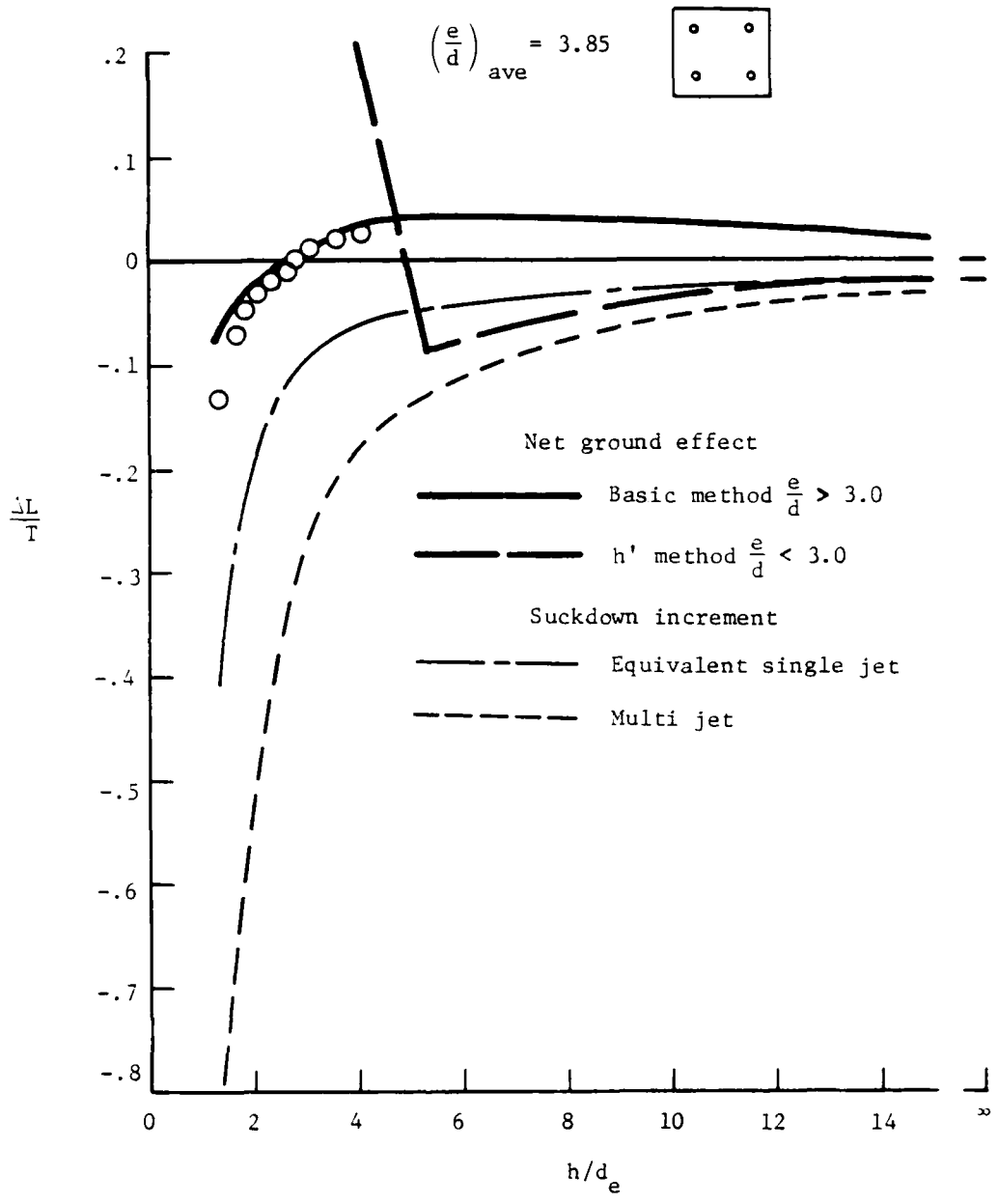

(a) Configuration 13 (ref 4)

Figure 20.- Comparison of calculated and measured ground effects for 3 and 4 jet configurations. Wide jet spacing; $\left(\frac{e}{d}\right)_{ave}$ >3.0.

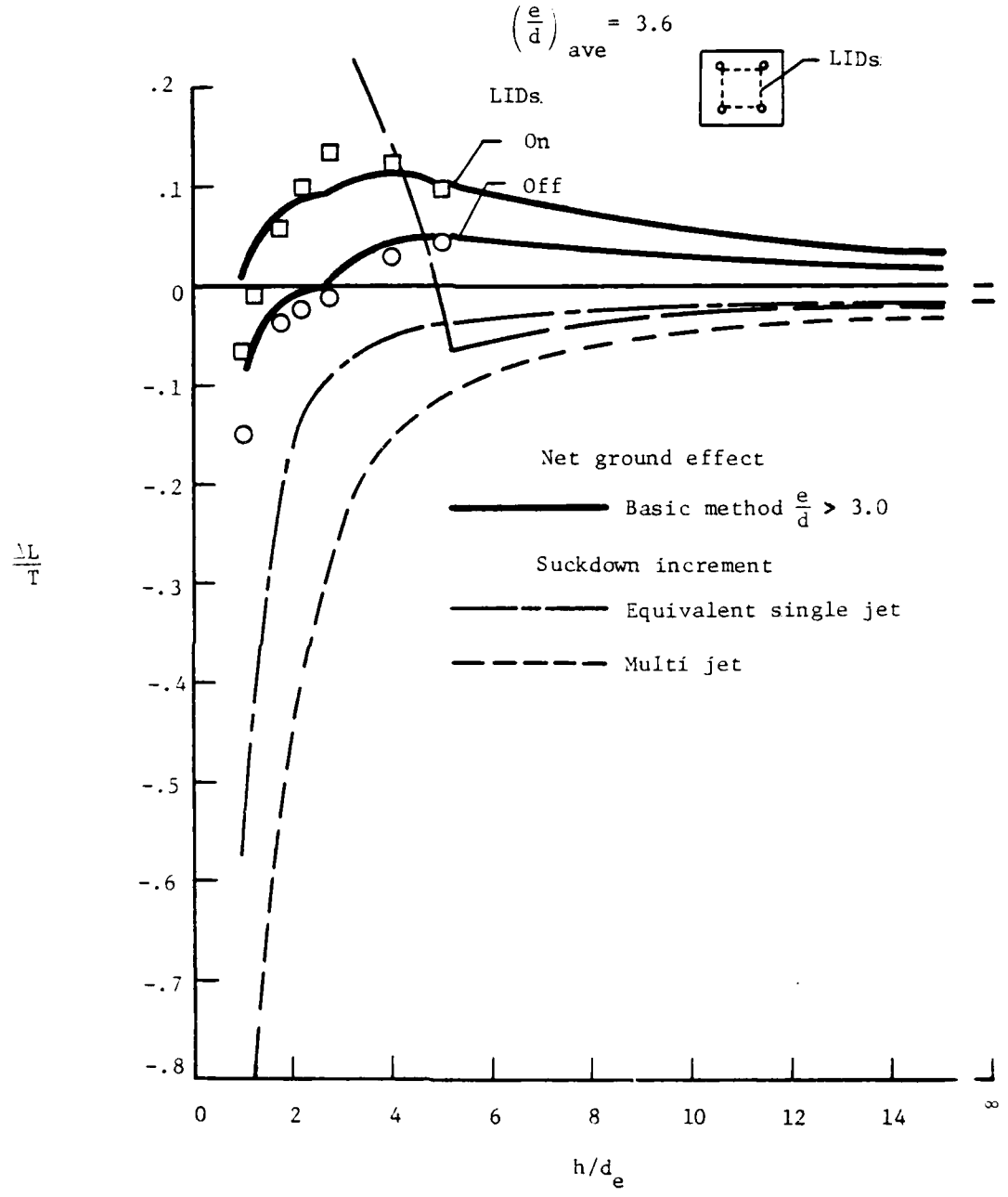

(b) Configuration 14 (ref 6).

Figure 20.- Continued.

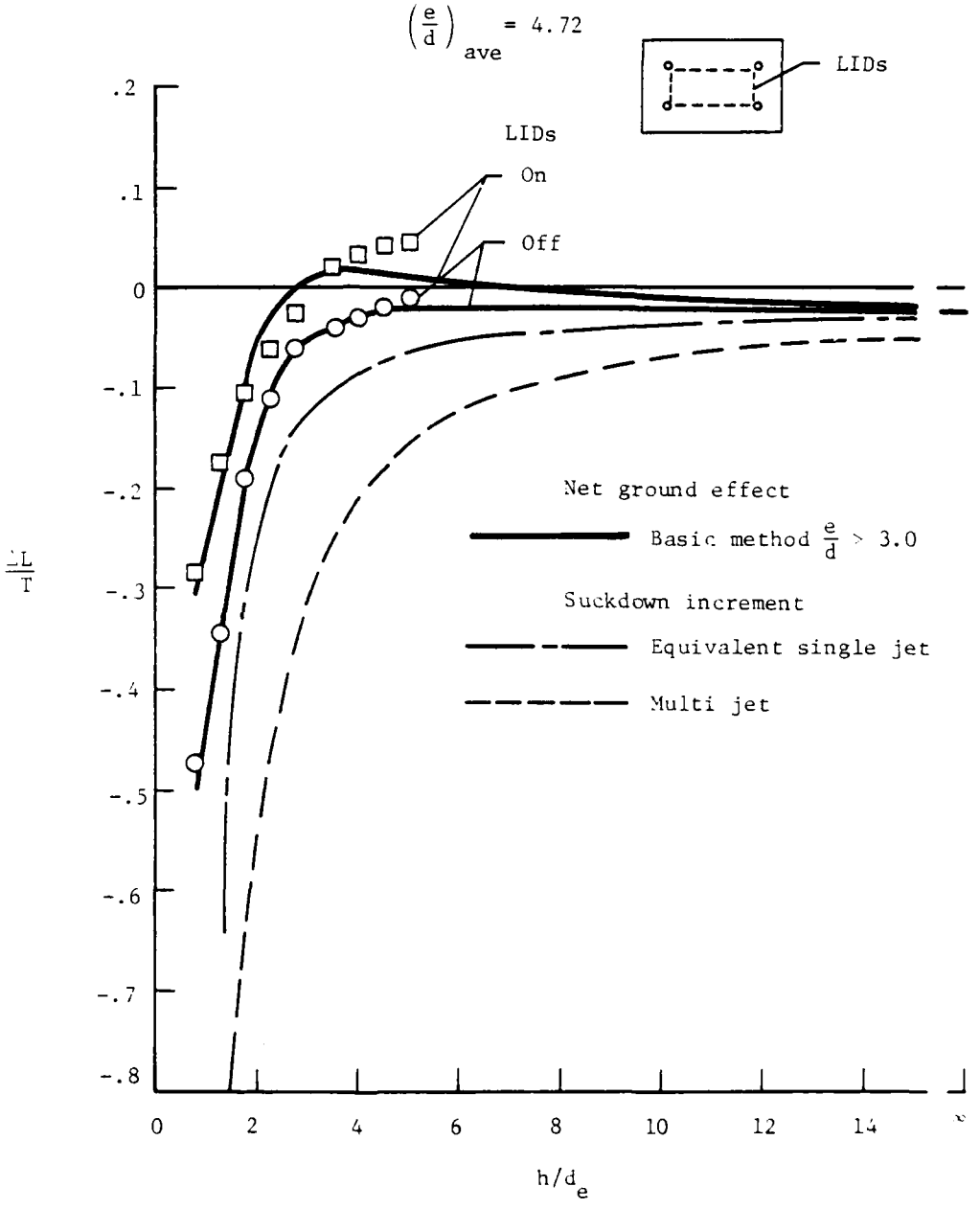

(c) Configuration 15 (ref 6).

Figure 20.- Continued.

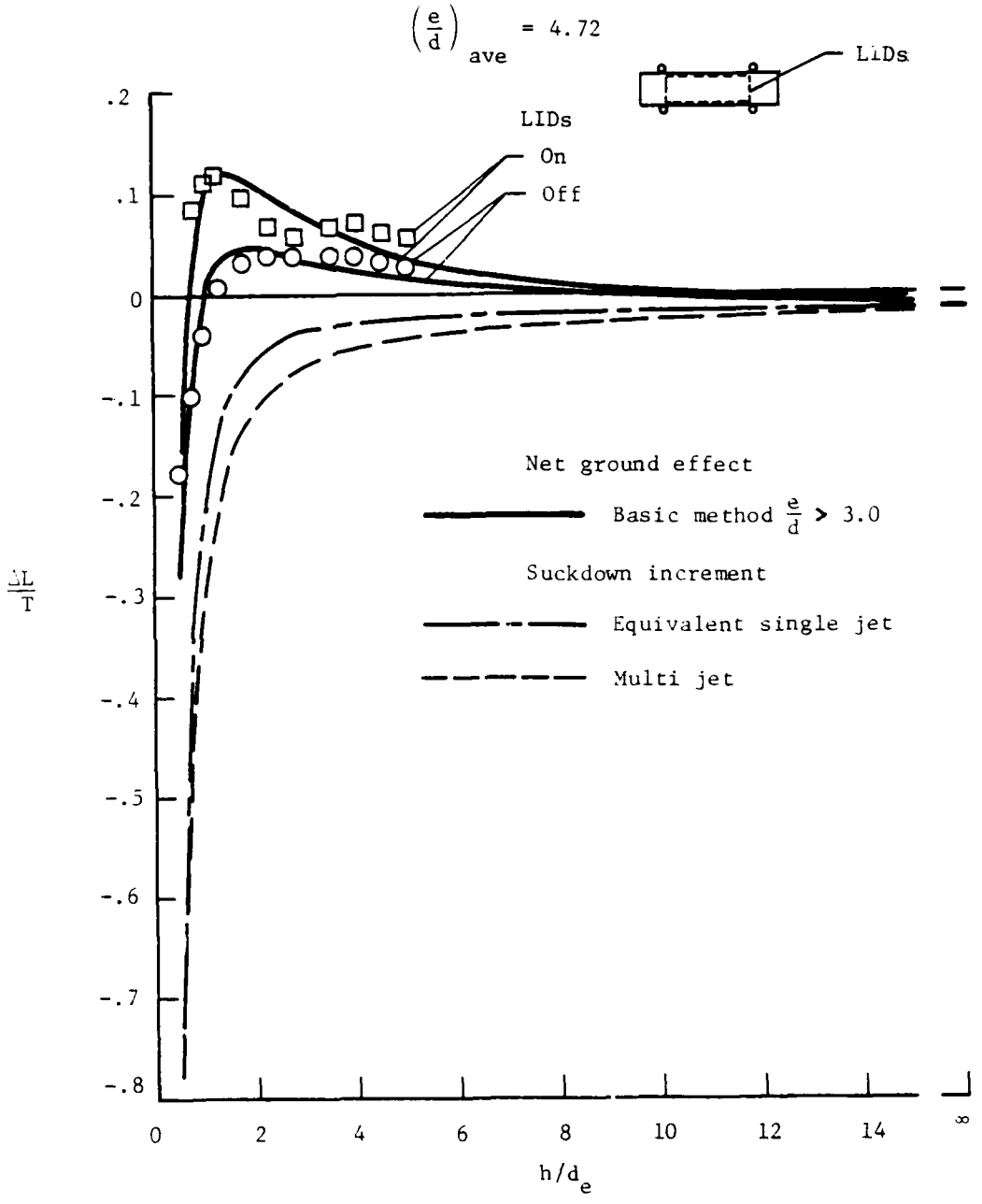

(d) Configuration 16 (ref 6)

Figure 20.- Continued.

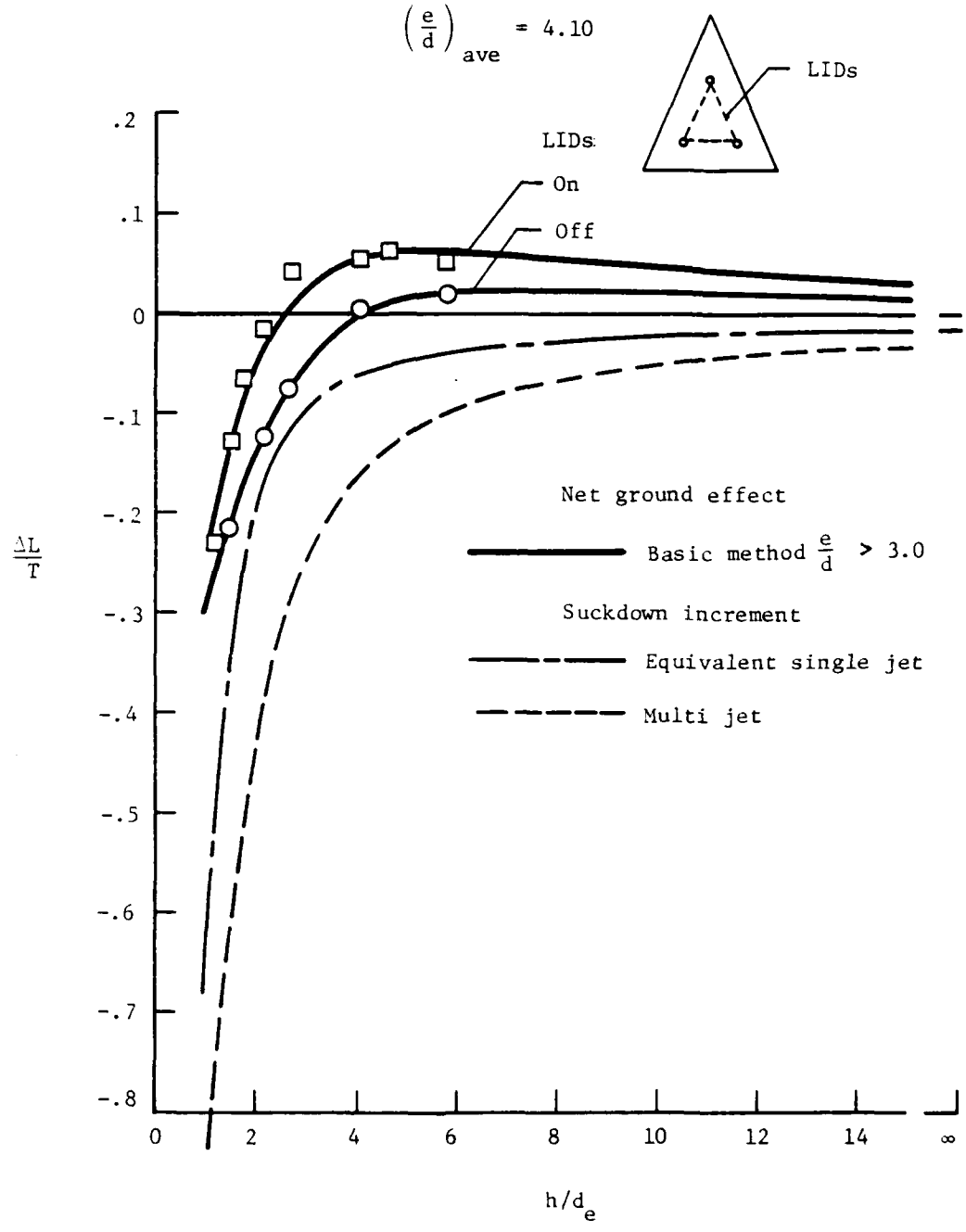

(e) Configuration 17 (ref 6).

Figure 20.- Continued.

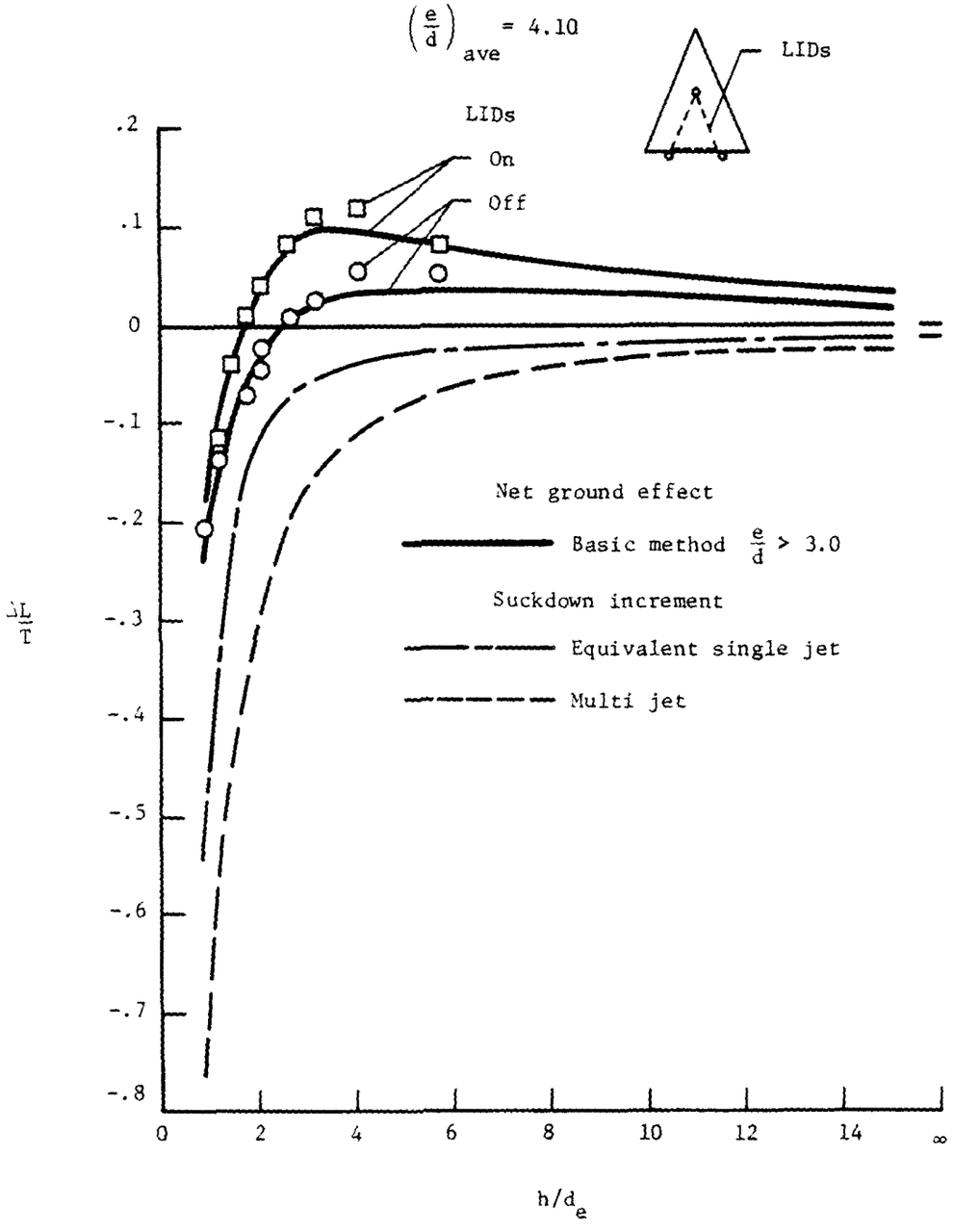

(f) Configuration 18 (ref 6).

Figure 20 .- Continued .

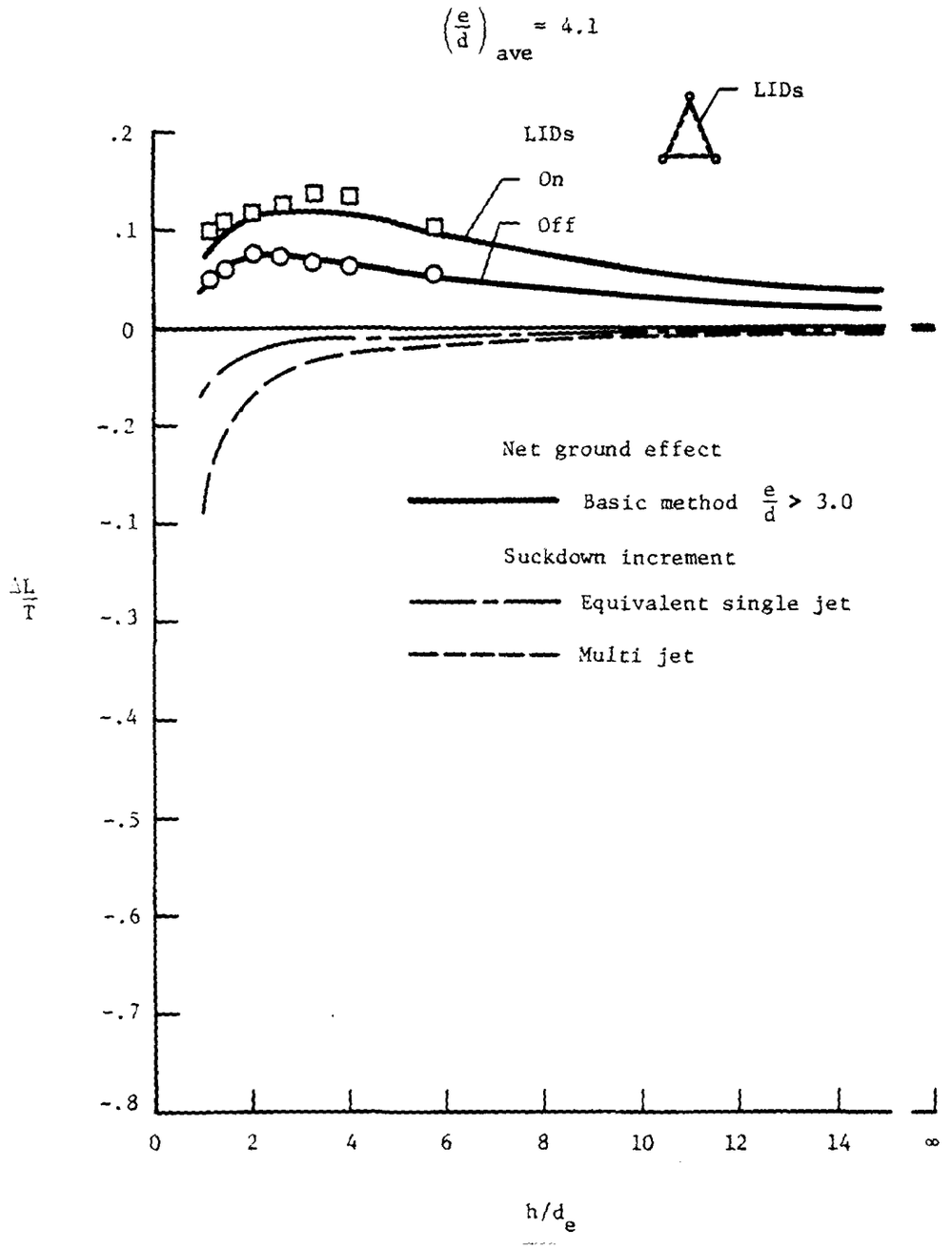

(g) Configuration 19 (ref 6).

Figure 20.- Continued.

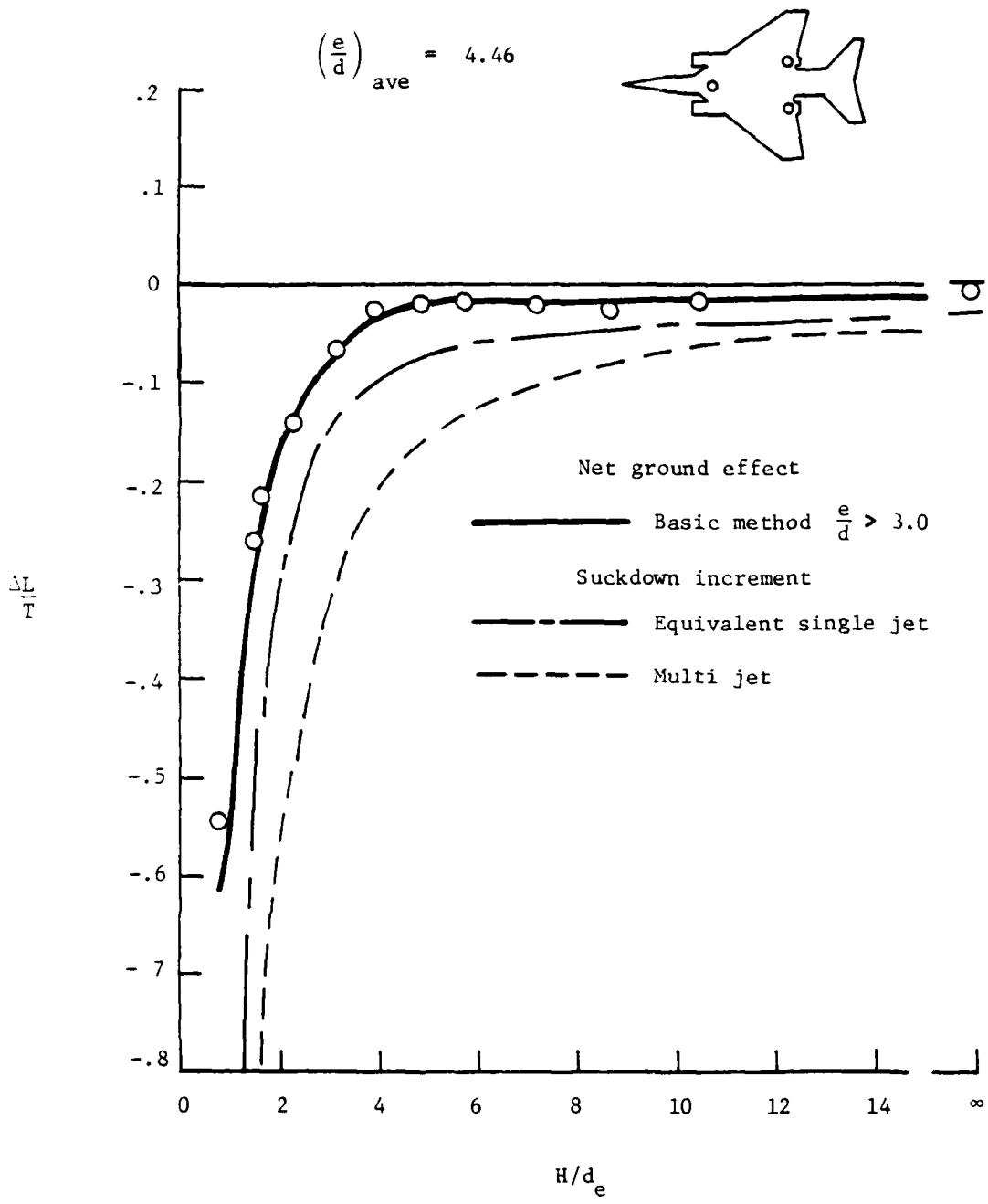

(h) Configuration 20 (ref 10).

Figure 20.- Continued.

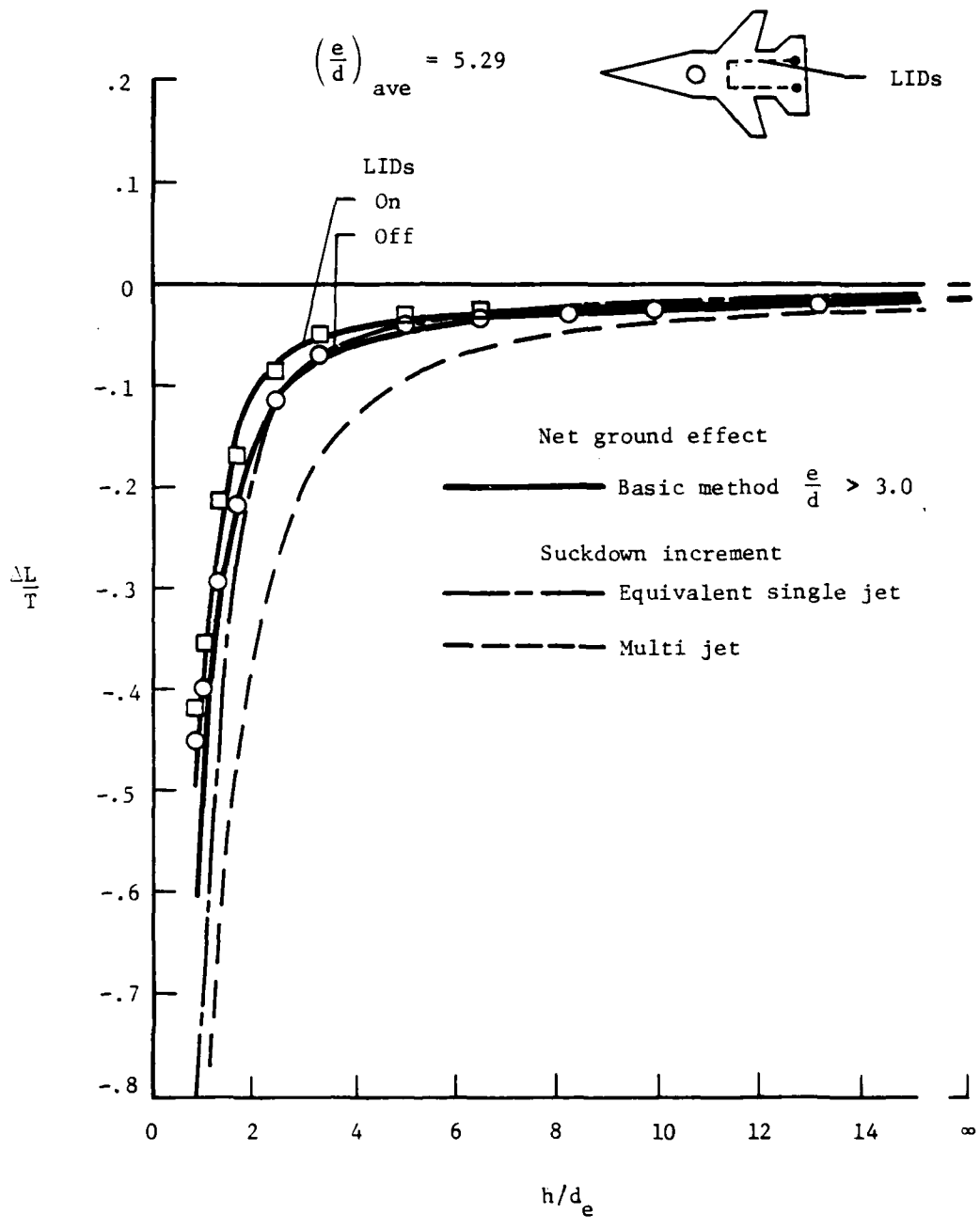

(i) Configuration 21 (ref 8).

Figure 20.- Continued.

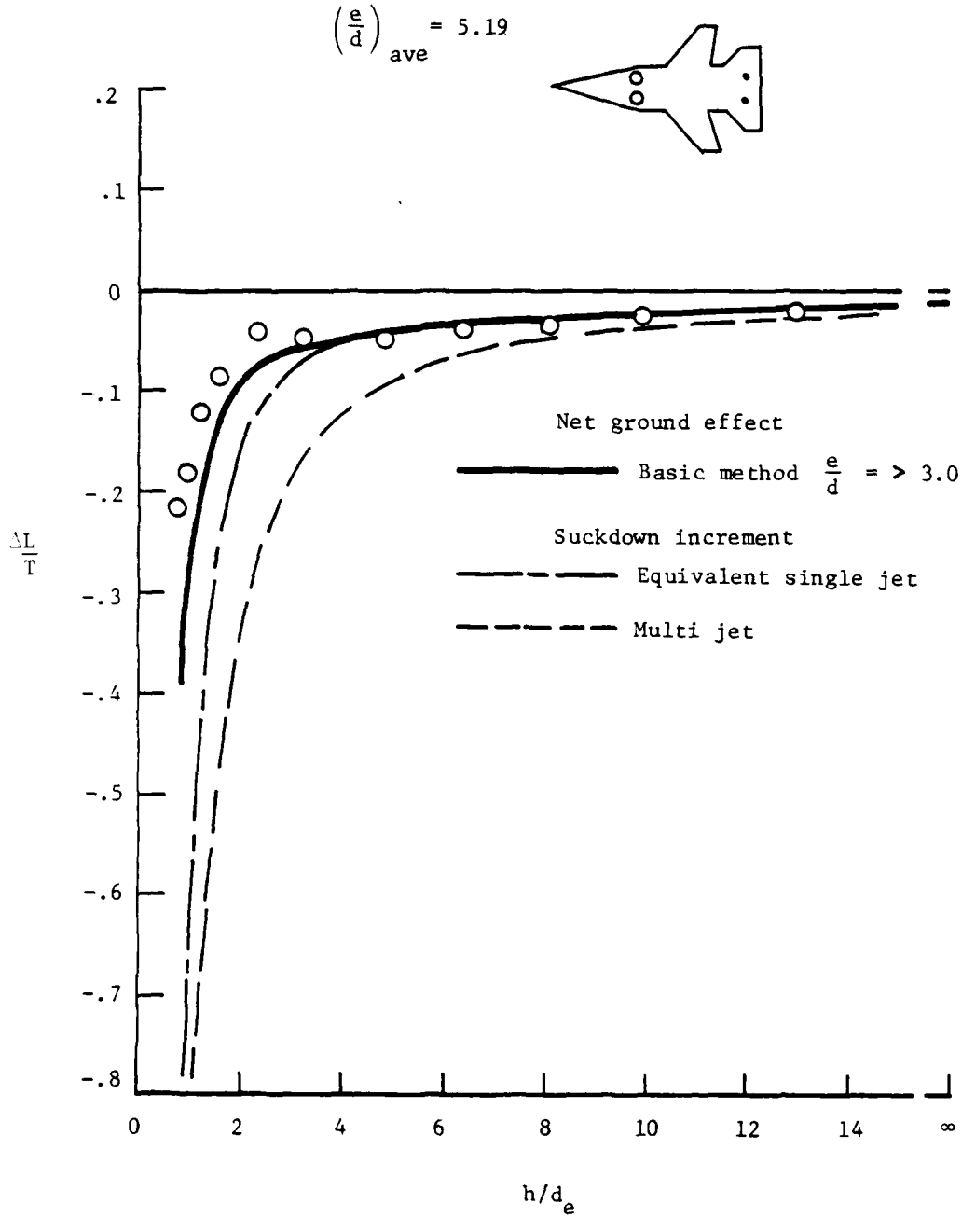

(j) Configuration 22 (ref 8).

Figure 20.- Continued.

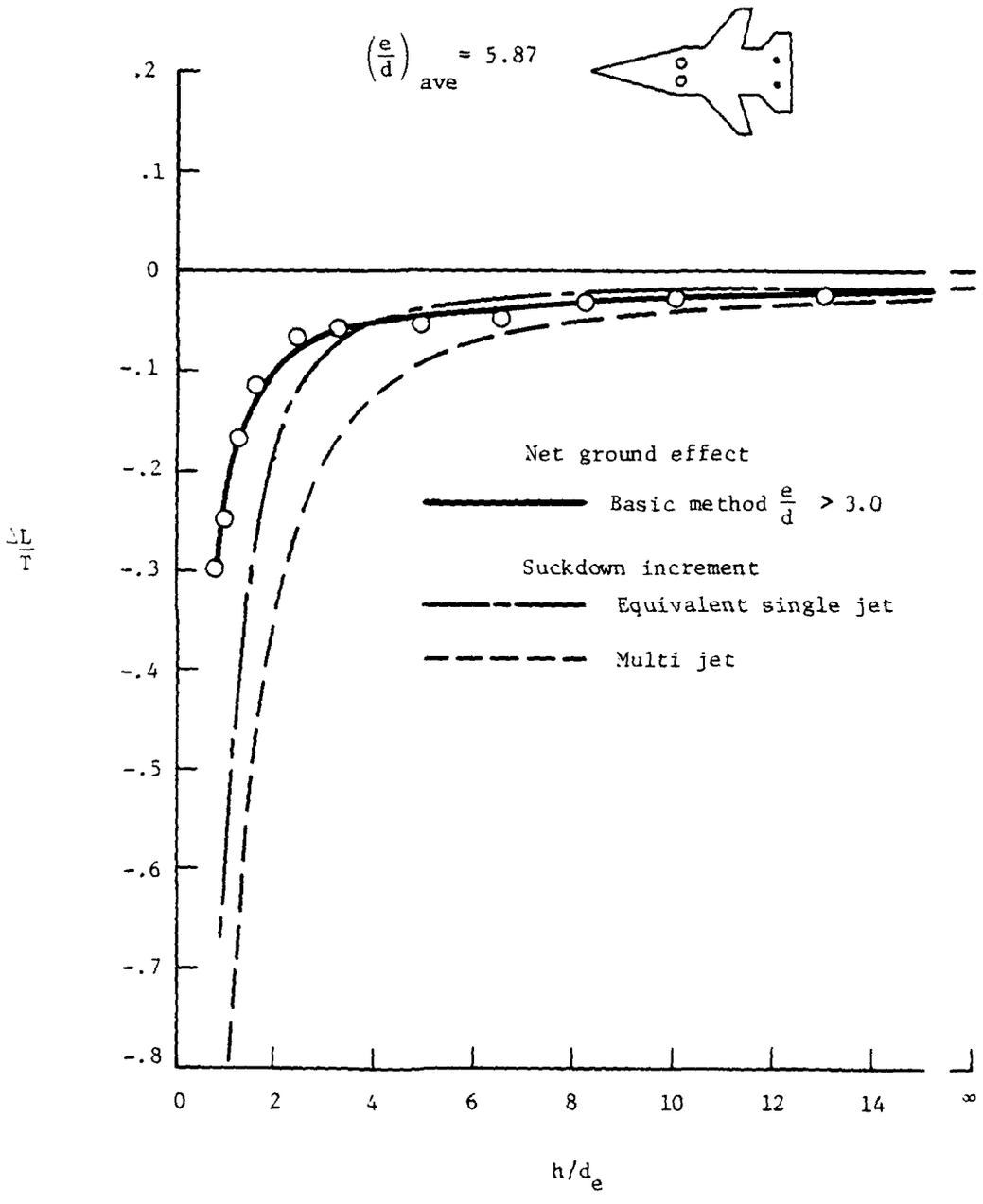

(k) Configuration 23 (ref 8).

Figure 20.- Concluded.

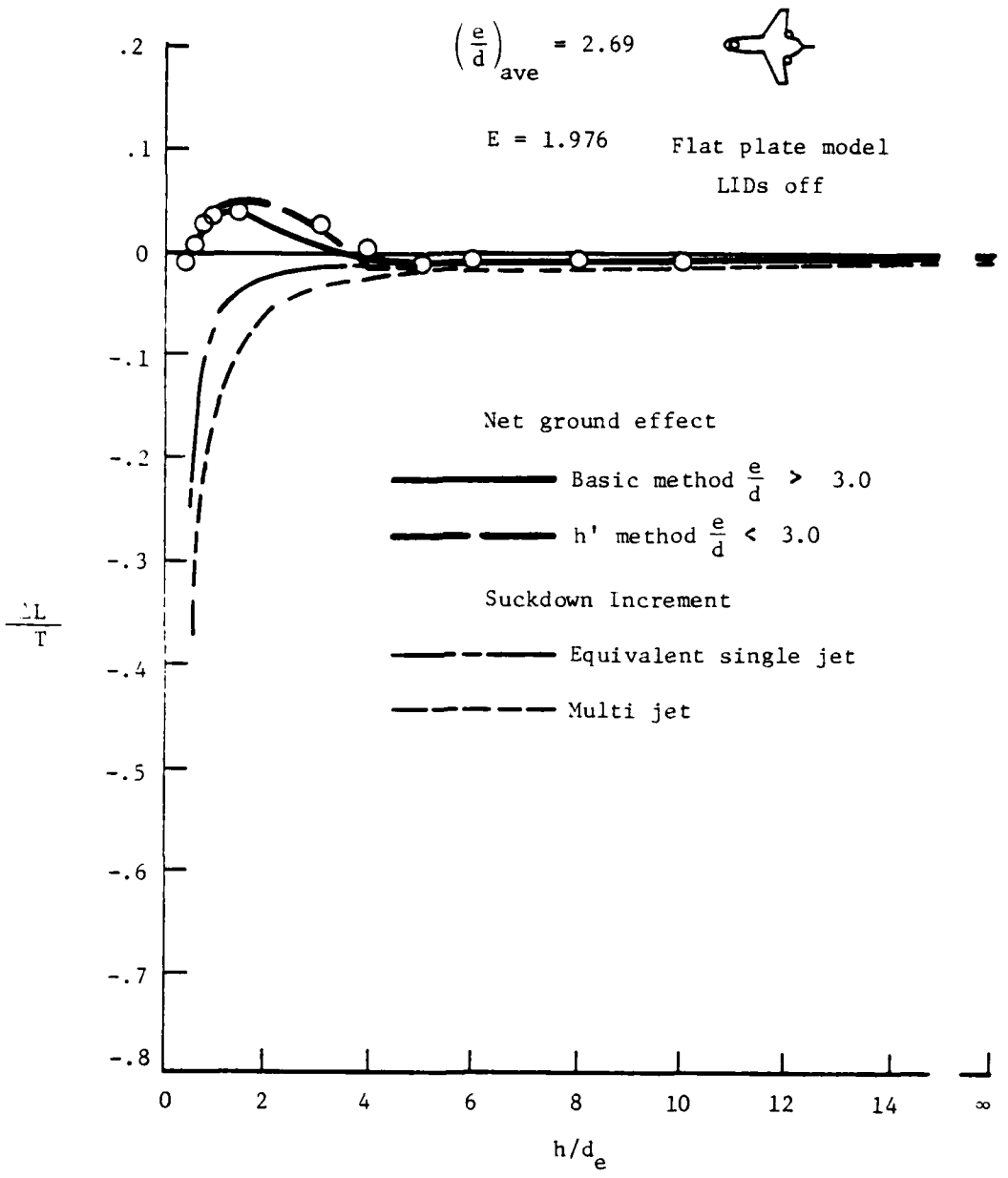

(a) Configuration 24 (ref 8).

Figure 21.- Comparison of calculated and measured ground effects for configurations with 3 or more jets. Close jet spacing $\frac{e}{d}_{ave}$ < 3.0.

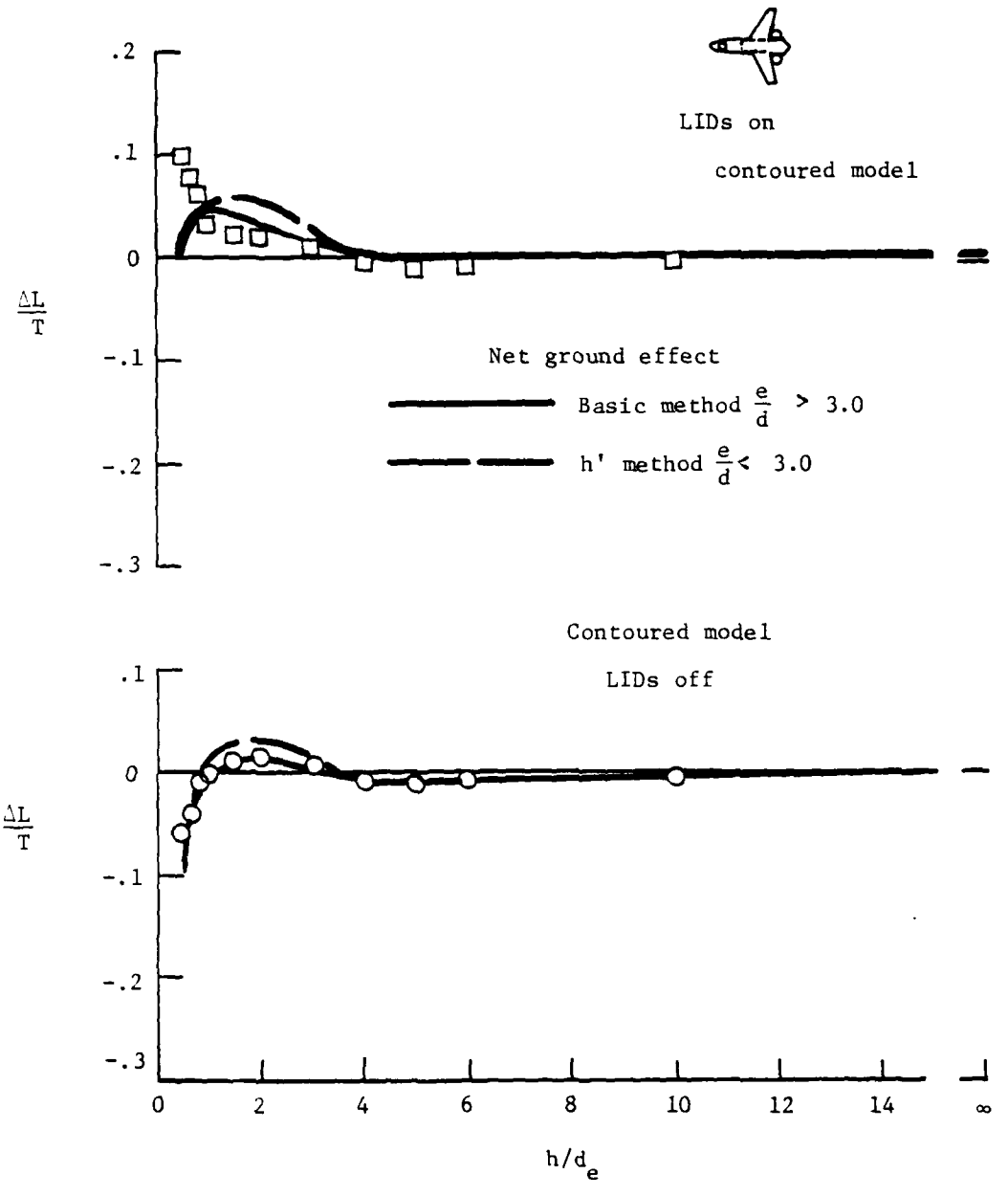

(b) Configuration 24 (ref 8).

Figure 21.- Continued.

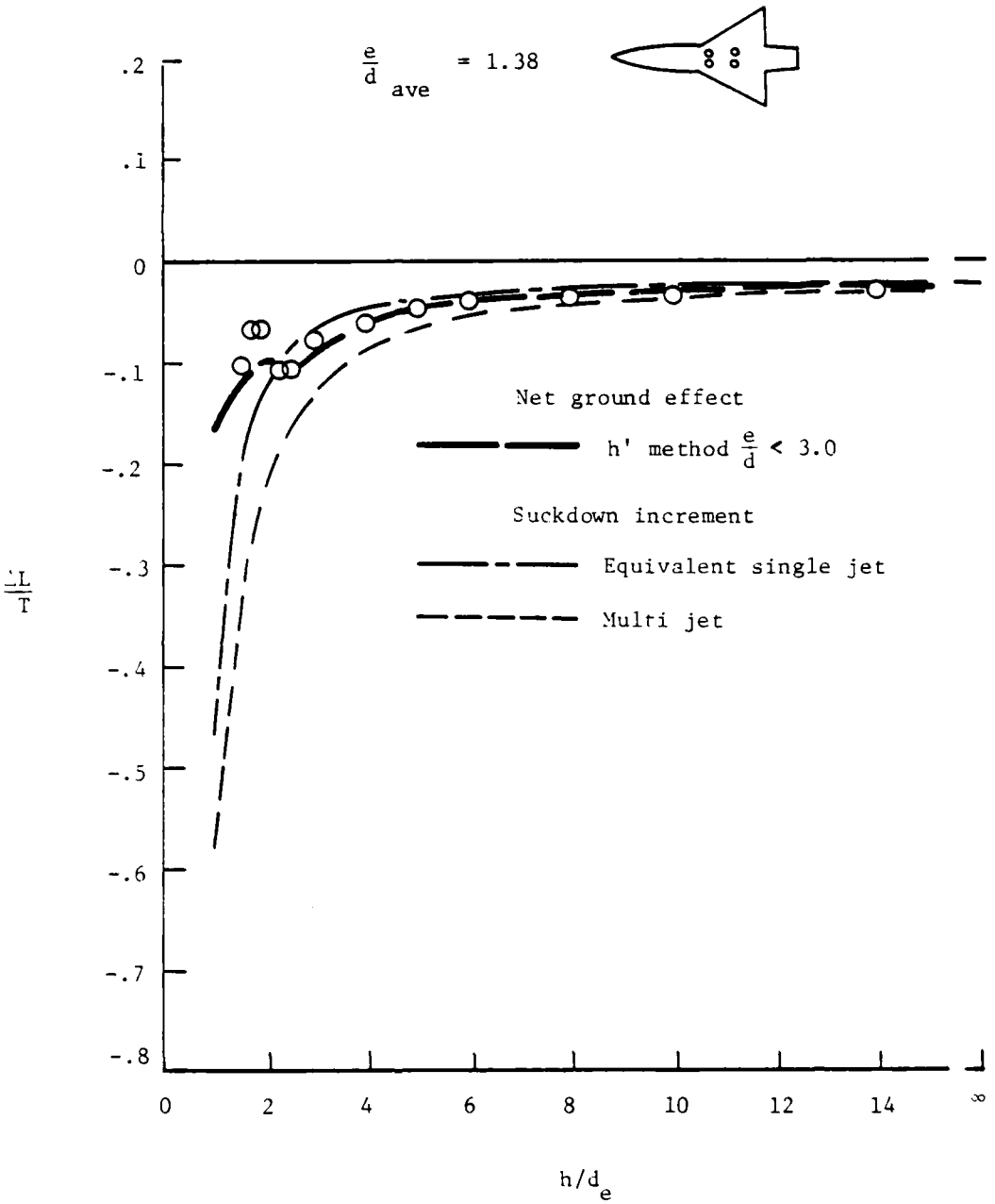

(c) Configuration 25a (ref 11).

Figure 21.- Continued.

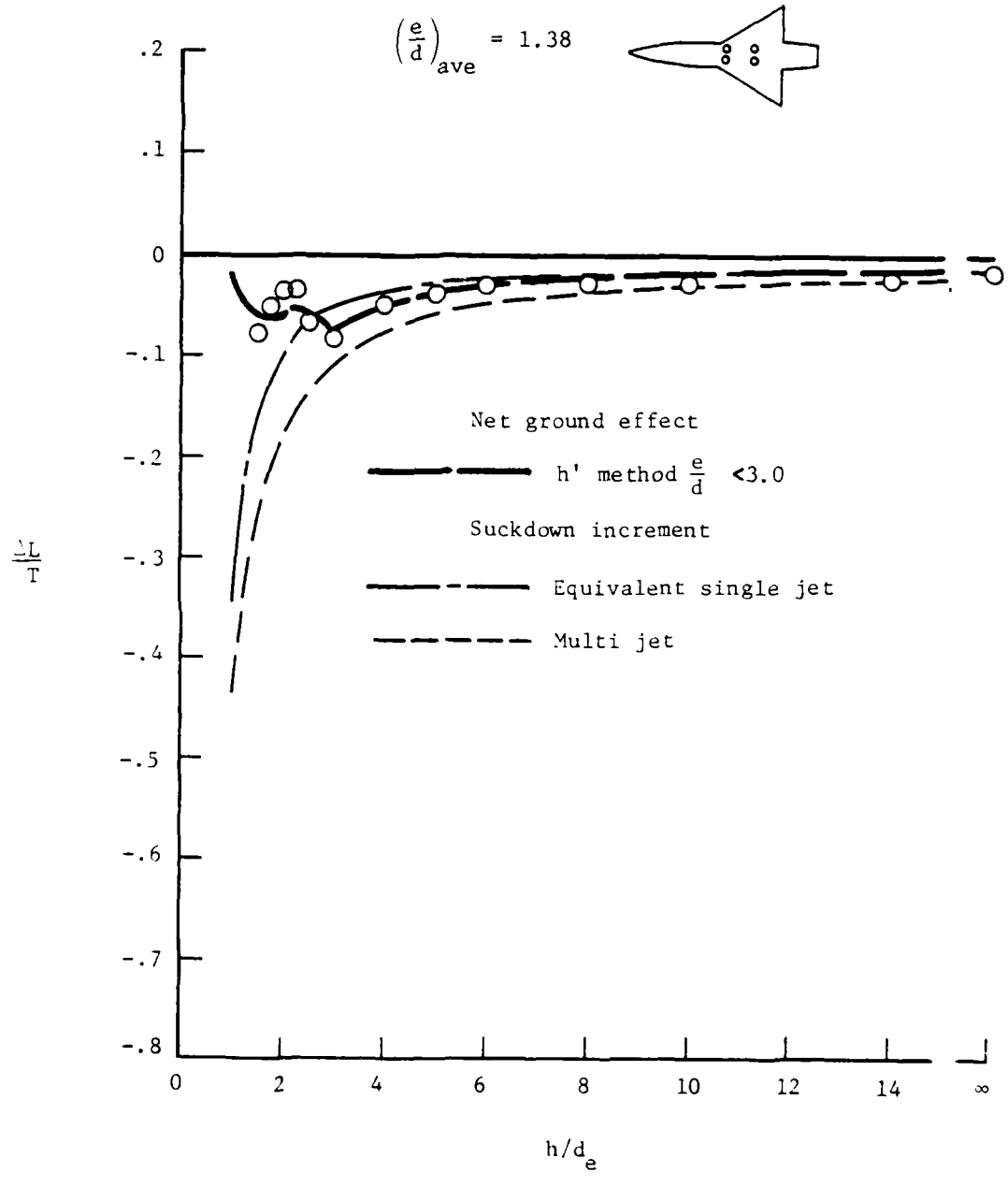

(d) Configuration 25b (ref 11)

Figure 21.- Continued.

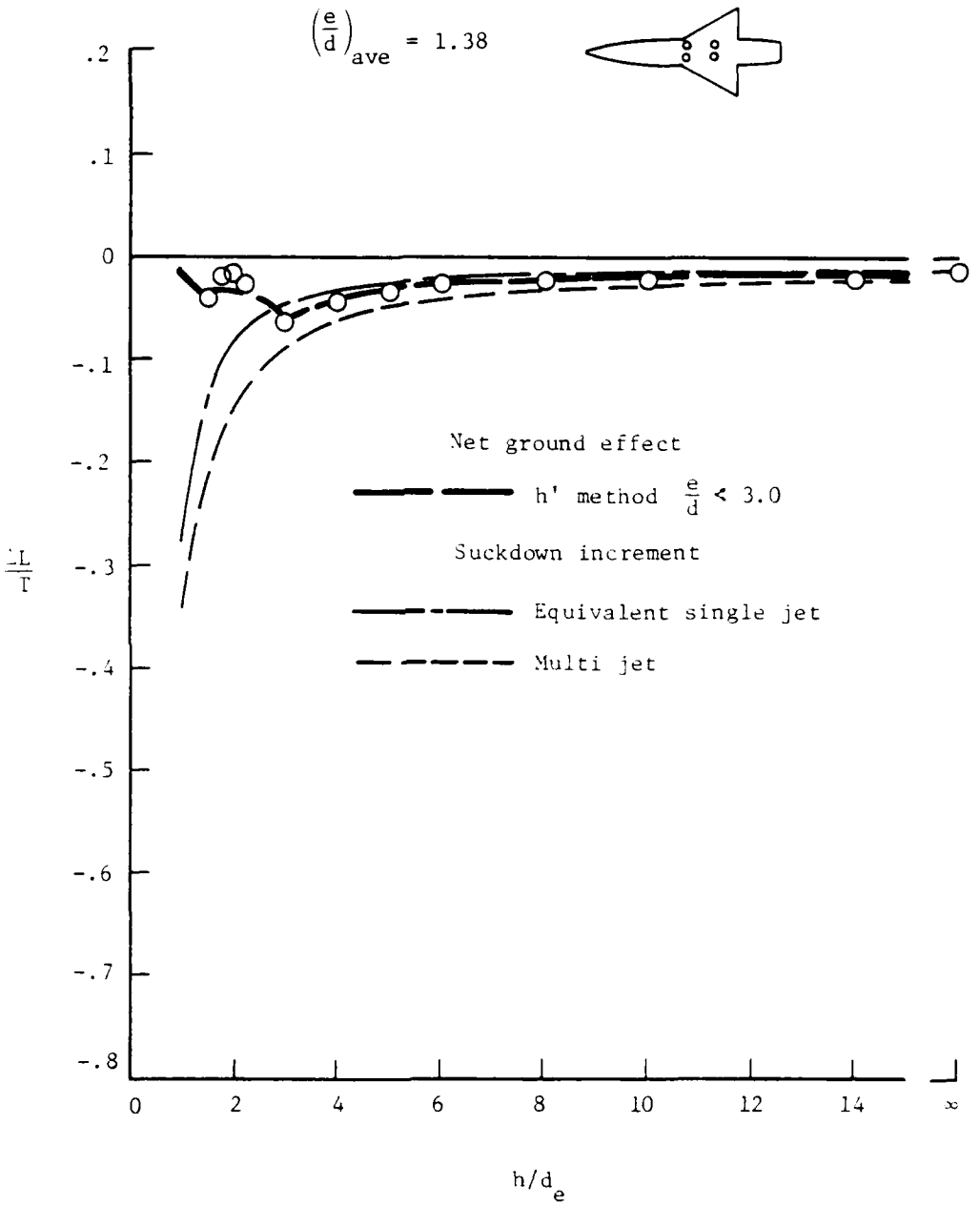

(e) Configuration 25c (ref 11).

Figure 21.- Continued.

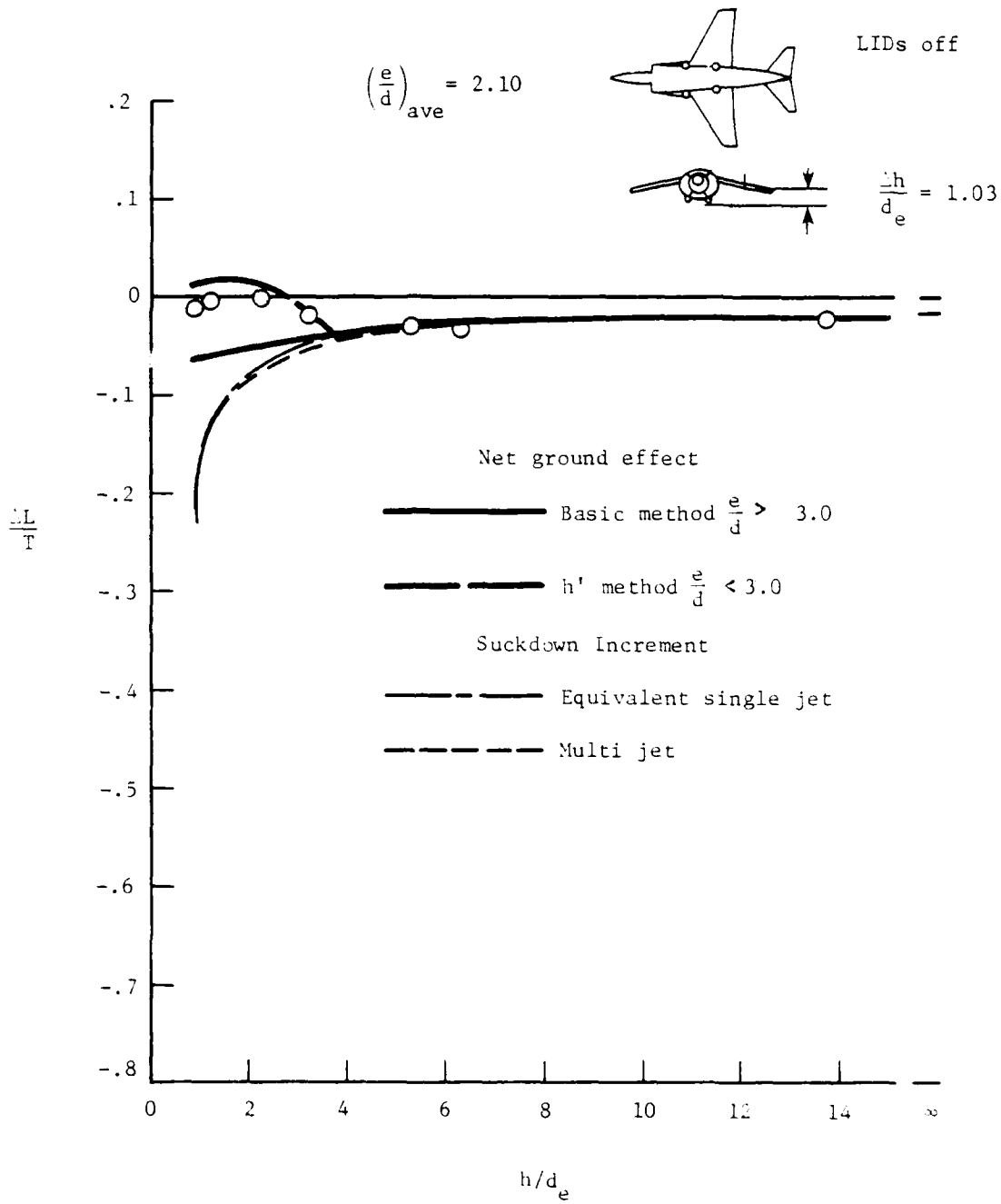

(f) Configuration 26a (ref 12).

Figure 21 continued.

AD-A098 509 KUHN (RICHARD E) NEWPORT NEWS VA F/G 20/4
AN ENGINEERING METHOD FOR ESTIMATING THE INDUCED LIFT ON V/STOL--ETC(U)
JAN 81 R E KUHN N62269-80-C-0366
UNCLASSIFIED NADC-80246-60 NL

END
DATE FILMED
5 81
DTIC

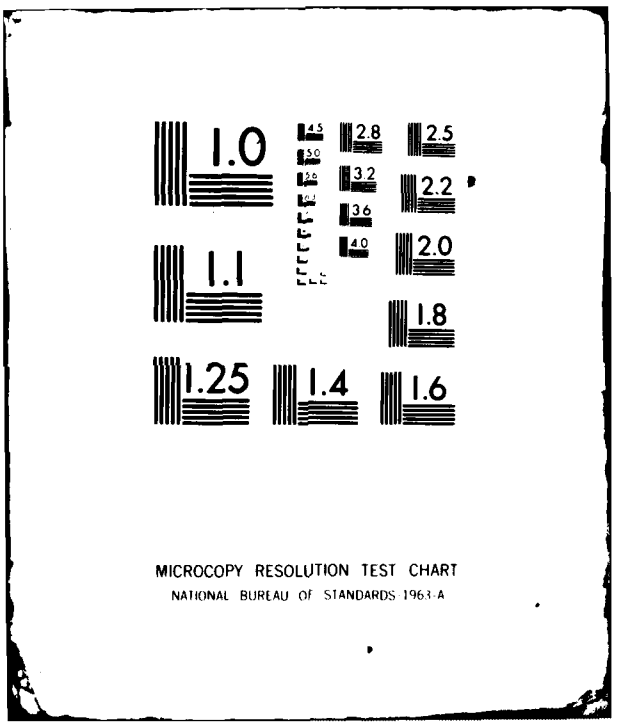
1.0
1.1
1.25
1.4
1.6
1.8
2.0
2.2
2.5
2.8
3.2
3.6
4.0
4.5
5.0
5.6
6.3
MICROCOPY RESOLUTION TEST CHART
NATIONAL BUREAU OF STANDARDS 1963-A

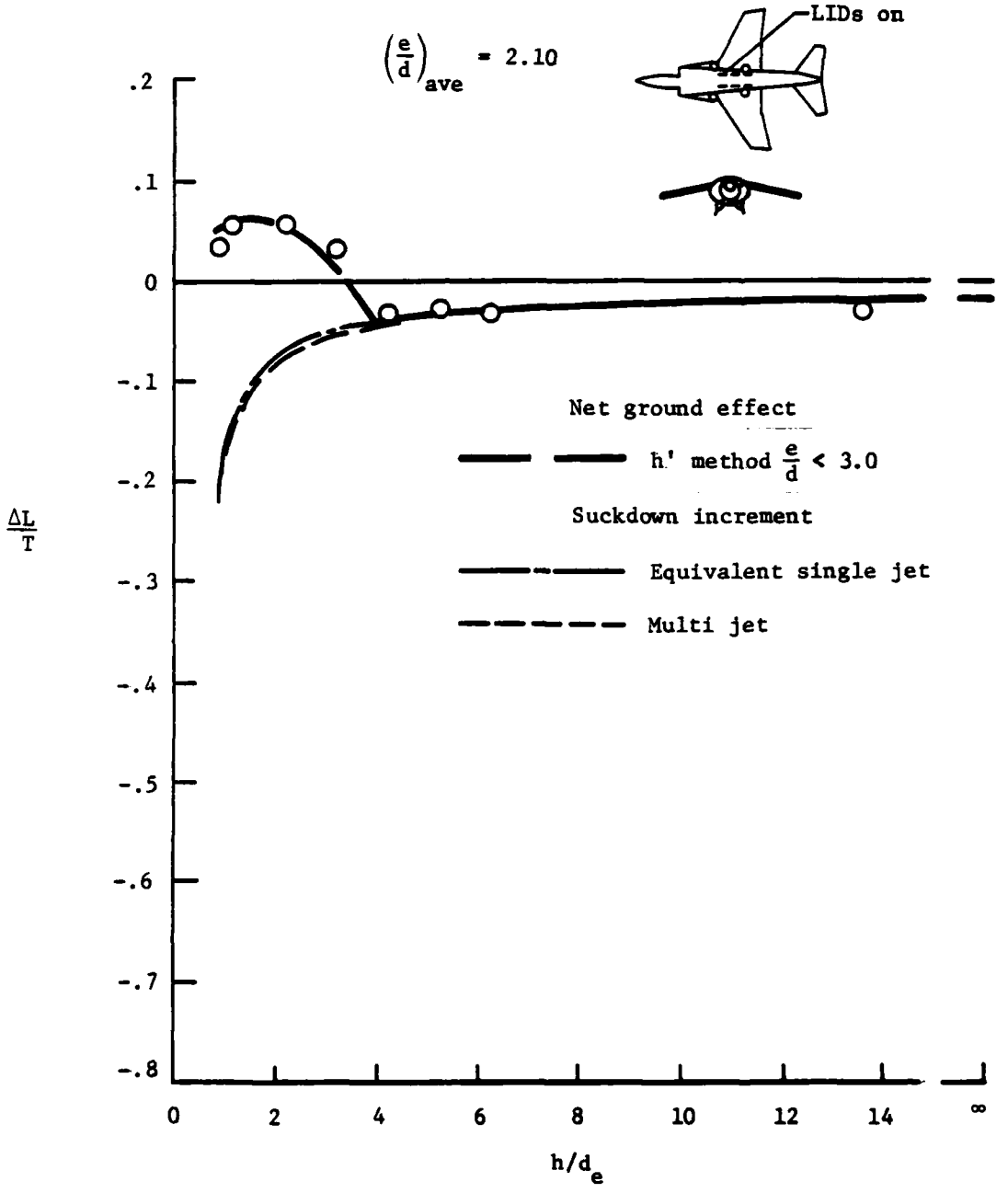

(g) Configuration 26b (ref 12)

Figure 21.- Continued.

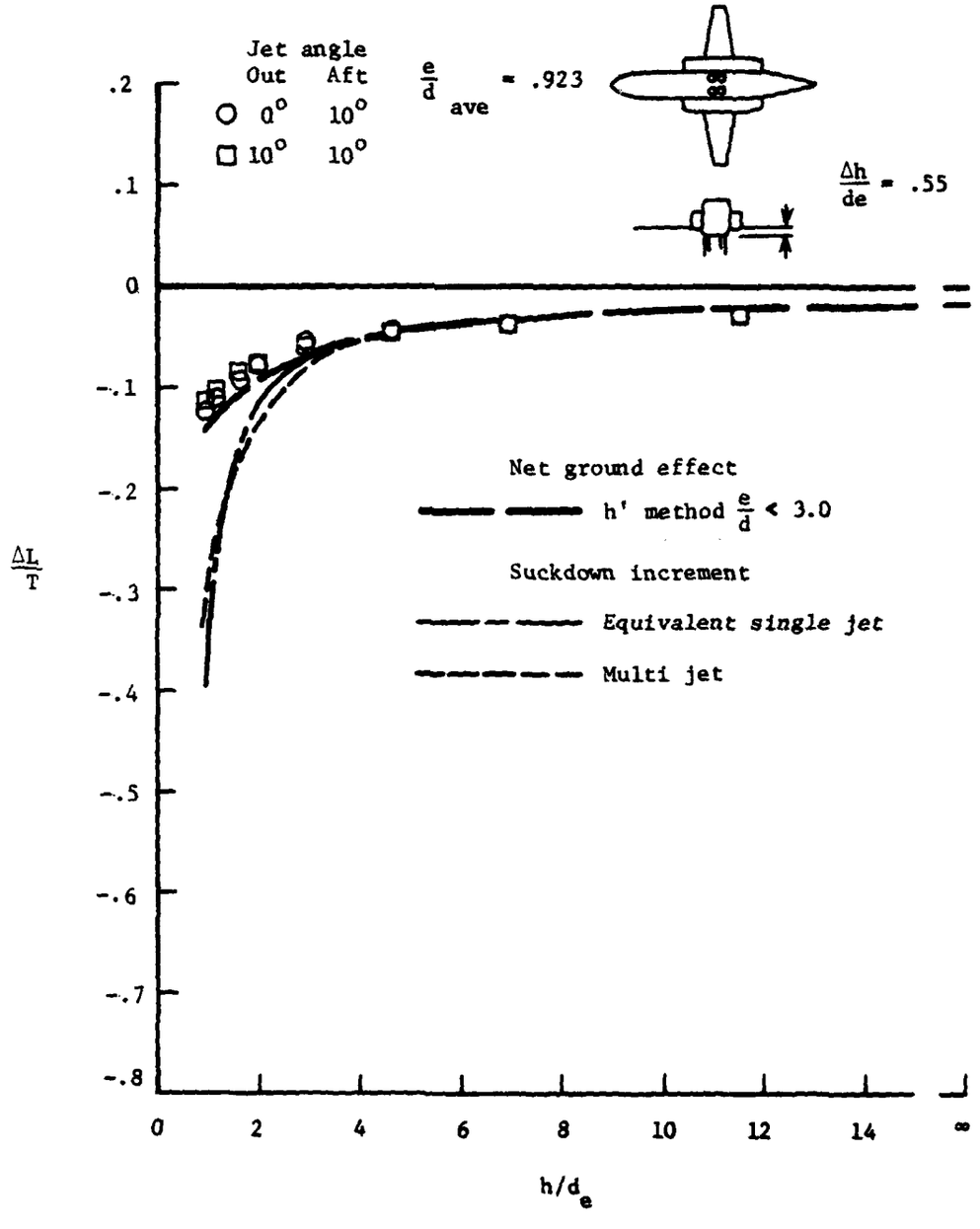

(h) Configuration 27 (ref 13)

Figure 21.- Continued.

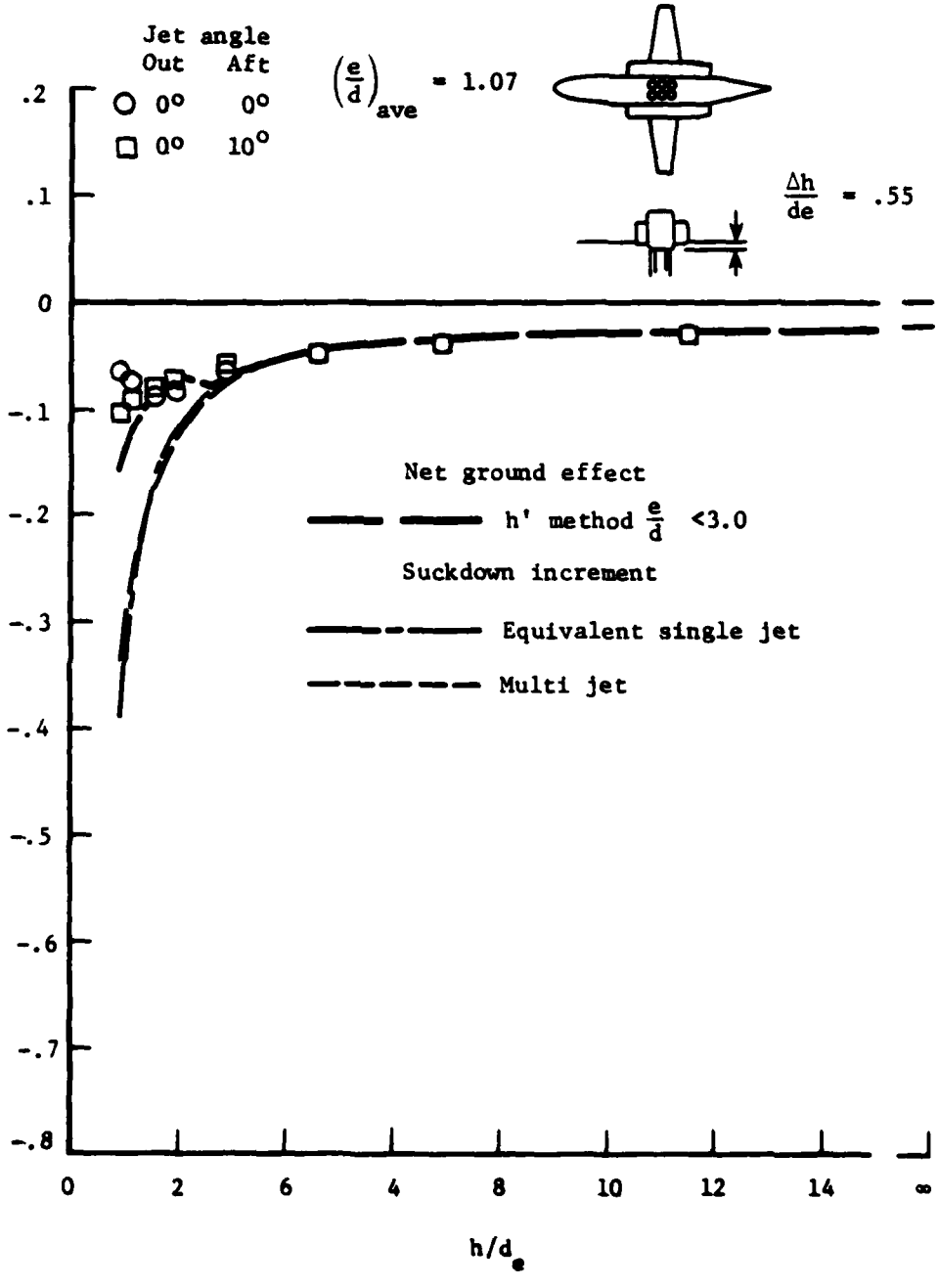

(i) Configuration 28 (ref 13)

Figure 21.- Continued.

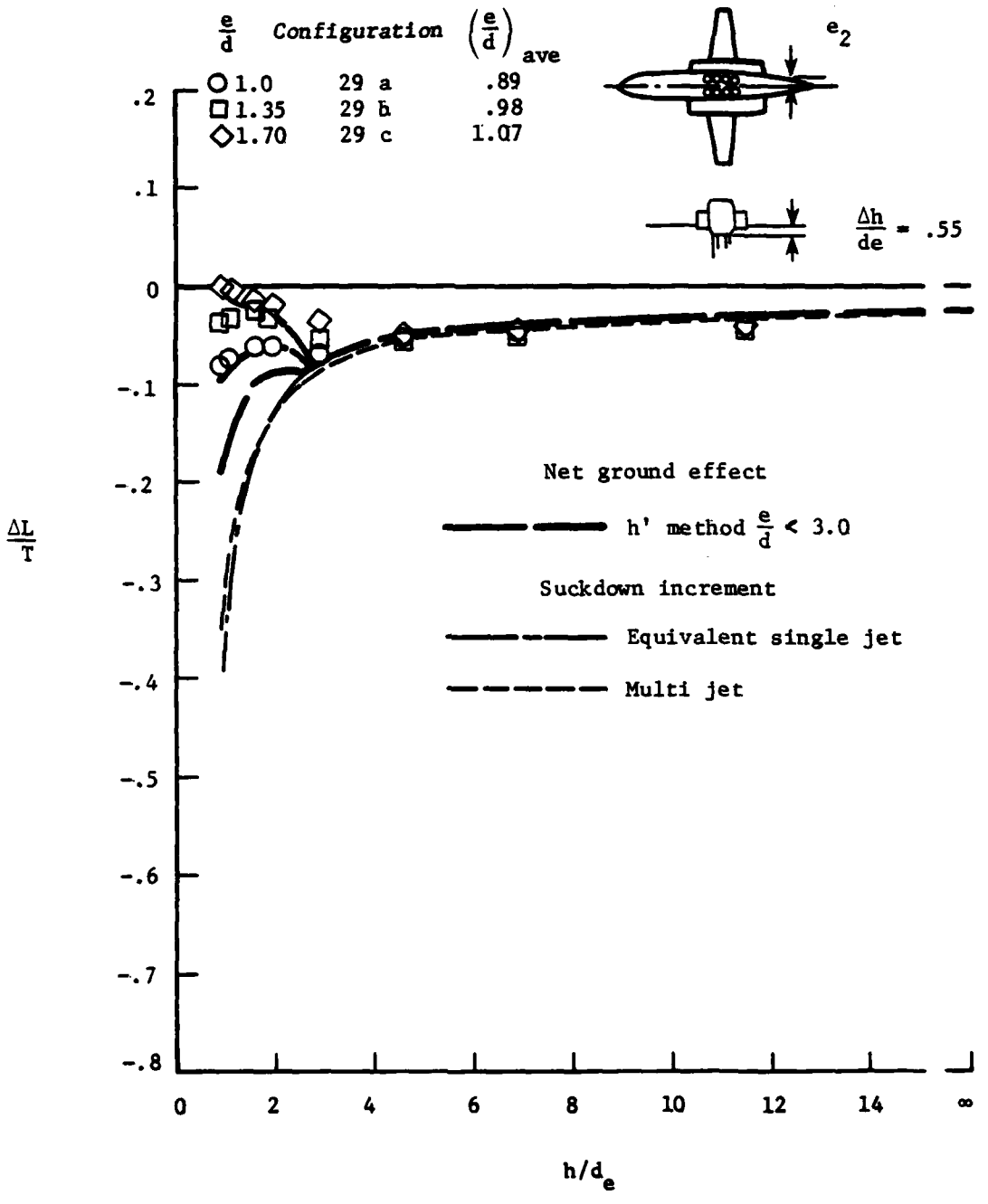

(j) Configuration 29 (ref 13).

Figure 21.- Continued.

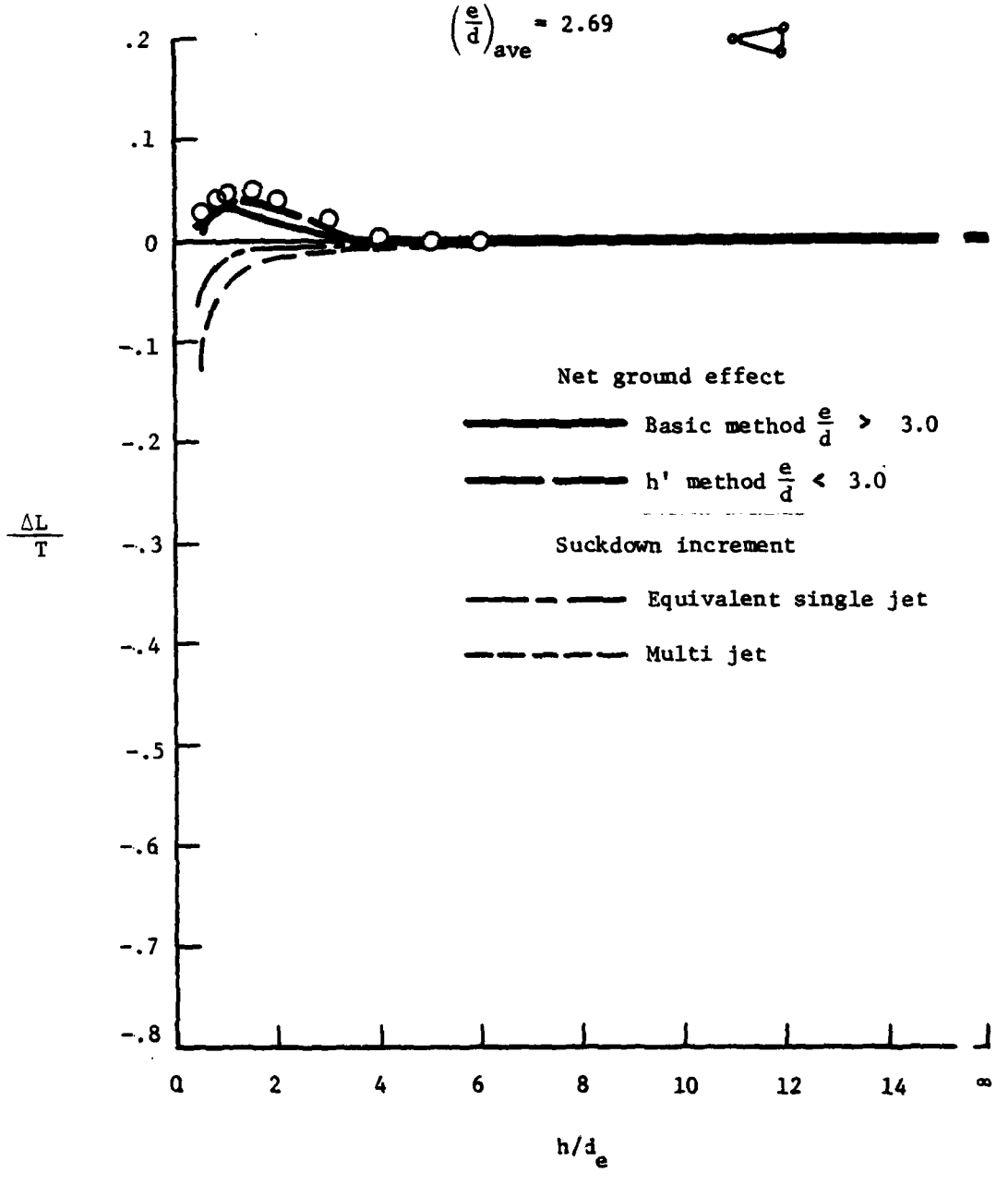

(k) Configuration 30 (ref 8).

Figure 21.- Concluded.

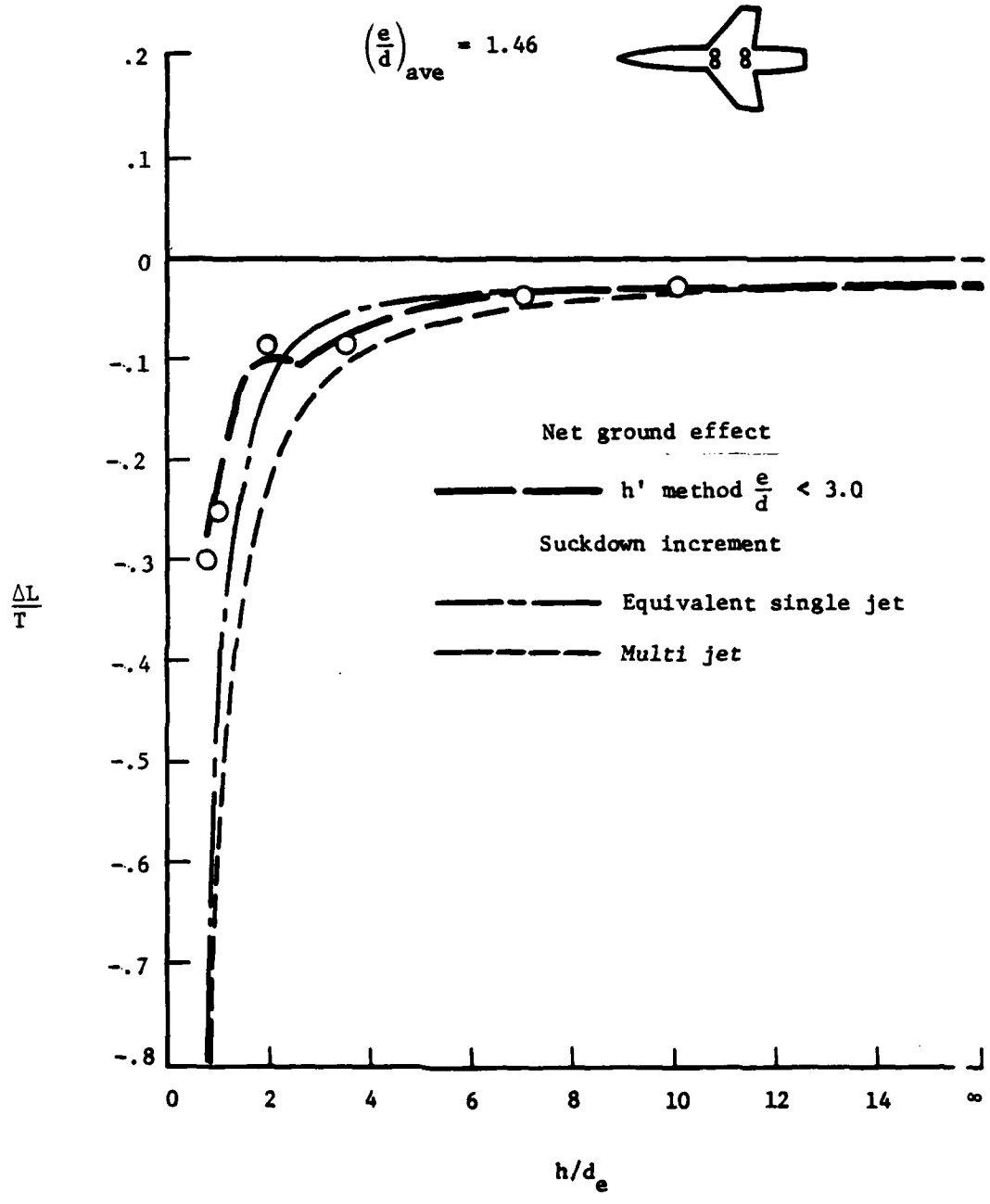

(a) Low wing.

Figure 22.- Effect of wing height on induced lift; Configuration 31, ref 14.

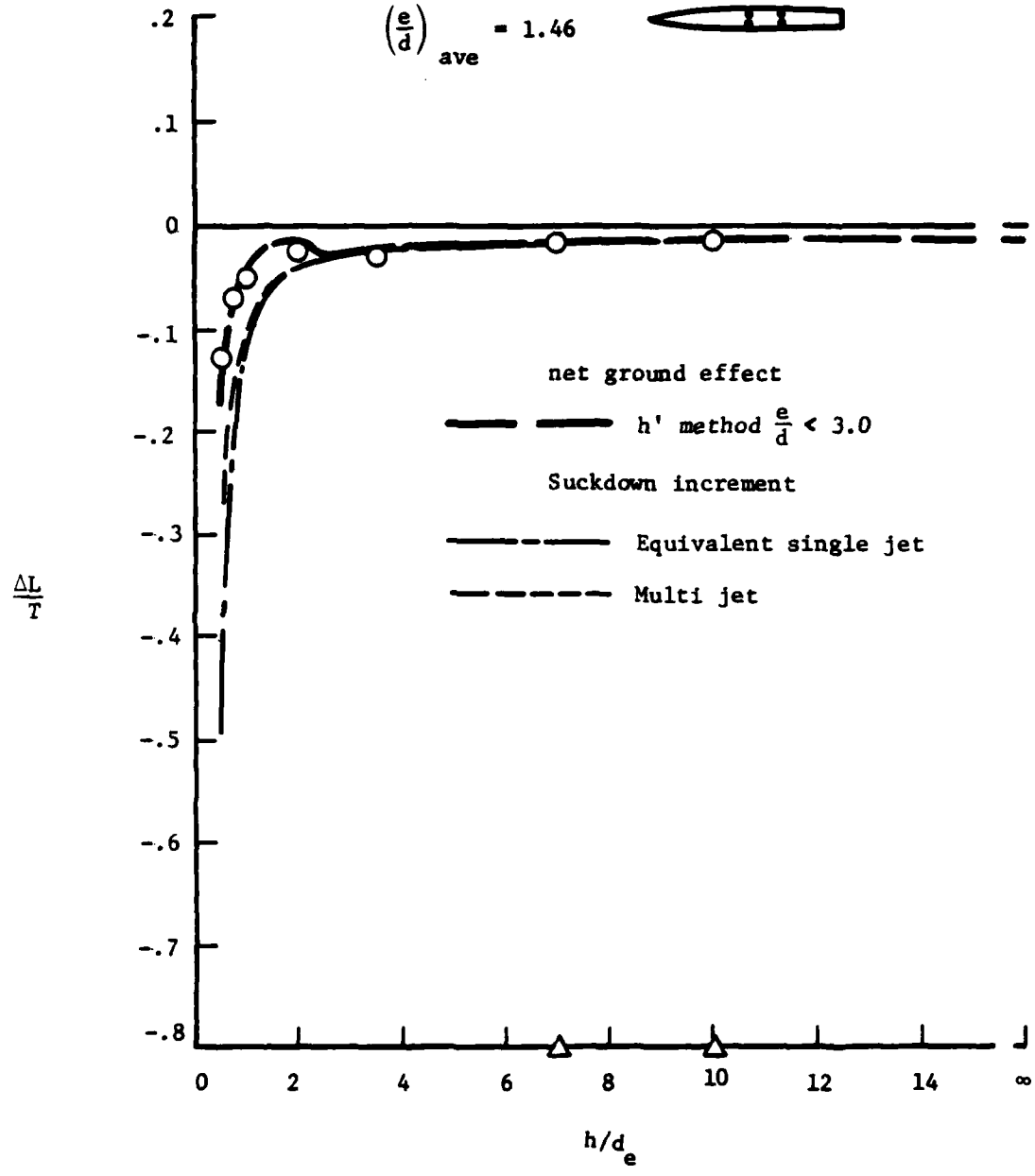

(b) Body alone.

Figure 22.- Continued.

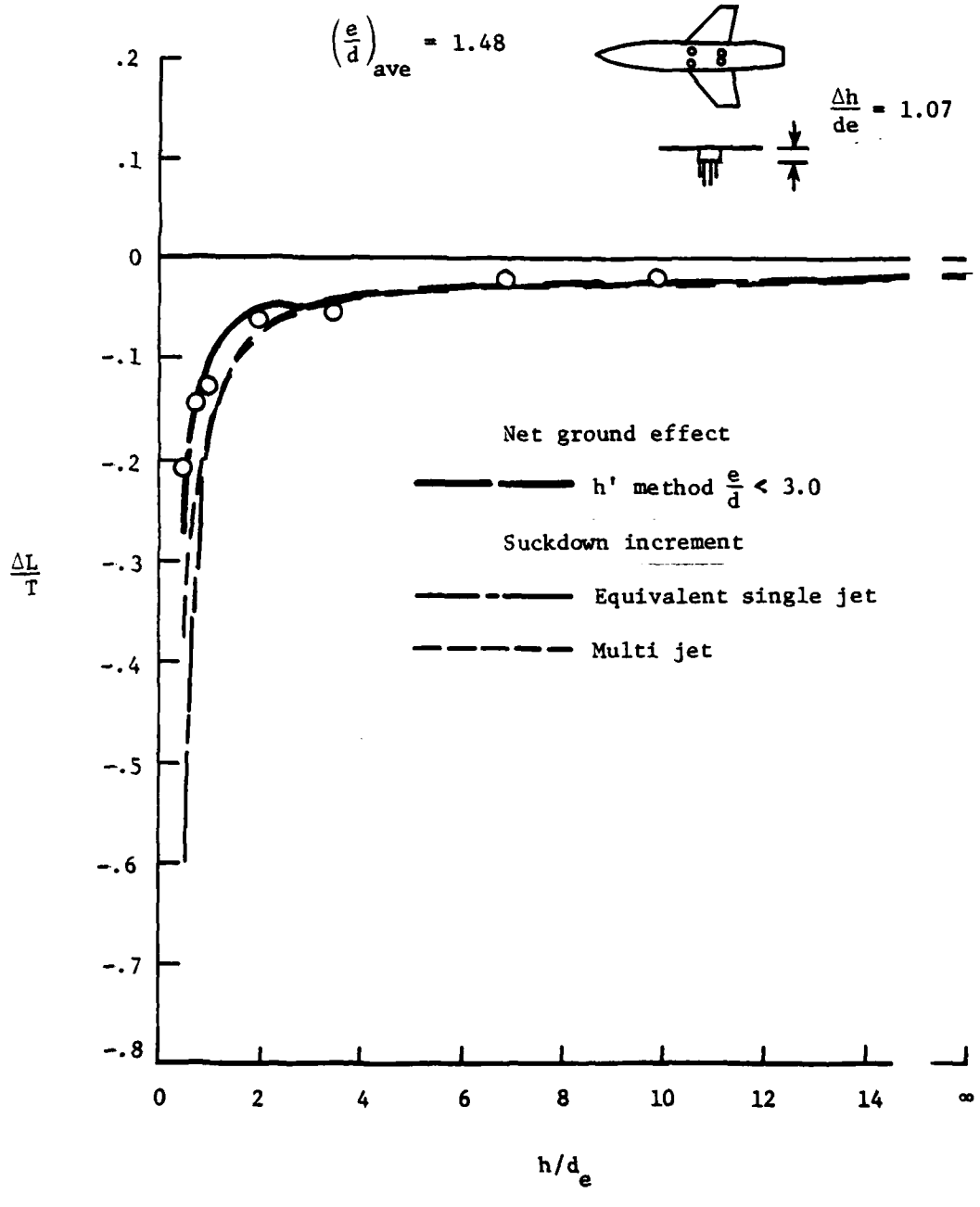

(c) High wing

Figure 22.- Concluded.

DISTRIBUTION LIST

REPORT NO. NADC-80246-60

AIRTASK NO. A03V-320D/01B/7F41-400-000

	No. of Copies
NAVAIRSYSCOM.	4
(2 for AIR-950D)	
(1 for AIR-320D)	
(1 for AIR-5301)	
NAVWPNCEN, China Lake, CA	1
NAVAIRPROPCEN, Trenton, NJ.	1
DTNSRDC, Bethesda, MD (Attn: Dr. H. Chaplin)	1
ONR, Arlington, VA (Attn: R. Whitehead).	1
NAVPGSCOL, Monterey, CA (Attn: M. Platzer)	1
NASA, Ames Research Center, Moffett Field, CA	2
(1 for D. Hickey)	
(1 for W. Deckert)	
NASA, Langley Research Center, Hampton, VA (Attn: R. Margason)	1
NASA, Lewis Research Center, Cleveland, OH.	1
Wright-Patterson AFB, Dayton, OH.	2
(1 for Flight Dynamics Lab)	
(1 for Aeronautical Systems Division)	
The Pentagon, Washington, DC (Attn: R. Siewert)	1
U.S. Army Aviation Systems Command, St. Louis, MO	1
U.S. Army Research Office, Durham, NC	1
DTIC, Alexandria, VA.	12
Boeing Company, Seattle, WA (Attn: E. Omar).	1
LTV Aerospace Corporation, Dallas, TX	2
(1 for T. Beatty)	
(1 for W. Simpkin)	
Rockwell International, Columbus, OH (Attn: W. Palmer)	1
General Dynamics Corporation, Ft. Worth, TX (Attn: W. Folley).	1
Nielson Engineering, Mountain View, CA (Attn: S. Spangler)	1
Univ. of Tennessee, Space Inst., Tullahoma, TN (Attn: W. Jacobs)	1
Lockheed-California Co., Burgank, CA (Attn: Y. Chin)	1
Northrop Corporation, Hawthorne, CA (Attn: P. Wooler).	1
Grumman Aerospace Corp., Bethpage, LI, NY (Attn: D. Migdal).	1
Royal Aeronautical Establishment, Bedford, England (Attn: A. Woodfield).	1
Fairchild-Republic, Corporation, Farmingdale, LI, NY.	1
Calspan, Buffalo, NY.	1
McDonnell Douglas Corp., St. Louis, MO (Attn: Dr. D. Kotansky)	1
V/STOL Consultant, Newport News, VA (Attn: R. Kuhn).	1
Georgia Inst., of Technology, Atlanta, GA (Attn: Dr. H. McMahon)	1
Penn State Univ., Univ. Park, PA (Attn: Prof. B. W. McCormick)	1

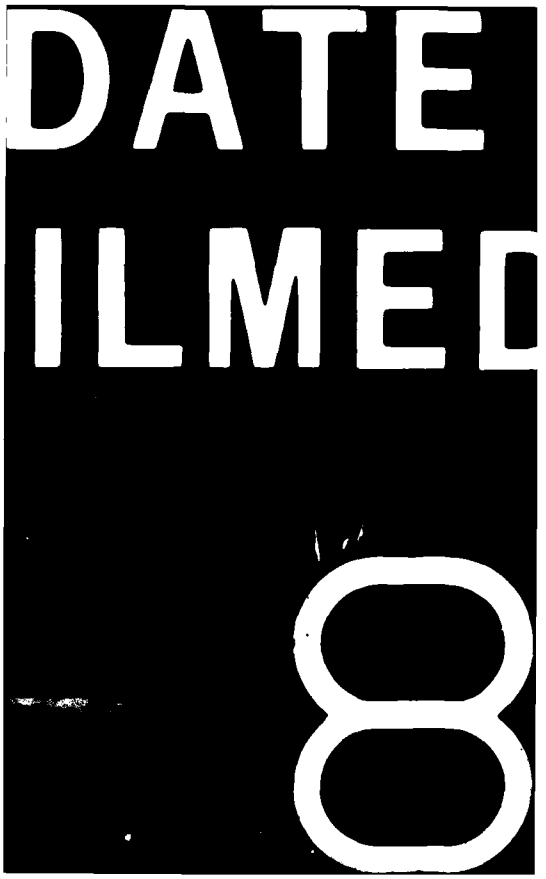
DATE
ILMED
8